CIVIL ENGINEERING STUDIES
Illinois Center for Transportation Series No. 21-025
UILU-ENG-2021-2025
ISSN: 0197-9191

Evaluation of Geosynthetics Use in Pavement Foundation Layers and Their Effects on Design Methods

Prepared By
Issam I. A. Qamhia, PhD
Erol Tutumluer, PhD

University of Illinois at Urbana-Champaign

Research Report No. FHWA-ICT-21-020

A report of the findings of

ICT PROJECT R27-193-3
Evaluation of Geosynthetics Use in Pavement Foundation Layers and Their Effects on Design Methods

https://doi.org/10.36501/0197-9191/21-025

Illinois Center for Transportation

August 2021

TECHNICAL REPORT DOCUMENTATION PAGE

1. Report No.	2. Government Accession No.	3. Recipient's Catalog No.
FHWA-ICT-21-020	N/A	N/A

4. Title	5. Report Date
Evaluation of Geosynthetics Use in Pavement Foundation Layers and Their Effects on Design Methods	August 2021
	6. Performing Organization Code N/A

7. Authors	8. Performing Organization Report No.
Issam I. A. Qamhia, https://orcid.org/0000-0002-2020-8437 Erol Tutumluer, https://orcid.org/0000-0003-3945-167X	ICT-21-025 UILU-2021-2025

9. Performing Organization Name and Address	10. Work Unit No.
Illinois Center for Transportation Department of Civil and Environmental Engineering University of Illinois at Urbana-Champaign 205 North Mathews Avenue, MC-250 Urbana, IL 61801	N/A
	11. Contract or Grant No. R27-193-3

12. Sponsoring Agency Name and Address	13. Type of Report and Period Covered
Illinois Department of Transportation (SPR) Bureau of Research 126 East Ash Street Springfield, IL 62704	Final Report 8/16/18–8/15/21
	14. Sponsoring Agency Code

15. Supplementary Notes

Conducted in cooperation with the U.S. Department of Transportation, Federal Highway Administration.
https://doi.org/10.36501/0197-9191/21-025

16. Abstract

This report presents findings of a research effort aimed at reviewing and updating existing Illinois Department of Transportation (IDOT) specifications and manuals regarding the use of geosynthetic materials in pavements. The project consisted of three tasks: evaluate current IDOT practice related to the use of geosynthetics; review research and state of the practice on geosynthetics applications, available products, design methods, and specifications; and propose recommendations for geosynthetic solutions in pavements to modernize IDOT's practices and manuals. The review of IDOT specifications revealed that geotextiles are the most used geosynthetic product in Illinois, followed by geogrids. Several of IDOT's manuals have comprehensive guidelines to properly design and construct pavements with geosynthetics, but several knowledge gaps and potential areas for modernization and adoption of new specifications still exist. Based on the review of the available design methods and the most relevant geosynthetic properties and characterization methods linked to field performance, several updates to IDOT's practice were proposed. Areas of improvement are listed as follows. First, establish proper mechanisms for using geogrids, geocells, and geotextiles in subgrade restraint and base stabilization applications. This includes using shear wave transducers, i.e., bender elements, to quantify local stiffness enhancements and adopting the Giroud and Han design method for subgrade restraint applications. Second, update IDOT's *Subgrade Stability Manual* to include property requirements for geogrids, geotextiles, and geocells suitable for subgrade restraint applications. Third, establish proper standards on stabilization, separation, and pumping resistance for geotextiles by incorporating recent research findings on geotextile clogging and permeability criteria. Fourth, promote the use of modern geosynthetic products, such as geotextiles with enhanced lateral drainage, and fifth, elaborate on proper methods for construction/quality control measures for pavements with geosynthetics.

17. Key Words	18. Distribution Statement
Pavements, Geosynthetics, Geogrids, Geotextiles, Geocells, Geofoams, Reinforcement, Stiffening, Drainage, Separation, Filtration, Climatic Effects, Bender Elements	No restrictions. This document is available through the National Technical Information Service, Springfield, VA 22161.

19. Security Classif. (of this report)	20. Security Classif. (of this page)	21. No. of Pages	22. Price
Unclassified	Unclassified	79 + appendices	N/A

ACKNOWLEDGMENT, DISCLAIMER, MANUFACTURERS' NAMES

This publication is based on the results of **ICT-R27-193-3: Evaluation of Geosynthetics Use in Pavement Foundation Layers and Their Effects on Design Methods**. ICT-R27-193-3 was conducted in cooperation with the Illinois Center for Transportation; the Illinois Department of Transportation; and the U.S. Department of Transportation, Federal Highway Administration.

Members of the Technical Review Panel (TRP) were the following:

- Heather Shoup, TRP Chair, Illinois Department of Transportation
- Veniecy Pearman-Green, TRP Co-chair, Illinois Department of Transportation
- Ally Kelley, Illinois Department of Transportation
- Andrew Stolba, Illinois Department of Transportation
- Bill Vavrik, Applied Research Associates Inc.
- Brian Laningham, Illinois Department of Transportation
- Charles Wienrank, Illinois Department of Transportation
- Dan Tobias, Illinois Department of Transportation
- Dennis Bachman, Federal Highway Administration
- Giancarlo Gierbolini, Illinois Department of Transportation
- Joe Olson, Illinois Department of Transportation
- Joe Vespa, Illinois Department of Transportation
- Megan Swanson, Illinois Department of Transportation
- Ryan Sheley, Illinois Department of Transportation
- Rustin Keys, Illinois Department of Transportation
- Scott Kassel, Illinois Department of Transportation
- Tim Peters, Illinois Department of Transportation

The authors would like to extend their appreciation to the TRP Chair and TRP members for their time and significant contributions to this research project, particularly for their help with providing the research team with special provisions, data, and materials related to the practice of IDOT and the use of geosynthetics in pavements in the State of Illinois. The feedback of the TRP members on the

proposed improvements to IDOT manuals and practice related to the use of geosynthetics as well as their feedback on the drafted design guides is much appreciated.

The authors would also like to extend their warm thanks to several PhD students at the University of Illinois's Department of Civil and Environmental Engineering—Mingu Kang, Han Wang, Zhongyi Liu, Wenjing Li, Kelin Ding, and Haohang Huang—for their contribution to compiling literature related to the use of geosynthetics in pavement applications. Their help and contribution to many sections in this report is highly appreciated.

Sincere thanks are extended to McCall Macomber for her help with editing this report, and to Kristi Anderson and Audrey Donoho for their contribution to ICT project management.

EXECUTIVE SUMMARY

This report aimed to evaluate the practice and specifications of the Illinois Department of Transportation (IDOT) related to the use of geosynthetic materials in pavement applications and identify knowledge gaps and potential areas of improvements. It also aimed to propose improvements to the current manuals and specifications to cover these knowledge gaps and modernize uses of geosynthetics (mainly to account for modern geotextile, geogrid, and geosynthetic products) as they relate to highway design and construction in the State of Illinois. Modern and up-to-date methods and uses for these products in subgrades, subbases, and bases as well as their potential benefits for the overall design and long-term performance of pavements were evaluated. Three major tasks were undertaken in this project. The first task covered the evaluation of the current IDOT practice related to the use of geosynthetics for highway applications. The second task involved the review of research and state of the practice on geosynthetics usage, available products, design methods, and specifications. The third task proposed recommendations and draft design guides to modernize IDOT's practices and manuals for effective solutions with modern geosynthetics in pavement applications.

As part of the first task (reviewing the current practice of IDOT), IDOT manuals and specifications were reviewed, and information was collected and summarized related to the current practices and specifications of IDOT for the use of geosynthetics in highway pavements. The revised IDOT manuals and specifications included the *Illinois Construction Manual* (2021a), *Geotechnical Manual* (2020), *Subgrade Stability Manual* (2005), *Bureau of Design and Environment Manual* (2021b), the *Standard Specifications for Road and Bridge Construction* (2016), and the *Bureau of Local Road and Streets Manual* (2018). In addition to these manuals and specifications, the Technical Review Panel (TRP) also provided the research team with several special provisions and project-specific documents for the use of geosynthetics in pavements. Such provisions entailed usage of geotextiles, geogrids, geofoams, and geocells. Based on the evaluation of IDOT documents, the researchers concluded that geotextiles are the most widely used geosynthetic material in Illinois, with applications covering subgrade restraint / soil stabilization, reflective crack control, drainage and separation applications, erosion control, slope stability, and retaining walls. Geogrids were the second most used geosynthetic product, but the specifications and applications were not well detailed. Other geosynthetic products were rarely mentioned in IDOT practice, except for some special provisions and specific projects. Thus, several knowledge gaps and lags in IDOT practice were identified for modernization and drafting of new specifications.

In the second task, previous research and state of the practice on geosynthetics usage, products, designs, and specifications were reviewed and evaluated. This task included a complete review of all design methods for geosynthetics (mostly geogrids, stiff geotextiles, and geocells) for unpaved and paved road applications, which are equivalent to subgrade restraint and base stabilization applications, respectively. Revised design methods included those by Steward et al. (1977), Giroud and Noiray (1981), Dutch (CROW) design (2002), US Army Corps of Engineers (2003), and Giroud and Han (2004a, 2004b) for unpaved roads. For paved road applications, reviewed design methods included those by US Army Corps of Engineers (2003), American Association of State Highway and Transportation Officials (AASHTO, 1993), Federal Highway Administration (FHWA) design manual

[Holtz et al. (2008)], AASHTO (2013), and other mechanistic-empirical design methods using finite-element and discrete-element modeling approaches. Design methods for geotextiles to ensure proper drainage, separation, and filtration were also fully reviewed and reported, including proper criteria to select the most suitable geotextile products to ensure that drainability, durability, and proper separation are achieved.

Further, available testing methods for geosynthetic materials and the geosynthetic properties reported by manufacturers were evaluated to determine best practices to select proper geosynthetic properties / products for serving a specific function in highway pavements. Some of the state-of-the art methods to characterize geosynthetic materials, such as using bender element piezoelectric sensors for local stiffness measurements in the proximity of a geogrid / stiff geotextile and evaluating the stiffness of the soil-geosynthetic composite (K_{SGC}), as proposed by Roodi and Zornberg (2017), were selected as the proper methods to determine the mechanisms that govern aggregate-geosynthetic interaction and properly evaluate the performance. Lastly, case studies and specific field data related to the use of geosynthetics for subgrade restraint, base stabilization, drainage, and mitigation of environmental effects resulting from expansive soils and frost heave were reviewed and reported. New and emerging geosynthetic products that serve specific functions were also investigated, such as woven geotextile products that can facilitate drainage in areas with silty soils and high capillary rise, or where shallow groundwater tables exist.

Based on the evaluation of IDOT's specifications and the review of the design methods with available products and characterization techniques, several improvements and changes were proposed to modernize IDOT's practice and ensure the state is making the most use of utilizing geosynthetic materials to design and construct more reliable, cost effective, and longer lasting pavements using geosynthetic products. The proposed modifications are summarized as follows:

1. Establish proper mechanisms for using geogrids, geocells, and stiff geotextiles in subgrade restraint and base reinforcement / stabilization applications. This entails adopting the Giroud and Han (2004b) design method to account for reinforcement and stabilization geosynthetics for unpaved road designs and/or designing with geosynthetics serving the subgrade restraint function. It also includes the use of bender elements to quantify local stiffness enhancements (due to geogrid-aggregate interlock) and to incorporate stiffening effects in design methods.

2. Propose improvements to the Subgrade Stability Manual (IDOT, 2005) to add minimum requirements and physical properties for geogrids and geotextiles suitable for subgrade restraint / stabilization applications.

3. Establish proper standards on stabilization, separation, and pumping resistance for geotextiles by considering the most recent research findings on geotextile clogging and permeability criteria. These standards can be used for filter fabrics, geotextile separation layers under concrete pavements, and geotextiles used for separation on top of weak and muddy subgrades.

4. Promote the use of modern geosynthetic products, such as geotextiles with enhanced (suction-driven) lateral drainage and geocells for subgrade restraint.

5. Elaborate on correct methods to construct pavements with geosynthetics and the utilization of proper quality control measures.

TABLE OF CONTENTS

LIST OF FIGURES

LIST OF TABLES

CHAPTER 1: INTRODUCTION

BACKGROUND AND MOTIVATION

Illinois Department of Transportation's (IDOT's) mechanistic-empirical (M-E) pavement design procedures have continually incorporated significant advances in material characterization, climate effects, performance prediction, and other elements of pavement design over the last few decades. However, the modernization of design and construction methods employed for foundation layers of pavements, including subgrade soils and base / subbase courses, has generally not kept up a similar pace. One important aspect where IDOT's design and construction manuals are lacking modernization is the use of geosynthetics in highway and pavement projects. IDOT has kept up with technical advancements on the use of geogrids / geotextiles with regards to applications such as retaining walls. However, employment of and specifications for geotextile and geogrid products in highway design and construction has not kept pace.

One of the objectives of this research project is to investigate proper usage of geotextiles and geogrids in pavement design and construction, to bring the most recent and up-to-date technologies and design methodologies to IDOT manuals, and to ensure proper use of geotextiles and geogrids in pavements. This will result in more economical pavement structures with reliable performance and durability. Other geosynthetic products such as geocells will be also reviewed and recommended to be brought to the practice and specifications of IDOT.

Geotextile and geogrid materials are the most used geosynthetics in transportation. They provide reinforcement or stabilization to the aggregate layer by laterally restraining the base or subbase and improving the bearing capacity of the system, decreasing wheel load stresses on the subgrade. A geogrid with good interlocking capabilities with aggregate particles through its apertures or a geotextile with good frictional capabilities can provide tensile resistance to lateral aggregate movement. The geosynthetic also increases the system bearing capacity by forcing the potential bearing surface under the wheel load to develop along alternate and longer mobilization paths.

Geotextile usage and properties have been widely investigated by researchers. Al-Qadi and Appea (2003) state that geotextiles are used between the aggregate layer (base / subbase) and subgrade and can decrease the required excavation depth on weak soil as they improve the performance of pavement sections constructed on weak soils. According to Yeo (2008), geotextiles have four main functions for use in highway design and construction: separation, reinforcement, filtration, and drainage.

Geotextiles can increase the interaction with soils to improve the shear capacity of the interface between aggregate layers and soils. Thus, geotextiles for reinforcement can improve the mechanical properties of earth structures, which allows for the use of local weak soils. According to Alungbe (2004), geotextiles perform two main mechanical functions in conventional pavement systems. First, geotextiles provide a physical separation between two layers of different natural material, while allowing the water to freely flow through the interface. Second, when geotextiles are in tension, they

generate tensile resistance to the soils near the interface, allowing the stresses in the base to redistribute more efficiently through the layer, increasing the load-bearing capacity.

Similarly, properties and uses of geogrids have been widely investigated by researchers. Geogrids are an attractive highway product due to their unique characteristics, and common experience indicates that pavement performance can be enhanced when geogrids are used. They have been used for three main pavement applications: (1) mechanical subgrade stabilization, (2) aggregate base reinforcement / stabilization, and (3) hot-mix asphalt (HMA) overlay reinforcement (US Army Corps of Engineers, 2003). One of the most attractive characteristics of geogrids is the ability to decrease the cost for highway projects, which requires that the geogrid cost be lower than the cost savings from thickness reduction of aggregate layers for the same pavement design life. This is known as the base course reduction (BCR). If base course thickness reduction is not the main goal, i.e., the same layer thickness design is applied with and without the geogrid, then the geogrid benefit is quantified by the life extension of pavement design, commonly referred to as the traffic benefit ratio (TBR).

Due to the popularity of geogrids in pavement applications, multiple research projects were undertaken to determine the reinforcement mechanisms of geogrids in pavements. The US Army Corps of Engineers (2003) identified lateral restraint as the primary reinforcement mechanism of geogrids and indicated that lateral restraint due to geogrid reinforcement contributes to an increase in the resilient modulus of the stabilized material. Three main reinforcement mechanisms have been identified by Perkins and Ismeik (1997) and IDOT's *Subgrade Stability Manual* (2005). These mechanisms are lateral restraint, improved bearing capacity, and tensioned membrane effect. Lateral restraint is when geogrids are used at the interface between the base / subbase layer and the subgrade. The interlock that occurs between the geogrid apertures and the base course aggregates as well as the frictional / shear interaction reduce the tensile strain that occurs on the layer interface due to traffic loading. Then, shear load is transferred from the base layer into the geogrid, and due to the high shear resistance of the geogrid and the aggregate-aperture interlock, the shear strains and lateral displacements are greatly reduced. Improved bearing capacity consists of a change in the potential failure surface that would initially extend into the soft subgrade into a failure surface that would extend only into the upper layer, which would have a greater mobilized shear resistance. The tensioned membrane effect is when a considerable amount of rutting occurs in the subgrade and the base course. This creates tension in the geogrid and, in turn, improves the vertical stress distribution, as tensile forces in the deflected geosynthetic (such as tensioned membrane) help to support traffic loading. Figure 1 presents a summary of these three mechanisms.

The efficiency of using geogrids / geotextiles for stabilization of weak soil layers or for reinforcing unbound aggregate layers has been studied extensively (Al-Qadi & Appea, 2003; Al-Qadi et al., 2009; Chen & Farsakh, 2012). Geogrids can be used to improve field performance, measured by lower rutting and rutting rate. For the purpose of stabilization, the geogrids can be applied at the interfaces between the subgrade and the base layer or the interface between the HMA layer and the base layer. Another use for geogrids is reinforcement of the unbound aggregate layers to provide lateral restraint to aggregate particles, thus improving the bearing capacity and minimizing rutting in the granular layer, eventually to be used for base / subbase layer thickness optimization. According to Al-Qadi et al. (2009), for aggregate base layers with thicknesses of 203–457 mm (8–18 in.), the optimal

position of the geogrid was determined to be at the interface of the unbound aggregate-subgrade boundary. For thicker base layers, the optimum location is at the top one-third of the base layer, and one more layer may be added at the interface with the subgrade for stability purposes.

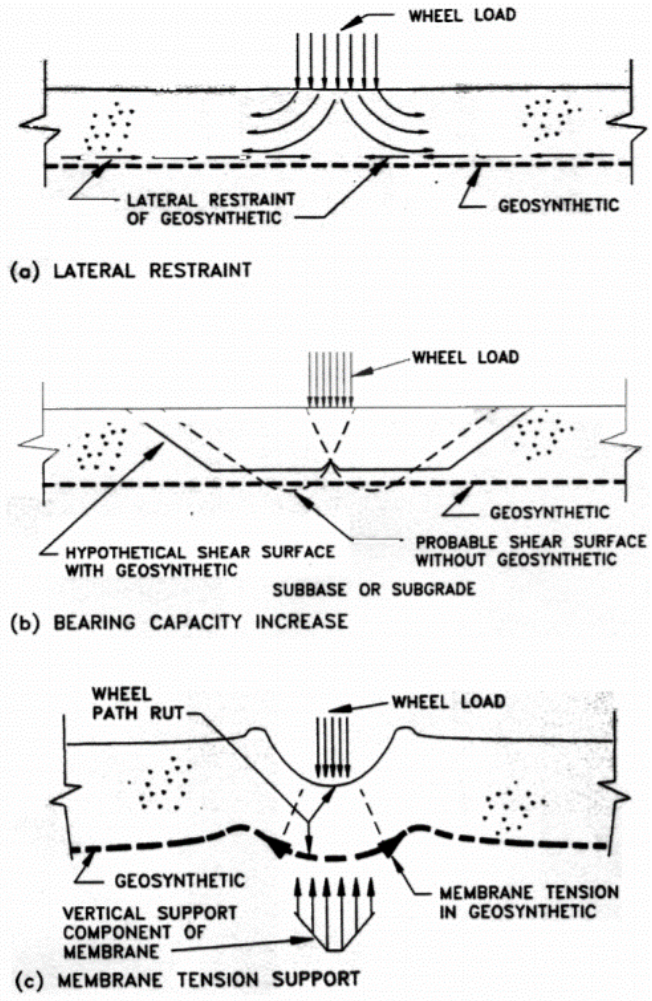

Figure 1. Illustration. Reinforcement mechanisms of geogrids and stiff geotextiles.

Source: IDOT (2005)

Figure 2 presents basic functions of geotextiles and geogrids when used in pavements. Accordingly, geogrids are primarily associated with the reinforcement function and geotextiles with separation and filtration. Geogrids have been shown to perform as interlocking elements with unbound aggregate particles to minimize lateral movement and increase layer stiffness (Kwon & Tutumluer, 2009). Subgrade restraint design is the use of a geosynthetic placed at the subgrade / subbase or subgrade / base interface to increase the bearing capacity or the support of construction equipment over a weak or soft subgrade (for cases with a California Bearing Ratio [CBR] of less than 3%). When placed in a granular base course, geogrids can restrain the lateral spreading of the granular base layer, and through interlocking between geogrid and aggregates, may develop a relatively “stiffer” layer surrounding the geogrid (Kwon & Tutumluer, 2009). Granular “base reinforcement /

stabilization" of geogrids could be crucial to ensuring their successful and beneficial application in low- to moderate-volume roads having thin HMA surfaces and CBRs between 3% to 8%. In addition to potentially reducing shear deformation in aggregates, the control of aggregate movement, especially in the upper part of the layer adjacent to the HMA, may also reduce HMA fatigue (Al-Qadi et al., 2009). Hence, a geogrid interlayer system can typically reduce the overall thickness of a pavement system for a target design life or extend the design life of the pavement.

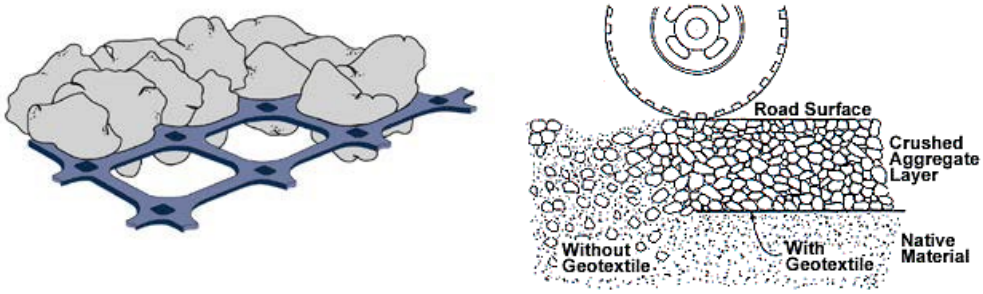

Geogrids (and Geocells)	**Geotextiles**
• Reinforcement / Stabilization	• Separation
• Interlock	• Filtration
• Confinement	• Drainage
• Separation	• Reinforcement / Stabilization

Figure 2. Illustration. Functions of geogrids and geotextiles listed in order of effectiveness.

OBJECTIVE AND SCOPE

The objective of this research project was to evaluate geosynthetics use in pavement foundation layers and their effects on design methods, particularly focusing on the use of geogrids and geotextiles. The research provided recommendations to modernize the beneficial uses of geosynthetics (mainly to account for modern geotextile and geogrid products) as they relate to highway design and construction in the State of Illinois. Modern and up-to-date methods and uses for these products in subgrades, subbases, and bases, as well as their potential benefits for the overall design and long-term performance of pavements were evaluated.

To achieve the overall objective of this project, the following tasks were conducted:

- Task 1—Review and evaluate current geosynthetics use in Illinois and practice of IDOT.
- Task 2—Review and evaluate previous research and state of the practice on geosynthetics usage, designs, and specifications.
- Task 3—Recommend revisions and draft design guides to modernize IDOT practices and manuals for effective solutions with modern geosynthetics in pavement applications.

REPORT ORGANIZATION

This report consists of five chapters, including this introductory chapter.

Chapter 2, titled "Review of IDOT's Current Geosynthetics Use and Practice," provides details for the geosynthetic materials currently used by IDOT, as well as their applications, minimum required specifications, selection criteria, and construction procedures. This chapter reviews a total of six IDOT manuals and specifications that describe geosynthetic materials and specifications related to their use, including the *Subgrade Stability Manual* (2005), *Geotechnical Manual* (2020), and the *Standard Specifications for Road and Bridge Construction* (*Standard Specifications*) (2016), among others. Special provisions related to some application of geosynthetic materials in specific IDOT projects are reviewed. The chapter also identifies the knowledge gaps and potential areas where IDOT practice related to the use of geosynthetics is lagging and requires improvement.

Chapter 3, titled "Review of Current State of the Practice of Geosynthetics Use in Roads," summarizes the state of the practice and state-of-the-art methods for geosynthetic design and evaluation, to bring these into the practice of IDOT. The chapter provides details on the up-to-date knowledge related to modern geosynthetic materials; the design methods used to account for the effects of using geogrids, geotextiles, and geocells in pavements; the relevant geosynthetic properties that should be considered for pavement design, including properties provided by the manufacturers; and the proper testing and evaluation methods to evaluate and account for geosynthetic effects in pavements. This chapter summarizes the historical design methods for geosynthetics in pavements and how these methods evolved over time to account for the right properties and effects on geosynthetics in pavements. The chapter also presents some modern geosynthetic materials and designs that can resolve pavement foundation issues related to environmental aspects, e.g., expansive soils, frost-heave effects, and moisture-related issues.

Chapter 4, titled "Recommended Modifications to IDOT Practices and Manuals," presents the efforts of the research team to propose changes to IDOT specifications and manuals that promote the adoption of the latest and most effective roadway transportation geosynthetics solutions into IDOT practices and to bring major improvements to pavement construction with geosynthetics. Specific details of the proposed changes to IDOT manual sections / pages that need to be updated are presented in this chapter. Further, this chapter presents a list of drafted design guides to promote using state-of-the-art methods for design, characterization, and evaluation of geosynthetic materials used in pavements, particularly geogrids, geotextiles, and geocells.

Chapter 5, titled "Summary and Conclusions," provides a summary of the recommendations and conclusions related to the use of geosynthetic materials to construct durable, economic, and sustainable pavements in Illinois. This chapter also discusses some recommendations for future research, such as using modern geosynthetic materials and evaluating these modern products through small-scale pilot projects and/or accelerated pavement testing.

CHAPTER 2: REVIEW OF IDOT'S CURRENT GEOSYNTHETICS USE AND PRACTICE

INTRODUCTION

This chapter presents the current practice of IDOT related to the use of geosynthetics in pavement applications. Information is collected and summarized related to the current practices / specifications of IDOT in highway pavements. IDOT specifications and manuals are reviewed, in addition to special provisions and project-related documents that involve the use of geosynthetics in pavements. Specifically, the following IDOT manuals / specifications were reviewed:

- The *Illinois Construction Manual* (2021a), issued by the Office of Highways Project Implementation, was last updated on March 31, 2021.
- The *Geotechnical Manual* (2020), issued by the Office of Highways Project Implementation—Bureau of Materials, was published on December 15, 2015, and last revised on December 4, 2020.
- The *Subgrade Stability Manual* (2005), issued by the Bureau of Bridges and Structures, was last updated on May 1, 2005.
- The *Bureau of Design and Environment Manual* (2021b), issued by the Bureau of Design and Environment, was published in September 2010 and revised in May 2021.
- The *Standard Specifications for Road and Bridge Construction* (2016), issued by the Office of Highways Project Implementation, Bureau of Design and Environment, was last updated on April 1, 2016. Note that supplemental specifications containing additions and revisions to the Standard Specifications are issued annually.
- The *Bureau of Local Roads and Streets Manual* (2018) was issued by the Bureau of Local Roads and Streets in April 2005 and underwent an intermittent revision in December 2018.

The research team reviewed these IDOT specifications and manuals as well as collected other special provisions and field applications. To cover all geosynthetics applications, the criteria used was to check all manuals for any mention of geosynthetics, or any specific products (e.g., fabrics, geotextiles, geogrids, etc.). Based on the modern geosynthetic materials available in the market and their suggested uses, the areas with knowledge gaps and those where IDOT practice is lagging will be highlighted and applications that require modernizations or adoption of new standards and techniques will be proposed.

In the following sections, IDOT's *current* use of geosynthetic materials is divided into six categories: (1) subgrade stabilization and soil reinforcement; (2) reflective crack control for pavement rehabilitation; (3) drainage-related applications—including separation and filtration; (4) erosion

control and slope stability applications; (5) retaining wall applications; and (6) other applications (e.g., membrane waterproofing, bridge deck protection, bicycle facilities, and fabric-reinforced elastomeric for concrete pavements).

GEOSYNTHETICS USE BY IDOT—GENERAL OVERVIEW

According to IDOT's *Geotechnical Manual* (2020), the past three decades witnessed rapid growth in the use of geotextiles and geocomposite materials in transportation engineering. Areas where geosynthetics are used by IDOT include road reinforcement, reinforcement in embankment and retaining wall construction, filtration and drainage, sediment erosion control, road material separation, and geocomposite drains behind walls.

The *Standard Specifications for Road and Bridge Construction* (IDOT, 2016) also addresses several application areas and geosynthetic materials, including: (1) fabric envelope for pipe underdrains; (2) geotechnical fabric for French drains; (3) geotextile fabric for ground stabilization; (4) filter fabric for use with riprap; (4) silt filter fence; (5) fabric for fabric-formed concrete revetment mats; (6) erosion control blankets; (7) geosynthetic soil reinforcement for retaining walls; and (8) geocomposite wall drain.

SUBGRADE STABILIZATION / SOIL REINFORCEMENT

Several IDOT manuals discuss using geosynthetics for subgrade stabilization and soil reinforcement applications. Geogrids and geotextiles are the two geosynthetic products listed in these manuals. The IDOT manuals and specifications that cover this application are the *Standard Specifications for Road and Bridge Construction* (2016), the *Bureau of Design and Environment Manual* (2021b), the *Subgrade Stability Manual* (2005), the *Bureau of Local Roads and Streets Manual* (2018), the *Geotechnical Manual* (2020), and the *Illinois Construction Manual* (2021a).

According to the *Subgrade Stability Manual* (IDOT, 2005), when the subgrade soil is soft or silty, the District Geotechnical Engineer (DGE) may require a geosynthetic fabric (i.e., a geotextile) to prevent intermixing of the subgrade and aggregate layers. Geosynthetics (i.e., geogrids and geotextiles) may be used for subgrade restraint and base reinforcement / stabilization. Subgrade restraint may occur when a geosynthetic is placed at the subgrade / aggregate interface to increase the support of the construction equipment over a weak subgrade and in unpaved roads. Base reinforcement or stabilization is considered for paved roads and for the purpose of long-term pavement performance (beyond the scope of the manual). Through the interlock between the grids-soil and grids-aggregate, geogrids are assumed to have higher friction and confining stresses than the smoother surface geotextiles. However, geogrids do not prevent intermixing of the subgrade and aggregate layers.

Based on analyses of geotextiles (woven and nonwoven) and geogrids, a table was added to the *Subgrade Stability Manual* (IDOT, 2005) as a guideline for preliminary aggregate thickness design when using geosynthetics for subgrade restraint. Use of geosynthetics should only be considered when the immediate bearing value (IBV) and cone index (CI) of the subgrade are 3% and 120 or less, respectively. The greatest benefits are achieved when the IBV / CI is 1.5% / 60 or less. Larger thickness reductions could be achieved for IBVs less than 1% or CIs less than 40, and the inspector

should consult the DGE for the proper thickness reduction. The aggregate cover or subgrade improvement thicknesses recommended by the *Subgrade Stability Manual* (IDOT, 2005) when a geogrid / geotextile is used are presented in Table 1.

Table 1. Guidelines for Aggregate Thickness Reduction Using Geosynthetics

IBV (%) / Cone Index	Aggregate Cover without Geosynthetics in. (mm)	Aggregate Cover with Geotextile in. (mm)	Aggregate Cover with Geogrid in. (mm)
1 / 40	22 (560)	16 (405)	15 (375)
1.5 / 60	18 (450)	12 (300)	12 (300)
2 / 80	16 (400)	12 (300)	10 (250)
3 / 120	12 (300)	12 (300)	9 (230)

Source: IDOT (2005)

Note that not all types and/or brands of geosynthetics have the same engineering properties. For this reason, IDOT currently does not have generic specifications that could be applied to all geosynthetic products used for subgrade restraint. This makes the performance and, consequently, the specifications of geosynthetics product specific. Some soils require both a geotextile for separation, to prevent intermixing of the subgrade and the aggregate, and a geogrid for subgrade restraint. This combined geotextile-geogrid option has been used but has proven to be cost prohibitive (IDOT, 2005). The DGE should be consulted for designing or specifying a geosynthetic for subgrade restraint. It has been recommended that the Central Geotechnical Unit verify the cost / benefits of using geosynthetics in new projects.

Chapter 6 of the *Geotechnical Manual* (IDOT, 2020) also emphasizes that geosynthetics should generally only be considered when IBV is 3% or less. The decision should be made based on economics. When employing a geotextile or geogrid to carry tensile stresses, it may prove beneficial to use materials with a moderate to high modulus. Further, a minimum of 6 in. of granular cover is desirable before exposure to vehicular traffic. The *Standard Specifications* indicate the minimum requirements of fabrics for ground stabilization (IDOT, 2016). If a fabric is required that is different from the *Standard Specifications* or a geogrid is required, then the construction contract documents must contain a project-specific special provision. Fabric of insufficient width or length shall be lapped or sewn. The minimum laps for lap-only areas are 600 mm (2 ft) and for sewn areas are 100 mm (4 in.). For local roads, the *Bureau of Local Roads and Streets Manual* states that the Central Bureau of Local Roads and Streets should be contacted for assistance in designing the appropriate granular thickness when geosynthetics are used (IDOT, 2018).

The *Standard Specifications* only list the criteria / specifications for fabric materials used for ground stabilization. Geogrid or other geosynthetic material properties are not clearly presented. According to the *Standard Specifications* (IDOT, 2016), the fabric for ground stabilization shall consist of woven or nonwoven filaments of polypropylene, polyester, or polyethylene. Nonwoven fabric may be needle

punched, heat-bonded, resin-bonded, or a combination thereof. The fabric shall be resistant to ultraviolet radiation and selected according to Table 2.

Table 2. Mechanical Properties of Geotextile Fabrics for Ground Stabilization

Physical Properties	Requirements
Grab Tensile Strength (lb.) ASTM D4632 (1) *	200 min.
Grab Elongation @ Break (%) ASTM D4632 (1)	12 min.
Burst Strength (psi)—ASTM D3786 (2) *	250 min.
Trapezoidal Tear Strength (lb.) ASTM D4533 (2) *	75
Weight (oz/sq yd)—ASTM D3776 *	4.0 min.

Source: IDOT (2016)

(1) For woven fabric, test results shall be referenced to orientation with warp or weave, whichever the case may be. Both woven and nonwoven fabric shall be tested wet.

(2) Test results may be obtained by manufacturer's certification.

* References: ASTM D4632 (2015a), ASTM D3786 (2018a), ASTM D4533 (2015b), ASTM D3776 (2020a)

REFLECTIVE CRACK CONTROL (PAVEMENT REHABILITATION)

Reflective crack control is a well-covered topic in IDOT's manuals and specifications. IDOT documents that discuss this application include the *Standard Specifications for Road and Bridge Construction* (2016), the *Bureau of Design and Environment Manual* (2021b), the *Bureau of Local Roads and Streets Manual* (2018), and the *Geotechnical Manual* (2020). Geosynthetics for reflective crack control are mainly used for concrete pavements overlain by HMA and for HMA pavements. The use of geosynthetic materials for crack control is covered in detail in IDOT manuals and is beyond the scope of this project.

According to the *Standard Specifications for Road and Bridge Construction* (IDOT, 2016), the following materials have been developed for the control of reflective cracking in HMA overlays. For each system, the standard specification lists the minimum requirements and specifications for the fabric (geotextile) materials to be coated with bitumen for crack control.

- System A is a nonwoven reinforcing fabric placed on a hot applied liquid asphalt binder over the prepared pavement surface.
- System B is a prefabricated waterproofing membrane interlayered with woven or nonwoven reinforcing fabric embedded in a layer of self-adhesive plasticized bitumen.
- System D is a composite three-layer system composed of a low-strength, nonwoven, geotextile bottom layer; a viscoelastic membrane middle layer; and a high-strength, woven geotextile top layer.

GEOTEXTILE / GEOCOMPOSITE USE FOR DRAINAGE-RELATED APPLICATIONS

Drainage-related application for geosynthetics (mostly geotextiles) is a popular topic among IDOT manuals. The specifications and manuals that discuss this application include IDOT's *Standard Specifications for Road and Bridge Construction* (2016), *Bureau of Design and Environment Manual* (2021b), *Bureau of Local Roads and Streets Manual* (2018), *Geotechnical Manual* (2020), and *Illinois Construction Manual* (2021a). Applications that use geotextiles for drainage-related purposes discussed in IDOT manuals include (1) slope drains, (2) pipe underdrains, (3) filter fabrics for multiple uses, (4) filter fabrics for aggregate ditches, (5) geocomposite wall drains, and (6) French drains.

Slope drains (see Figure 3) include flexible tubing or a rigid pipe, generally used in conjunction with a diversion dike or channel, to convey concentrated runoff down the face of a cut or fill slope without causing erosion on or at the base of the slope. One of the design considerations is to place slope drains on compacted soil that is covered with a Class B geotextile filter fabric (following AASHTO M 288 specifications [AASHTO, 2017] for a Class B geotextile).

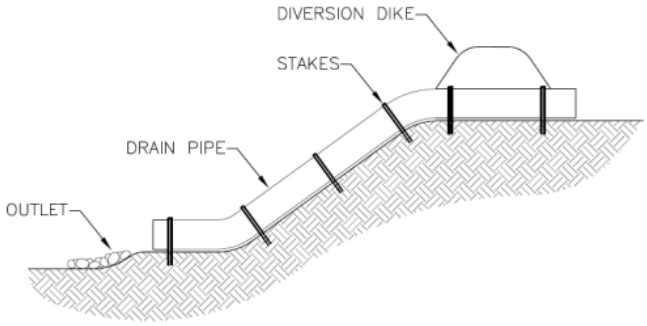

Figure 3. Illustration. Slope drain.

Source: IDOT (2021b)

For aggregate ditches, Section 283.03 of the *Standard Specifications* (IDOT, 2016) states that a stone aggregate ditch shall be constructed on filter fabric without any bedding material. For the filter fabric, the edges along the centerline of the ditch shall be turned down and buried 150 mm (6 in.), the upstream and downstream edges shall be turned down and buried 300 mm (12 in.), and securing pins at overlaps shall be inserted at each edge of the ditch bottom and at intervals no greater than 1.5 m (5 ft) extending up the slopes.

Several IDOT manuals discuss subsurface drainage design considerations using geosynthetics, particularly the *Geotechnical Manual* (2020) and the *Standard Specifications* (2016). Because it is desirable to maintain the pavement system and subgrade free of excess water, subdrains are frequently employed. In certain localized areas, drainage must be provided for seepage water entering the pavement subgrade system laterally, or from below the subgrade. Various geosynthetic products have become favorable as a substitute for conventional soil filters, as they offer excellent drainability at considerable cost savings. Geotextile filter fabric can be economically designed by methods similar to those for aggregate filters.

Section 6.17 of the *Geotechnical Manual* (IDOT, 2020) specifies using a combination of materials (e.g., granular aggregates and a geosynthetic) such that both head loss and movement of fines are avoided. The optimal or ideal particle size distribution of a granular filter material and the required properties of a geosynthetic material are dependent upon the soils being protected. Filtration systems are used for several drainage applications mentioned throughout the manual. The filter system used for any of these drainage applications should meet the following criteria:

- To avoid head loss in the filter, $D_{15\ (filter)} / D_{15\ (protected\ layer)}$ must be greater than 4, and the permeability of the filter must be adequate for the drainage system. Where:
    - $D_{15\ (filter)}$ is the diameter through which 15% of the filter material will pass by weight.
    - $D_{15\ (protected\ layer)}$ is the diameter through which 15% of the protected layer material will pass by weight.
- To avoid movement of particles from the protected layer:
    - $D_{15\ (filter)} \div D_{85\ (protected\ layer)} < 5$;
    - $D_{50\ (filter)} \div D_{50\ (protected\ layer)} < 25$; and
    - $D_{15\ (filter)} \div D_{15\ (protected\ layer)} < 20$.
- To avoid movement of the filter into the drain pipe perforation or joints:
    - $1.2 < D_{85\ (filter)} \div$ slot width < 1.4; and
    - $1.0 < D_{85\ (filter)} \div$ hole diameter < 1.2.
- To avoid segregation, the filter should contain no particle size larger than 76 mm (3 in.).
- To avoid internal movement of fines, the filter should have no more than 5% passing No. 200 (0.075 mm) sieve.

When the above criteria cannot be satisfied without using a multifilter media, the use of a suitable geosynthetic fabric can be included with a granular material. In this application, the fabric may be used to wrap the pipe in order to satisfy the opening requirements, or to line the trench so that it is protected from the movement of fines into the collector (serving drainage, separation, and filtration functions).

Section 1040.07 of the *Standard Specifications* (IDOT, 2016) details the design requirements for a geocomposite wall drain. The geocomposite shall be in direct contact with the wall and secured with concrete nails. The drainage core shall provide support to and be bonded to the geotextile at intervals not exceeding 30 mm (1 1/8 in.) in any direction and shall permit unobstructed flow through

no less than 75% of the geotextile. All seams, splices, bottom caps, top caps, and end caps shall be constructed so that backfill material cannot enter the geocomposite during or after construction.

Section 601 of the *Standard Specifications* (IDOT, 2016) provides design details for pipe underdrains and pipe underdrains in backslopes. Four designs (Types 1, 2, 3, and special) are provided for pipe underdrains, and three designs (Types 1, 2, and 3) are provided for underdrains in backslopes. Some of these designs (e.g., Type 2 pipe underdrain) involved the use of a fabric material. Fabric materials for pipe underdrains are detailed in Section 1080.01 of the *Standard Specifications* (IDOT, 2016) and are provided in Table 3. Note that the *Standard Specifications* (IDOT, 2016) reference provides several tables that list geotextile properties for underdrains, French drains, and general filter fabric requirements.

Table 3. Physical Properties of Geotextile Fabrics for Pipe Underdrains

Property	Knitted [1/]		Woven or Nonwoven	
Min. Weight (oz/sq. yd)	3.5 applied 4.8 relaxed	ASTM D3887 * ASTM D3887	3.5	ASTM D3776 *
Min. Wet Grab Tensile Strength (lb.)	–	–	100	ASTM D4632 [2/]
Grab Elongation @ Break (%)	–	–	20 min.	ASTM D4632 [2/]
Apparent Opening Size (AOS No.)	30 max.	ASTM D4751 [3/ *]	30 max. nonwoven [3/] 50 max. woven [3/]	–
Static Puncture Strength (psi)	116 min.	ASTM D6241 [3/ *]	–	–

Source: IDOT (2016)

1/ Knitted fabric shall be Type A according to ASTM D 6707 (2019a).

2/ For woven fabric, test results shall be referenced to orientation with warp or fill, whichever the case may be.

3/ Manufacturer's certification to meet test requirements.

* References: ASTM D3887 (1996), ASTM D3776 (2020a), ASTM D4632 (2015a), ASTM D4751 (2020b), ASTM D6241 (2014a).

Lastly, Section 41-3 of the *Bureau of Design and Environment Manual* (IDOT, 2021b) lists the following drainage and sedimentation applications that require the use of a geosynthetic material (geotextile):

- Sediment Traps: A small, temporary ponding area either excavated or impounded by embankments. It detains runoff for a sufficient time to allow sediment to drop out of suspension prior to discharge. For outlets consisting of a coarse aggregate and riprap section, locate the stone at the low point of the trap and extend vertically to 300 mm (1 ft) below the top of the embankment. Place coarse aggregate (CA 3) on the upstream side of outlet, separated by filter fabric from riprap (RR 3) on the downstream side of outlet.

- Pipe (Culvert) Inlet Silt Fence Barriers: A temporary permeable barrier of entrenched filter fabric used to protect a pipe inlet. A pipe (culvert) inlet silt fence barrier promotes the

deposition of sediment from sediment-laden runoff prior to discharge from the construction site.

- Drop Inlet Prefabricated Barriers: Manufactured, temporary sediment control barriers constructed of geosynthetic fabric and foam or an equivalent. Drop inlet prefabricated barriers are installed around drop inlets to intercept and pond sediment-laden runoff prior to entering the storm sewer.

- Stabilized Construction Entrance / Exits: A stabilized pad of coarse aggregate, underlain with geotextiles or a commercially available prefabricated unit designed to vibrate accumulated sediment from tires and under chassis.

- Above-grade Drop Inlet Filters: Fabric-covered, polyethylene-framed barriers that are installed over area drains. Above-grade inlet filters protect storm drains from ingress of sediment during construction activities.

EROSION CONTROL AND SLOPE STABILITY APPLICATIONS

IDOT manuals that discussed the use of geosynthetic materials in these applications include the *Standard Specifications for Road and Bridge Construction* (2016), *Bureau of Design and Environment Manual* (2021b), *Bureau of Local Roads and Streets Manual* (2018), *Geotechnical Manual* (2020), and *Illinois Construction Manual* (2021a). Erosion control measures include vegetation, mulch (weed barrier fabric), flow controls, and outlet protection controls. Note that erosion control and slope stability applications that use geosynthetics were reviewed but proposing modifications to these applications is beyond the scope of this project. A list of the applications and the manual sections that presented them are listed below:

- Embankment stability (*Geotechnical Manual*, 2020, Section 6.4.3).

- Slope mattress and gabions (*Standard Specifications for Road and Bridge Construction*, 2016, Section 284).

- Concrete revetment mat (*Standard Specifications for Road and Bridge Construction*, 2016, Section 285).

- Fabric-formed concrete revetment mat (*Standard Specifications for Road and Bridge Construction*, 2016, Section 1080.04).

- Weed barrier fabric (*Standard Specifications for Road and Bridge Construction*, 2016, Section 1081.14).

- Temporary erosion control materials (*Standard Specifications for Road and Bridge Construction*, 2016, Section 1081.15).

RETAINING WALL APPLICATIONS

Several IDOT manuals discussed the use of geosynthetic materials in retaining wall applications. These include the *Standard Specifications for Road and Bridge Construction* (2016), *Bureau of Design and Environment Manual* (2021b), *Geotechnical Manual* (2020), and *Illinois Construction Manual* (2021a). These applications will be beyond the scope of this project for proposing modifications to IDOT practice, but the following applications were found to utilize geosynthetics as part of IDOT's standard practice:

- Soldier pile retaining walls (*Standard Specifications for Road and Bridge Construction*, 2016, Section 522.08). When required, a geocomposite wall drain is installed. Wall drains shall be installed on the concrete-facing side of the lagging with the fabric side of the drain installed to face the lagging. When a concrete facing is not specified, the fabric side of the drain shall be installed to face the soil.

- Precast modular retaining wall systems (*Standard Specifications for Road and Bridge Construction*, 2016, Section 522.10). The system shall consist of precast concrete modules, select fill, joint separation material, geotextile, and a concrete or aggregate leveling pad. The rear face of all precast concrete module joints shall be covered by a geotextile filter fabric.

- Segmental concrete block retaining walls (*Standard Specifications for Road and Bridge Construction*, 2016, Section 522.12). When a fine aggregate is selected, the rear of all block joints shall be covered by a nonwoven needle-punched geotextile filter material. All fabric overlaps shall be 150 mm (6 in.) and non-sewn.

- Geotextile retaining wall (*Standard Specifications for Road and Bridge Construction*, 2016, Section 522.11 and 1080.06). Geotextile retaining walls shall consist of successive layers of geotextile fabric anchored by placing select fill retained at the face by extending the fabric over a removable form brace and re-embedding the remaining fabric back into the select fill. The geotextiles shall satisfy the requirements of Article 1080.05 (*Standard Specifications*, 2016).

OTHER APPLICATIONS

In addition to the five broad areas where geosynthetic materials are used in IDOT practice, other additional applications that specify the use of geosynthetic materials were also listed in IDOT manuals and specifications. These typically involve the use of a geotextile fabric and include the following applications:

- Membrane waterproofing for railway structures (*Standard Specifications for Road and Bridge Construction*, 2016, Section 580).

- Fabric-reinforced elastomeric for Portland cement concrete (*Standard Specifications for Road and Bridge Construction*, 2016, Section 1028). Fabric-reinforced elastomeric shall

consist of a fabric and an elastomer compound. The composite of the fabric and elastomer compound shall have a minimum tensile strength of 700 × 700 lb/in. according to ASTM D378 (2016a). The minimum elongation at ultimate tensile strength shall be 30% according to ASTM D412 (2021a). The minimum thickness of the fabric-reinforced elastomeric shall be 3.175 mm (1/8 in.).

- Special provision for cold in-place recycling with emulsified asphalt, effective as of April 1, 2012 (*Bureau of Local Roads and Streets Manual*, 2018—section LR400-5). When a paving fabric is encountered, at least 90% of the shredded fabric in the recycled material is no more than 3,200 mm^2 (5 in^2). No fabric piece shall have any dimension exceeding a length of 100 mm (4 in.).

- Bicycle facilities design guidelines (*Bureau of Local Roads and Streets Manual*, 2018, Chapter 42). For crushed aggregate surfaces, a geotextile fabric mat is used if the soil is soft or unstable.

- Bridge deck protection (*Bureau of Local Roads and Streets Manual*, 2018, Chapter 36). For precast prestressed concrete deck beams, placement of mortar fairing course and waterproofing membrane system prior to surfacing with bituminous overlay is recommended for bridge decks without deicing agents and is required for bridge decks with deicing agents.

IDOT SPECIAL PROVISIONS AND PROJECTS INVOLVING GEOSYNTHETICS

Section 6.18.2 of IDOT's *Geotechnical Manual* (2020) states that "if a geosynthetic material is recommended, and it is not referenced by the Standard Specifications, then a Special Provision must be developed." To review IDOT practices and current use of geosynthetics, several special provisions were reviewed, most of which are guide bridge special provisions (GBSP), special provisions by the Bureau of Design and Environment, or district or project-specific special provisions. For brevity and space limitations, only the names, source, and a brief description of the most relevant special provisions are listed in this section:

- GBSP #38: Mechanically Stabilized Earth Retaining Walls. This special provision was effective February 3, 1999, and revised October 5, 2015. The work listed in this special provision includes preparing the design, furnishing the materials, and constructing the mechanically stabilized earth retaining wall.

- GBSP #51: Pipe Underdrains for Structures. This special provision was effective May 17, 2000, and revised January 22, 2010. The work contains furnishing and installing a pipe underdrain system as shown in the plans. The fabric surrounding the drainage aggregate shall be geotechnical fabric for French drains according to Article 1080.05 of the *Standard Specifications* (2016).

- GBSP #77: Weep Hole Drains for Abutments, Wingwalls, Retaining Walls, and Culverts. This special provision was effective February 3, 1999, and revised October 5, 2015. If a

geocomposite wall drain according to Section 591 is not specified, a prefabricated geocomposite strip drain according to Section 1040.07 shall be placed at the back of each drain hole. The strip drain shall be 600 mm (24 in.) wide and 1.220 m (48 in.) tall. The strip drain shall be centered over the drain hole with the bottom located 300 mm (12 in.) below the bottom of the drain hole.

- Geotechnical Reinforcement—District 1 Special Provision for geogrid. This special provision was effective November 30, 2010, and revised April 10, 2014. The work consisted of furnishing and installing an integrally formed polypropylene geotechnical grid reinforcement material. Table 4 lists the geogrid requirements specified in the special provision. The supplier should provide a certification that their product meets these requirements.

Table 4. Specified Geogrid Properties

Material Characteristics	Test Method	Unit	Data
Polymer type	–	–	polypropylene
Carbon black content	ASTM D4218 *	–	0.50% (min.)
Open area	CW 02215 +	%	75 (max.)
Unit weight	ASTM D5261 *	oz/yd^2	5.0 (min.)
Junction efficiency	GRI-GG2 #	%	90 (min.)

* References: ASTM D4218 (2020c), ASTM D5261 (2018d)

+ Method was used in the United States until 1993. Equivalent opening size (EOS) of a geogrid / geotextile is determined by sieving uniform glass beads or sand of known size. Successively finer sizes are tested to find the smallest size of particles where 5% or less by mass pass through the geosynthetic, and that size is denoted as the EOS of the respective geosynthetic product.

This test method by the Geosynthetic Research Institute (GRI) was dicontinued and replaced by ASTM D7737 (2015d)

- District 3 Special Provision on Filter Fabric, Special for application in infiltration trenches and the infiltration basins. Strength properties shall be according to Class 1, as defined in Table 1 of AASHTO M 288 (AASHTO, 2017). Ultraviolet stability shall be according to Table 2 of AASHTO M 288. Permittivity and apparent opening size shall be for soils with less than 15% passing the No. 200 sieve, according to Table 2 of AASHTO M 288. Woven slit film geotextiles shall not be used. All other requirements of AASHTO M 288 shall apply.

- District 7 Special Provision on Soil Stabilization Using Cellular Confinement System. This special provision was issued as part of Contract No. 74794 for Clark County, Section 12-51 I, Route FAI 70. It involves constructing a cellular confinement system of a geocell material into which specific infill materials are to be placed (See Figure 4). The geocell shall be a perforated polyethylene sheet strip assembly, connected by a series of offset full-depth

ultrasonic seams. Items shall consist of furnishing, placing, and compacting 4" of topsoil in a manner compatible with a cellular confinement system constructed of a geocell material.

Figure 4. Photos. Soil stabilization using the cellular confinement system (District 7).

- Geofoams were utilized on Contract 60W55 in 2016. Members of the Technical Review Panel (TRP) who are familiar with this project mentioned they had not heard of any issues thus far. Figure 5 presents construction photos from this project. Another project involving geofoams in Cook County for Project No. NHPP-VQ14(255) was also reviewed. In this project, the expanded polystyrene (EPS) geofoam blocks conformed to the minimum requirements listed in Table 5. Sand layers were placed underneath the first level of EPS geofoam blocks and compacted to satisfaction.

Table 5. Min. Allowable Values of Parameters for EPS Geofoam Blocks for Project NHPP-VQ14(255)

Property	EPS40 (EPS 15)	EPS50 (EPS 19)	EPS70 (EPS22)	EPS100 (EPS29)
Minimum Density (lb/ft^2) Whole Block	1.0	1.25	1.5	2.0
Minimum Density (lb/ft^2) Individual Test Specimens	0.9	1.15	1.35	1.8
Minimum Compressive Resistance at 1% Deformation (lb/in^2)	5.80	7.20	10.15	14.50
Initial Tangent Young's Modulus (lb/in^2)	580	725	1015	1450
Minimum Flexural Strength (lb/in^2)	25	30	40	50
Minimum Oxygen Index, Volume %	24.0	24.0	24.0	24.0
Maximum Water Absorption by Total Immersion, Volume %	4.0	3.0	3.0	2.0

Figure 5. Photos. Using geofoams on IDOT's contract no. 60W55.

- Geotechnical Fabric for Pipe Underdrains and French Drains—Bureau of Design and Environment (BDE) Special Provision. This special provision was effective on November 1, 2019. It updates the physical properties of fabrics for pipe underdrains and French drains in accordance with AASHTO specifications. Knitted fabric (BDE) envelope shall be Type A according to ASTM D6707 (2019a). Woven or nonwoven fabric (BDE and Type 2) shall be Class 3 according to AASHTO M 288 (AASHTO, 2017). Woven slit film geotextiles (i.e., geotextiles made from yarns of a flat, tape-like character) shall not be permitted.

- Silt Fence, Ground Stabilization, and Riprap Filter Fabric—BDE Special Provision. This special provision was effective on November 1, 2019. It states that fabric for a silt filter fence shall consist of woven fabric meeting the requirements of AASHTO M 288 for an unsupported silt fence. The fabric for ground stabilization shall consist of woven yarns or nonwoven filaments of polyolefins or polyesters. Woven fabrics shall be Class 2 and nonwoven fabrics shall be Class 1 according to AASHTO M 288 (See Table 6). The riprap filter fabric shall consist of woven yarns or nonwoven filaments of polyolefins or polyesters. Woven fabrics shall be Class 3 for riprap gradations RR 4 and RR 5 and Class 2 for RR 6 and RR 7, according to AASHTO M 288 (AASHTO, 2017).

Table 6. Physical Properties of Fabrics for Silt Fences and Ground Stabilization

	Silt Fence Woven	Ground Stabilization Woven	Ground Stabilization Nonwoven
Grab Strength, lb (N) ASTM D4632 *	123 (550) MD 101 (450) XD	247 (1100) min.	202 (900) min.
Elongation/Grab Strain, % ASTM D4632	49 max.	49 max.	50 min.
Trapezoidal Tear Strength, lb (N) ASTM D4533 *	–	90 (400) min.	79 (350) min.
Puncture Strength, lb (N) ASTM D6241 *	–	494 (2200) min.	433 (1925) min.
Apparent Opening Size, Sieve No. (mm) ASTM D4751 *	30 (0.60) max.	40 (0.43) max.	40 (0.43) max.
Permittivity, sec-1 ASTM D4491 *		0.05 min.	
Ultraviolet Stability, % retained strength after 500 hours of exposure ASTM D4355 *	70 min.	50 min.	50 min.

* References: ASTM D4632 (2015a), ASTM D4533 (2015b), ASTM D6241 (2014a), ASTM D4751 (2020b), ASTM D4491 (2021b), ASTM D4355 (2021c).

LEARNING OUTCOMES, KNOWLEDGE GAPS, AND POTENTIAL AREAS FOR IMPROVEMENT

Based on the review of IDOT standards and specifications, the following learning outcomes, knowledge gaps, and potential areas for improvement could be identified. These gaps and areas of improvement will be further discussed in Chapter 4, after the current state of the practice and available knowledge base for geosynthetics material use in pavements is discussed in Chapter 3.

Learning outcomes from reviewing IDOT current practices related to the use of geosynthetic materials in pavements include:

- The most used geosynthetic products in IDOT practices are geotextiles and geogrids. Some specific projects reported the use of geocells for slope stability and geofoams.
- IDOT manuals often lack proper specifications / descriptions needed for using geosynthetic materials in various applications. To remedy this, some manuals and special provisions refer to standards and specifications (e.g., ASTM standards). These should be revised as some are outdated or withdrawn.

- Many areas for potential improvement in IDOT's practices exist to take advantage of beneficial uses of geosynthetics. They include applications for (1) subgrade restraint for subgrade replacement and subbase, (2) base reinforcement / stabilization, (3) drainage, (4) separation, and (5) mitigation of reflective cracking.

- Reflective cracking mitigation is well documented in IDOT manuals.

- Other pavement areas can benefit from improved specifications and consideration of recent developments in geosynthetic materials and characterization techniques.

Potential areas of improvement to modernize IDOT practices related to the use of geosynthetics to design and construct long-lasting and cost-effective pavements are listed below. These areas are kept in mind when a literature survey study is conducted for up-to-date geosynthetic products, design methods, and functions in Chapter 3.

- Collect information on and promote use of new geosynthetic materials with well-documented advantages to pavement performance.

- Better understand mechanisms and take advantage of using geogrids in subgrade restraint and base reinforcement / stabilization applications.

- Draft proper and more relevant specifications based on proven mechanisms for characterizing geogrids and geogrid-aggregate interactions.

- Areas of improvement regarding use of geotextiles:

    - Establish proper standards on separation and pumping resistance, considering criteria for clogging and permeability.

    - Consider foundation improvements (uniformity, drainability, and stability) for rigid pavements using geosynthetics. This area was covered in a recent project by the research team (R27-193-5) recommending the use of a geotextile fabric at the subgrade / subbase interface for concrete pavements constructed on top of daylighted unbound aggregate subbases up to a traffic factor of 10.0 (Qamhia & Tutumluer, 2021).

- Improve guidelines for geotextile and geogrid benefits in the *Subgrade Stability Manual* (IDOT, 2005) through an assessment of proper mechanisms provided by geogrids and geotextiles related to aggregate cover thickness reductions.

CHAPTER 3: REVIEW OF CURRENT STATE OF THE PRACTICE OF GEOSYNTHETICS USE IN ROADS

Geosynthetics have drastically changed the way roads are designed and constructed since the first use of nonwoven geotextiles in the late 1960s to successfully construct access roads at construction sites where driving trucks was otherwise impossible. The second major step in the development of the use of geosynthetics in roads was the advent of geogrids in the 1980s (Giroud, 2009). Other major steps are expected in the future, perhaps related to the development of new geosynthetics or to the growing use in roads of existing geosynthetics such as geocells.

The geosynthetics currently used in roads include geotextiles (woven and nonwoven), geogrids with different geometries, geocells, drainage geocomposites, wicking geotextiles, etc. These geosynthetics perform several functions, as discussed by Zornberg (2017a, 2017b). As a result, geosynthetics are highly beneficial to roads by providing better performance and increased service life. Alternatively, geosynthetics can be used to allow a smaller thickness of the road cross section or the use of lower quality construction materials.

Geosynthetics perform several functions to benefit from their uses in roads, which are detailed for highlighting the current state of the practice in this chapter. The geosynthetic functions performed in a road structure (i.e., excluding functions performed in geotechnical bodies associated with roads, such as slopes and embankments) include reinforcement, stabilization, stress-relief interlayer, separation, fluid barrier, drainage, and filtration. The order in the list of functions does not imply any hierarchy between functions. For the sake of clarity, mechanical functions are listed first, followed by functions related to water. Note that the stress-relief interlayer application related to mitigating reflective cracking in HMA is not discussed in this chapter as it was adequately included in IDOT's practice.

GEOSYNTHETIC APPLICATIONS IN PAVEMENT FOUNDATIONS

Subgrade Restraint or Stabilization

The objective of subgrade restraint or stabilization with geosynthetics is to increase the bearing capacity of soft subgrade soils. The identified mechanisms include vertical restraint of the subgrade and membrane effect. The vertical restraint accounts for the increased vertical confinement induced by the geosynthetics and provides a relevant contribution to subgrade stabilization. The membrane effect, in contrast, requires significant deflection of the subgrade, often in excess of 100 mm (4 in.) to be mobilized. The functions of reinforcement, stiffening, separation, and filtration are all involved. The primary function (reinforcement) is to increase the bearing capacity of subgrade soils and restrain soils against shear failure at low stress (stiffening). Note that the stiffening function is also relevant to complement stabilization of the subgrade with that of the base (Zornberg, 2017a). The development of local shear failure in the subgrade may lead to significant deflections, as illustrated in Figure 6-A and Figure 6-B, and illustrates the impact of geosynthetics in increasing the bearing capacity of subgrade soils.

The main mechanisms to take place include vertical restraint beyond the wheel path and some membrane-induced tension under the wheel path. Such subgrade restraint can decrease time-dependent rutting by minimizing vertical and shear stresses in the subgrade under the wheel path and redistributing shear and normal stresses beyond the wheel path. Note that higher deformation is required to mobilize such a mechanism. Therefore, subgrade restraint is particularly applicable for projects with subgrade California Bearing Ratio (CBR) less than 3%. Typical applications include:

- Facilitate expediency in construction of roadways over very weak subgrade.
- Reduce aggregate thickness and depth over excavation for pavement construction over weak subgrade.
- Some rutting is allowed for the initial lift in construction.
- A serious alternative to other stabilization options when thick granular backfill is required and / or subgrade soil has high gypsum or sulfate content.

Figure 6. Illustration. Use of geosynthetics in stabilization of road subgrades: (a) roadway designed without geosynthetics and (b) roadway designed with geosynthetics.

Source: Zornberg (2017a)

Unbound Aggregate Base Stabilization

The aim of unbound aggregate base / subbase stabilization using geosynthetics is to provide initial compaction. The aim is also to increase the construction-bound modulus and decrease the time- and trafficking-dependent modulus of unbound aggregate layers. Stiffening is the primary function that can lead to decreased lateral displacements within the aggregate-geosynthetics composite (Zornberg, 2017a). The identified mechanism is the development of lateral restraint through tension and shear transfer to minimize the lateral displacement of unbound aggregates. The typical placement location to facilitate constructability is at the interface between the base being stabilized and the underlying subgrade. Multiple layers of geosynthetics can be used in aggregate layers thicker than 450 mm (~18 in.).

The degradation of the base layer happens when lateral displacement of aggregate particles occurs under repeated traffic loading, and significant displacement usually happens in the lower portion of the base layer, directly below the wheel path, where tensile stresses are more prone to develop (Zornberg, 2017a). The potential lateral displacement within the base layer under a wheel load is illustrated in Figure 7-A. The base material modulus is expected to decrease due to the resulting decreased lateral stresses. The higher modulus the base material holds, the wider the distribution of vertical loads can be achieved, and, in turn, a smaller vertical stress is applied at the base-subgrade interface. The function of geosynthetics in base stabilization is illustrated in Figure 7-B. The shear stress from the base material is taken by lateral restraint and the geosynthetic in tensile stresses. Additionally, the tensile stiffness of the geosynthetic contributes to limit lateral strain development. Note that both friction and interlocking contribute to the base stabilization. Stabilization is often associated with a paved road and an aggregate base constructed over a subgrade having CBR ranging from 3 to 8 (FHWA, 2008). The main benefits of unbound aggregate base stabilization include (1) decreasing time-dependent rutting by providing an increased modulus of unbound aggregates at the time of construction and added confinement from compaction-induced geosynthetic tension and (2) minimizing degradation of the modulus of unbound aggregates over time by proper control of lateral displacements in unbound aggregates and maintaining initial confinement of unbound aggregates.

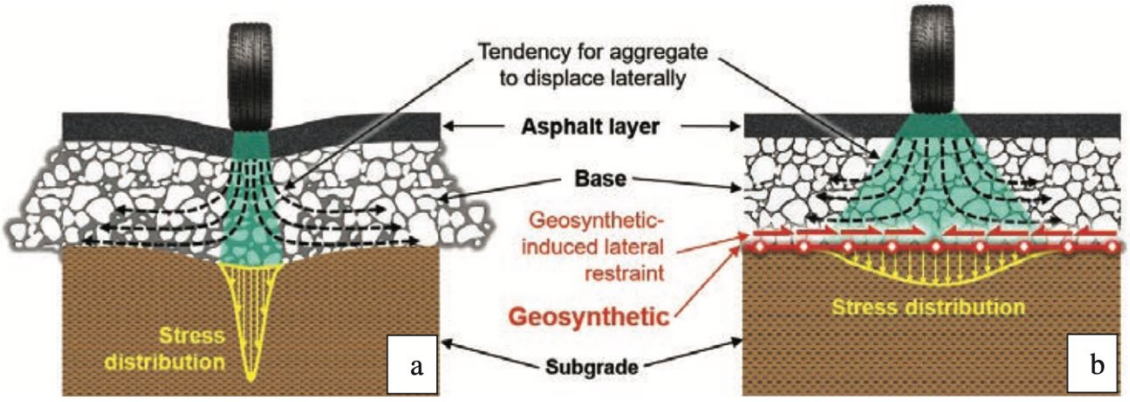

Figure 7. Illustration. Use of geosynthetics in stabilization of road base: (a) roadway designed without geosynthetics and (b) roadway designed with geosynthetics.

Source: Zornberg (2017a)

Reduction of Layer Intermixing

Reduction of pavement layer intermixing is essential for building a permanent road foundation. The objective is to avoid contamination of unbound aggregate layers with fine-grained subgrade soils. Identified mechanisms include (1) pumping of subgrade fine-grained soils, which causes fines to migrate from the subgrade into aggregate voids and migration results from pore water pressures generated in the subgrade, and (2) intrusion of base aggregates through localized penetration of individual aggregate particles into the subgrade and induced by local bearing capacity type failure mechanisms. Separation is the primary function, and filtration is also considered a secondary effect when designing a proper separation geosynthetic, commonly a geotextile fabric. The use of geosynthetics in separation and reduction of layer intermixing is illustrated in Figure 8. The benefits in

pavement performance include maintaining the as-designed structural capacity by minimizing / eliminating time- and serviceability-related decrease in base / ballast or subbase / subballast layer thickness and reducing the quality of aggregate materials.

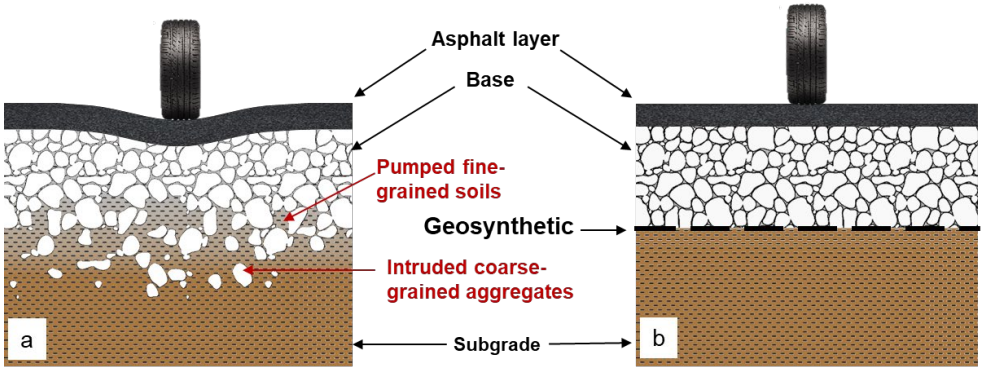

Figure 8. Illustration. Use of geosynthetics in separation and reduction of layer intermixing: (a) roadway designed without geosynthetics and (b) roadway designed with geosynthetics.

Source: Zornberg (2017a)

Reduction of Moisture in Structural Layers

In the case of properly draining or reducing moisture in unbound and bound structural layers, the objective is to provide in-plane drainage to minimize access and accumulation of moisture within structural layers. Identified mechanisms include conventional (gravity-driven) lateral drainage and enhanced (suction-driven) lateral drainage (Zornberg, 2017b). The conventional gravity-driven case involves in-plane flow that occurs under saturated soil conditions along the soil-geotextile interface. In the case of nonwoven geotextiles, this happens through large void spaces within their open structure. For woven geotextiles, drainage takes place through void spaces between crossed-over yarns. Gravity-driven lateral drainage does not allow flow that would decrease moisture stored within soil pores under unsaturated conditions. Whereas, in the case of enhanced (suction-driven) lateral drainage, in-plane flow occurs due to capillarity and allows a decrease of soil moisture stored within the soil pores under unsaturated conditions. Drainage is the main geosynthetic function, and separation and filtration both have secondary effects in the design of moisture reduction application. The use of geosynthetics to reduce moisture in pavement layers by providing improved internal drainage is illustrated in Figure 9. The benefits in pavement performance include avoiding or minimizing generation of positive pore water pressures (due to traffic loading in near-saturated layers), and as a result, reducing the increase of moisture content in unsaturated layers (to maintain adequate modulus and shear strength over time).

Mitigation of Distress Induced by Shrink / Swell Subgrades

High-plasticity clays often are associated with expansive behavior upon moisture content increase and inundation. This phenomenon is also known as high shrink / swell (volume change) behavior of such soils upon drying and wetting. A similar excess moisture-related volume increase also happens in frost-susceptible silty soils when a freezing front in winter penetrates pavement foundation layers and causes continuous ice lens formation due to suction-driven vertical upward movement of

capillary water from the groundwater table. To mitigate potential distress induced to pavements due to high shrink / swell subgrades, geosynthetics can be used to retard or eliminate environmental longitudinal pavement cracks induced by volume changes due to expansive or frost-susceptible subgrade soils. Identified mechanisms include (1) maintaining uniformity and integrity of the unbound aggregate layer to minimize stress concentration by developing lateral restraint through tension and shear transfer to minimize lateral displacement of unbound aggregates, as well as adding ductility to unbound aggregate layers and minimize stress concentrations; (2) controlling moisture distribution on top of the subgrade to maintain integrity of unbound aggregates; and (3) minimizing access of moisture to subgrade soils (Zornberg & Tutumluer, 2020). Stiffening is the main geosynthetic function for unbound aggregate stabilization in the design of distress mitigation induced by high shrink / swell subgrades. The benefits in pavement performance include maintaining integrity of asphalt surface course and reducing or eliminating degradation mechanisms, such as environmental longitudinal cracks along roadways, which are triggered by water content fluctuations and frost action in the subgrade.

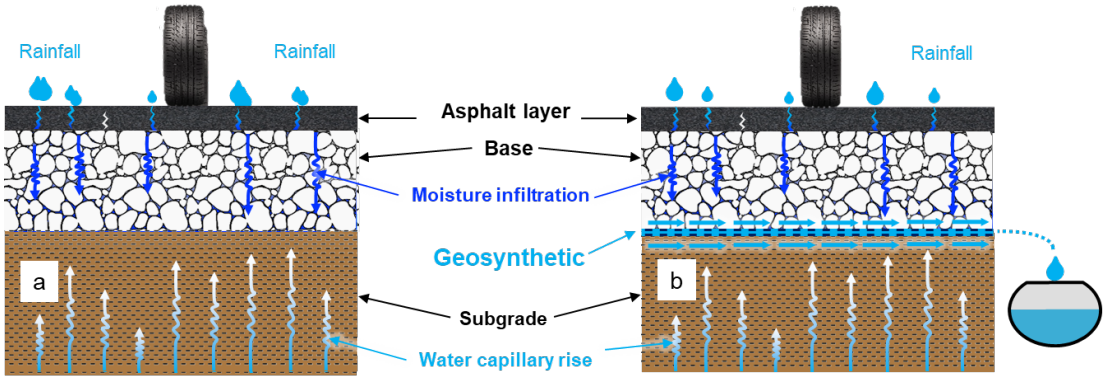

Figure 9. Illustration. Use of geosynthetics in improved internal drainage: (a) roadway designed without geosynthetics and (b) roadway designed with geosynthetics.

Source: Zornberg (2017b)

DESIGN METHODS FOR UNPAVED ROADS

Geotextiles and geogrids have been used for over four decades and are proven effective in facilitating the construction and improvement of unpaved, low-volume road performance on weak subgrades. The inclusion of geosynthetics in the design of unpaved roads can help reduce rutting caused by bearing capacity failure of the base or subgrade layer and the lateral movement of base course or subgrade material. In terms of the unbound aggregate base, the application of geosynthetics can improve the wheel load distribution and provide lateral restraint of the base course material. For the subgrade, the reduced wheel load impact can bring about better soil resilient modulus and provide vertical restraint. Meanwhile, the potential tensioned membrane effect can facilitate load transfer. The separation between the base and subgrade can prevent the intermixing of base aggregate particles and soft, fine-grained subgrade soil. As such, the geosynthetic increases the load-bearing capacity, creates an effective shear layer at the base-subgrade interface, and reduces / retards rut accumulation with traffic loads.

Geosynthetics can impart tensile stiffness at the bottom of the base and create a shear layer through several mechanisms: a) interface friction between a geosynthetic and base material; b) confinement of the base material by a geosynthetic; and c) the tensioned membrane effect (only when significant ruts occur). The existence of interface friction and confinement depends on both the geosynthetics and the soil. Interface friction will occur when a geotextile or the flat ribs of some types of geogrids (woven and welded geogrids) are used. In the case of stretched geogrids, the ribs are narrow. No significant friction with the aggregate is presented, and interlocking is the only mode of interaction. In the case of welded and woven geogrids, the ribs are wide. There are both friction and interlocking mechanisms between geogrids and aggregates. Note that interlocking works only with a coarse granular material, and interlocking is the key mechanism in geogrid-stabilized unpaved roads. The size and shape of geogrid aperture as well as the shape, stiffness, and junction of ribs all govern interlocking.

With the application of geotextiles and geogrids, more traffic is usually allowed given the same aggregate layer thickness, or a smaller aggregate layer thickness is required under the same traffic condition compared to when no geotextile is used. Many approaches in designing pavements with geosynthetics particularly involve geotextiles and geogrids, as proposed over recent decades. Six methods will be discussed in the following section. Note that most of the design methods for unpaved roads are based on bearing capacity equations given the designs are for soft subgrade (usually with CBR less than 3) and fine-grained, wet, saturated soils, including SC, CL, CH, ML, MH, OL, OH and Pt. (See Unified Soil Classification System for more details on these soil classifications.) Some methods were originally developed for geotextiles but are extended to geogrids.

Steward et al. (1977) Method

The design method proposed by Steward et al. (1977) is based on the subgrade restraint function using geotextiles. The concept of reducing soil movement and soil strain is emphasized, and the geotextile used for confinement can restrain soils against shear failure at low stresses. The soil is expected to hold higher bearing capacity given the soil and geotextile interaction. Such restraint mechanism will predominate only for weak soils stressed to levels at which the soil would fail or rut without the inclusion of a geotextile. Subgrades with CBR values less than or equal to 2 or 3 hold economic benefits in reducing structural thickness based on the restraint mechanism, while for subgrades with CBR values higher than 2 or 3, the separation or filtration function will also be considered predominant functions. The design procedure and the limitations of the Steward et al. (1977) method are described in detail in Appendix A.

Giroud and Noiray (1981) Method

The Giroud and Noiray (1981) method was established as an improvement to the Steward et al. method to more accurately reduce the base thickness when geotextiles were used in the design. The method presented by Giroud and Noiray is also for cohesive subgrade soils and mostly applicable to roads subjected to light to medium traffic. The design procedure, assumptions, design charts, and limitations are presented in detail in Appendix A.

Dutch (CROW) Design (2002) Method

The Dutch (CROW) Design (2002) method also emphasizes the important function of geosynthetics in terms of base layer thickness reduction. The method is based on calculating the required base thickness for an unreinforced section, then determining the reduction in the layer thickness based on the type of geosynthetic reinforcement (e.g., nonwoven or woven geotextile, welded geogrid) and the strength of the subgrade. The design procedure and base thickness reduction charts are detailed in Appendix A.

Army Corps of Engineers (2003) Method

The design method employed by the US Army Technical Manual 5-818-8 (U.S. Departments of the Army and Air Force, 1995) for geotextile-reinforced low-volume unpaved roads is based on the methodology proposed by Steward et al. (1977), which considers the reinforcement function of geotextile in increasing load-bearing capacity of subgrade. Tingle and Webster (2003) studied the US Army Corps of Engineers (USACE) approach and modified the criteria for the addition of stiff biaxial geogrid. Historical data were reviewed from a full-scale test section constructed in 1995 under controlled conditions and trafficked with military vehicles. The results of the full-scale test were used for comparison with the design method by the US Army Technical Manual 5-818-8. The aggregate thickness and subgrade strength of each test item were used to back-calculate the experimental values of the bearing capacity factor, N_c, which are presented in Table 7. Tingle and Webster (2003) recommended the N_c of 5.0 continue to be used until additional conclusive evidence is developed for its revision. However, for a conservative design of geotextile-reinforced unpaved roads, N_c of 3.6 should be used. N_c of 5.8 should be used for the design of unpaved roads reinforced with both a geotextile and a geogrid under soft cohesive subgrade conditions. More details on this method are presented in Appendix A.

Table 7. Theoretical and Experimental Bearing Capacity Factors

Section	Rut mm (in.)	Traffic *	Bearing Capacity Factor N_c	
			Theoretical	Experimental
Unreinforced	$< 50\ mm\ (2\ in.)$	$> 1{,}000$	2.8	2.6
Geotextile	$< 50\ mm\ (2\ in.)$	$> 1{,}000$	5.0	3.6
Geotextile and Geogrid	–	–	–	5.8

Source: Tingle & Webster (2003)

* Sections were trafficked with a M923 5-ton military truck loaded to a gross vehicle weight of 43.5 kips (194 kN).

Giroud and Han (2004) Method

A method for geosynthetic design for unpaved roads was proposed by Giroud and Han (2004a). The design method was developed for geogrid-reinforced unpaved roads, although it can also be used for geotextile-reinforced unpaved roads and unreinforced roads with appropriate values of relevant parameters. The method is based on Burmister's two-layer solution and data from cyclic plate load tests by Gabr (2001). This methodology has several improvements over the method by Giroud-Noiray (1981). These improvements, the design method, design charts, design equations, and the limitations of this method are presented in Appendix A.

Currently, this is the most used methodology for the design of geosynthetic-reinforced unpaved roads. A single expression is developed that determines the required base course thickness shown in Figure 10.

$$h = \frac{0.868 + (0.661 - 1.006J^2)\left(\frac{r}{h}\right)^{1.5} logN}{1 + 0.204[R_E - 1]}\left[\sqrt{\frac{\frac{P}{\pi r^2}}{\left(\frac{s}{f_s}\right)\left[1 - 0.9exp\left(-\left(\frac{r}{h}\right)^2\right)\right]N_c \cdot f_c \cdot CBR_{sg}}} - 1\right]r$$

Figure 10. Equation. Thickness design equation by Giroud & Han (2004b).

where *h* is the base course thickness (m); R_E is limited modulus ratio of base course to subgrade soil; *r* is equivalent radius for the contact area of the tire (m); *P* is wheel load (kN); *J* is aperture stability modulus of the geogrid; f_s is rut depth factor (often assumed 75 mm); f_c is factor relating CBR of subgrade to equivalent undrained cohesion (equal to 30 kPa); *s* is allowable rut depth (mm); *N* is number of equivalent standard (80-kN or 18-kip) axle passes; N_c is bearing capacity factor (5.71 for geogrid reinforcement, 5.14 for geotextile reinforced, and 3.14 for unreinforced); and CBR_{sg} is the California Bearing Ratio of the subgrade soil.

Illinois Department of Transportation *Subgrade Stability Manual* (2005)

According to IDOT, remedial procedures are required for any subgrade with immediate bearing value (IBV), less than 6. In the current IDOT *Subgrade Stability Manual* (*SSM*) (2005), when a geosynthetic is placed at the subgrade / aggregate interface, subgrade restraint may occur to increase the support. The guidelines for the preliminary aggregate thickness design when using geosynthetics for subgrade restraint are recommended by IDOT as presented in Table 1. The geosynthetics should only be considered when the subgrade is very weak (with an IBV / CI smaller than 3 / 120); the greatest benefits can be achieved when the IBV / CI is 1.5 / 60 or smaller. More details about this method are presented in Appendix A.

FHWA NHI-07-092 Manual (Holtz et al., 2008)

The FHWA NHI-07-092 Manual (Holtz et al., 2008) adopted the method proposed by Giroud and Han (2004a, 2004b). The design procedure requires the following steps: (1) determine soil subgrade strength; (2) determine the maximum single-, dual-, and dual-tandem wheel loads; (3) estimate the maximum amount of traffic anticipated for each design vehicle class; (4) select allowable rut depth depending on the road use, and calculate the radius of the equivalent rut depth; (5) check the capacity of subgrade soil to support wheel load without reinforcement; and finally (6) determine the required base course thickness for reinforced or unreinforced roads using the equation presented in Figure 10. More details on the procedure and the detailed equations are presented in Appendix A.

DESIGN METHODS FOR PAVED ROADS

There is a difference between unpaved and paved roads regarding the mechanisms of road improvement. Among the mechanisms involving geosynthetics that improve the performance or the service life of an unpaved road from a mechanical standpoint, only the lateral restraint of the base

material and the resulting load distribution improvement play a significant role in the improved performance and/or increased service life of a paved road. Both mechanisms are related to the same stiffening and stabilization function of the unbound aggregate layer.

Based on the foregoing discussion of relevant mechanisms, the design methods for paved roads incorporating geosynthetics are focused on the structural improvements that geosynthetic stabilization provides to the pavement layers. The state of the practice consists of using the traditional empirical methods (such as the US Army Corps of Engineers and AASHTO methods) with factors that account for the beneficial effect of geosynthetics on the associated layers. At the same time, mechanistic-empirical design methods that account for the beneficial effect of geosynthetics are being developed.

US Army Corps of Engineers (2003)

The USACE developed a methodology for aggregate-surface reinforced pavement design and flexible pavement design (US Army Corps of Engineers, 2003). This methodology was based on empirical data obtained from full-scale pavement sections tested at the US Army Engineer Research and Development Center. The procedure for flexible pavement design consists of determining the load-bearing capacity of the subgrade and the wheel load of the heaviest vehicle expected. Once these two design inputs have been chosen, the required aggregate thickness is determined from different charts depending on axle load configuration by using the subgrade shear strength multiplied by a factor corresponding to the type of geosynthetic and the expected wheel load. The main application for subgrades with CBR < 0.5 is subgrade stabilization, while the applications are subgrade stabilization and base reinforcement for subgrades with 0.5 < CBR ≤ 4.0 and base reinforcement for subgrades with CBR > 4.0. Just as in the aggregate-surface design, the shear strength of each pavement layer is determined. Next, the expected traffic load and number of passes are chosen as the design index (DI). Once this index has been determined, a minimum AC thickness is chosen as a function of this design index. Finally, by using a graph and entering the supporting layer's shear strength (C), the total thickness above the supporting layer is determined. A sample chart for determining the total thickness is presented in Figure 11.

The concept of confinement or "lateral restraint" is illustrated in USACE (2003). Lateral restraint is a unique characteristic of geogrid stabilization. The particle "strike-through" (i.e., particle presence in geogrid apertures) results in confinement of the aggregate during loading, leading to an increase in stiffness of the aggregate-geogrid composite material. This stiffness enhancement leads to an improvement of both vertical and horizontal stress distribution, resulting in a reduced maximum pressure being applied to the pavement subgrade. Through the interlock between the geogrids and aggregate, geogrids are assumed to have higher friction and confining stresses than the smoother surfaced geotextiles. This is in part due to the additional bearing resistance created in the geogrid ribs as aggregate particles provide the interlock in the geogrid apertures. When placed in a granular base course, geogrids, through interlocking, may restrain the lateral spreading of the granular base layer, thereby developing a relatively "stiffer" layer surrounding the geogrid. Interlock is therefore essential to the performance of any geogrid in mechanical stabilization.

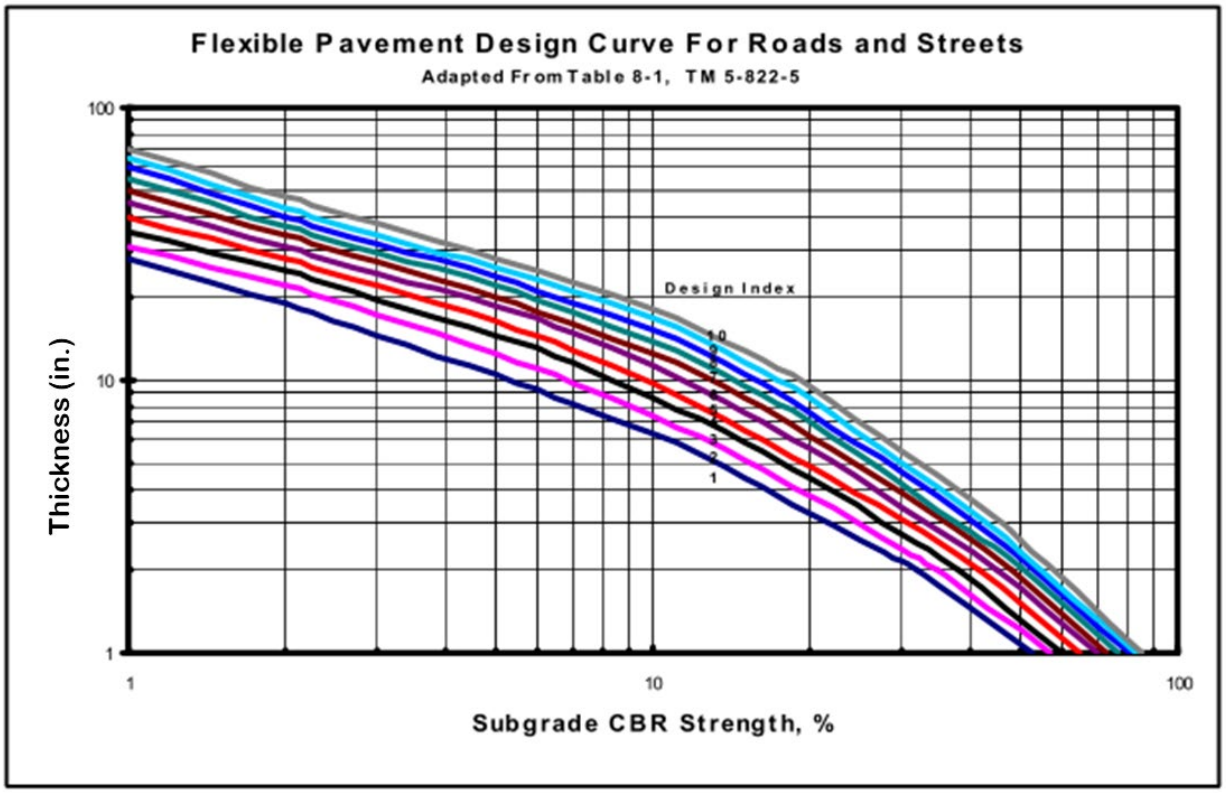

Figure 11. Plot. USACE flexible pavement thickness design curve.

Source: US Army Corps of Engineers (2003)

AASHTO Design Method

Based on the American Association of State Highway Officials (AASHO) Road Test in Ottawa, Illinois, equations were developed that related loss in serviceability, traffic, and pavement thickness. The AASHTO *Guide for Design of Pavement Structures* (1993) considers pavement performance, traffic, roadbed soil, construction materials, environment, drainage, reliability, life cycle cost, and shoulder design. The design equations have some limitations, such as limited pavement types, loads, age, and environment, because they were developed for the specific conditions of the AASHO Road Test. The empirical AASHTO design method was the predominant method for road design in the United States until 2008.

The AASHTO design equation defines a structural number (SN), which is an abstract number expressing the structural strength of a pavement required for given combinations of soil support, and total traffic in terms of 18 kip single-axle loads, terminal serviceability, and environment. The required SN should be converted to the thickness of the surface, base, and subbase layers by means of proper layer coefficients representing the relative strength of the materials. The SN is calculated using a recently modified equation for geosynthetics presented in Figure 12.

$$SN = a_1 D_1 + LCR \times a_2 D_2 m_2 + a_3 D_3 m_3$$

Figure 12. Equation. Structural number for AASHTO flexible pavement design.

Source: AASHTO (2013)

where a_i is ith layer coefficient, D_i is ith layer thickness, m_i is ith layer drainage coefficient, and *LCR* is a layer coefficient ratio. LCR is an empirical dynamic stabilization factor that varies depending on HMA layer thickness, aggregate thickness, aggregate quality, subgrade resilient modulus, moisture, traffic, and so on. The effect of mechanical stabilization using geosynthetics can be incorporated into the LCR. AASHTO (2013) provides guidance to design geosynthetic-reinforced aggregate base courses in flexible pavement structures and outlines the overall design considerations. In Section 3, AASHTO (2013) states that "Because the benefits of geosynthetic reinforced pavement structures may not be derived theoretically, test sections are necessary to obtain benefit quantification." In Section 5, the document states that the design procedure uses experimentally derived input parameters that are often geosynthetic specific and users of this document are encouraged to affirm their designs with field verification of the reinforced pavement performance. The document later states that "traffic benefit ratio (TBR) and base course reduction factor (BCR) are the parameters that need to be quantified through full-scale testing." TBR is the ratio of the number of load cycles of a reinforced pavement structure to reach a defined failure state to the number of loads for the same unreinforced section to reach the same defined failure state (see Figure 13).

$$TBR = \frac{\boldsymbol{Geogrid}\ Section\ ESALs}{\boldsymbol{Control}\ Section\ ESALs}$$

Figure 13. Equation. Traffic benefit ratio.

Source: AASHTO (2013)

BCR is the percentage of the base or subbase thickness in a reinforced pavement compared to the base or subbase thickness in an unreinforced pavement with the same material components, such that equal life cycles for a defined failure state result between the two (see Figure 14).

$$BCR = \frac{Thickness\ of\ Base\ Layer\ in\ \boldsymbol{Geogrid}\ Section}{Thickness\ of\ Base\ Layer\ in\ \boldsymbol{Control}\ Section} \times 100$$

Figure 14. Equation. Base course reduction factor.

Source: AASHTO (2013)

In conclusion, the AASHTO (2013) design method specifies the benefit of the geogrid stabilization as design values, i.e., BCR, TBR, and LCR, while it requires product-specific research from the test sections to quantify the benefit.

FHWA NHI-07-092 Manual (Holtz et al., 2008)

The FHWA NHI-07-092 (Holtz et al., 2008) design manual includes two types of procedures for the design of geogrid-reinforced base courses in flexible pavements. First, the state of the practice for the design of geogrid-reinforced base courses following AASHTO PP 46-01 guidelines (a previous version of AASHTO R50-09, 2018) was suggested with nine steps, which refer to Berg et al. (2000), as follows:

- Step 1: Perform initial assessment of geosynthetic applicability. Required assessment areas include subgrade strength, aggregate thickness required for unreinforced section, characteristic of base / subbase materials, seasonal variation in moisture levels, reinforcing mechanisms, and value added by geosynthetics.

- Step 2: Use an established method for design of unreinforced pavements. The structural layers, the type of material, and the thicknesses are determined for a pavement section without geosynthetics.

- Step 3: Investigate potential benefits of using geosynthetics reinforcement. This requires a review of available data to define potential and target benefits for the specific project. The conditions for which various geosynthetic products should be considered for this application are summarized in Figure 15.

- Step 4: Define reinforcement benefits in terms of TBR or BCR factor. This requires a review of successful applications, field studies, and lab test results.

- Step 5: Use TBR for the design of a reinforced pavement section based on the AASHTO design guide.

- Step 6: Conduct a cost-benefit analysis to evaluate the benefits. A reduction in initial construction cost or reduction in life cycle costs can be used to justify the use of geosynthetics, depending on the priorities of the user.

- Steps 7–8: Develop specifications, bid documents, and construction drawings.

- Step 9: Monitor construction and document performance.

Roadway Design Conditions		Geosynthetic Type					
		Geotextile		Geogrid [2]		GG-GT Composite	
Subgrade	Base / Subbase Thickness[1] (mm)	Nonwoven	Woven	Extruded	Knitted or Woven	Open Graded Base[3]	Well Graded Base
Soft (CBR < 3) (M_R <30 MPa)	150 – 300	❹	●	●	❑	●	⑤
	> 300	❹	❹	◗	◗	◗	⑤
Firm - Very Stiff (3 ≤ CBR ≤ 8) (30 ≤ M_R ≤ 80)	150 – 300	❍	◗	●	❑	●	⑤
	> 300	❍	❍	❍	❍	❍	❍

KEY: ● — usually applicable ◗ — applicable for some conditions
❍ — usually not applicable ❑ — insufficient information at this time ❹⑤ — see note

NOTES: 1. Total base or subbase thickness with geosynthetic reinforcement. Reinforcement may be placed at bottom of base or subbase, or within base for thicker (usually > 12 in {300 mm})) thicknesses. Thicknesses less than 6 in. (150 mm) not recommended for construction over soft subgrades. Placement of less than 6 in. (150 mm) over a geosynthetic not recommended.
2. For open graded base or thin bases over wet, fine grained subgrades, a separation geotextile should be considered with geogrid reinforcement.
3. Potential assumes base placed directly on subgrade. A subbase also may provide filtration.
❹ Reinforcement usually applicable, but typically addressed as subgrade stabilization.
⑤ Geotextile component of composite likely is not required for filtration with a well graded base course, therefore, composite reinforcement usually not applicable.

Figure 15. Illustration. Qualitative review of reinforcement application potential for paved permanent roads (after Berg et al., 2000). GG stands for geogrid, and GT stands for geotextile.

Source: Holtz et al. (2008)

The second design procedure suggested by the FHWA NHI-07-092 (Holtz et al., 2008) design manual adopts a mechanistic-empirical (M-E) method for design of pavement systems. In the original scope of the M-E design guide, geosynthetics materials have not been included but the opportunity to utilize the M-E concept to rationalize the design has been recognized by the geosynthetics community. The FHWA NHI-07-092 (Holtz et al., 2008) design manual introduced the initial research projects designed to define and quantify the benefits of geosynthetics within the M-E design framework. The numerical modeling of geosynthetic-stabilized pavements and design methods with an M-E design framework are described in the following sections.

Numerical Modeling of Geosynthetic-stabilized Flexible Pavements

The structural performance of a layered pavement system is usually improved by including geogrids and high-strength geotextiles as base and subbase stabilization geosynthetics. For mechanistic pavement analysis, finite element method (FEM) and discrete element method (DEM) tools are commonly used for the characterization and analysis of geosynthetic-aggregate interactions and stabilization effects.

Finite Element Method—Geosynthetic-stabilized Pavement Analysis

FEM approaches analyze geosynthetic-stabilized flexible pavements as soil-fabric-aggregate systems. Perkins (2001) used the ABAQUS™ contact model for modeling geogrid interface behavior and

reported that the predicted pavement responses obtained from 3D analyses were affected considerably by the elastic slip input of the Coulomb contact friction model. Eiksund et al. (2002) developed a 2D axisymmetric model for geogrid-stabilized flexible pavements using the ABAQUS™ program. The Coulomb interface friction contact was used to model the soil / aggregate–geosynthetic interface. Kwon et al. (2005) developed a 2D axisymmetric model based on a GT-PAVE finite element program for analyzing geogrid-stabilized flexible pavements. For continuum layers such as HMA, base / subbase, and subgrade, eight-noded axisymmetric solid elements were used in the FEM analysis. For the geosynthetic, three-noded axisymmetric membrane elements were used to simulate the geosynthetic inclusion. The membrane elements take only tension but not compression in the radial and tangential directions. Moreover, the soil / aggregate–geosynthetic interface was modeled by connecting the membrane elements with neighboring continuum elements through the six-noded interface elements, as illustrated in Figure 16. Normal and shear springs placed between neighboring continuum and membrane elements provided relative movements depending upon the spring shear and normal stiffnesses. Using the model, Kwon and Tutumluer (2009) further investigated the appropriate geosynthetic property assignments including geogrid modulus, built-in residual stress, etc.

Discrete Element Method—Geosynthetic-stabilized Pavement Analysis

In contrast to FEM approaches, which model geosynthetic material as interaction between continuum elements, DEM approaches consider realistic geosynthetic geometries, such as geogrid and aggregate interlocking, when investigating the stiffening effect in the vicinity of geosynthetic. This microscale numerical simulation approach is fully capable of modeling the most realistic interaction of soil–aggregate particles, which is predominantly the interlock between geogrid and aggregate particles.

Jewell et al. (1984) identified early on the important mechanisms of soil and geogrid interactions using large shear box testing. Seven granular soils associated with a biaxial geogrid with an aperture width 17.3 mm (0.68 in.) were tested. Direct shear tests for the various soil gradations adopted indicated that the granular soil particle size and gradation compared to the geogrid aperture size had an influence on the size of the shear zone. The findings of Jewell et al. (1984) laid the foundation for understanding the fundamental mechanisms by which geogrids stabilize pavement systems by entertaining the idea of choosing the type of geogrid for the intended aggregate particle sizes and gradation.

A 3D particle flow code, the PFC3D computer program, was used for investigating aggregate and geogrid interactions and modeling confinement effects (Konietzky & Keip, 2005; McDowell et al., 2006). In DEM, multiple interacting bodies undergoing large dynamic motions can be modeled by computing their motion and the overall behavior of the assembly. The findings of DEM modeling studies covered the areas of interaction between geogrids and surrounding soil–aggregate, load transfer mechanisms, deformation, particle rearrangements, etc. The developed interlocking between particles and geogrids after unloading can be simulated as illustrated in Figure 17.

Besides the grain size distribution, aggregate shape properties, especially the flat and elongated (F&E) ratio, angularity index (AI), and surface texture (ST) index, are key indices quantified by the Enhanced

University of Illinois Aggregate Image Analyzer (E-UIAIA) (Tutumluer et al., 2000; Rao et al., 2002; Moaveni et al., 2013). Representative samples of granular materials for base course in pavements or ballast in railroad tracks are typically scanned and analyzed using the E-UIAIA to determine the values of the F&E ratio, AI, and ST index, which can be used as the essential morphological data to generate ballast particle shapes as 3D polyhedrons, i.e., individual discrete elements utilized in the ballast DEM models. These aggregate particles generated for the assembly deformation behavior DEM simulations are typically rigid individual elements to match the gradation and shape properties quantified from sieve analysis and E-UIAIA.

The DEM simulation approach developed at the University of Illinois adopts real polyhedral particles and has the capability to create actual aggregate particles as 3D polyhedron elements having the same particle size distributions and imaging quantified average shapes and angularities. This DEM approach was calibrated by the laboratory large-scale direct shear test results for ballast size aggregate application (Tutumluer et al., 2006) and has been successfully utilized to simulate complex ballast behavior, such as effects of multi-scale aggregate morphological properties, gradation, and fouling (Tutumluer et al., 2006, 2007, 2008, 2009). Ongoing research efforts at the University of Illinois successfully quantified the benefits of geogrid-stabilized ballast aggregates on the shear strength and permanent deformation behavior from large-scale triaxial testing in the laboratory. With the capability to create actual ballast aggregate particles as 3D polyhedron elements having the same particle size distributions and imaging quantified average shapes and angularities, the DEM simulations were able to capture the ballast behavior with and without geogrids reasonably accurately (Qian et al., 2013, 2018).

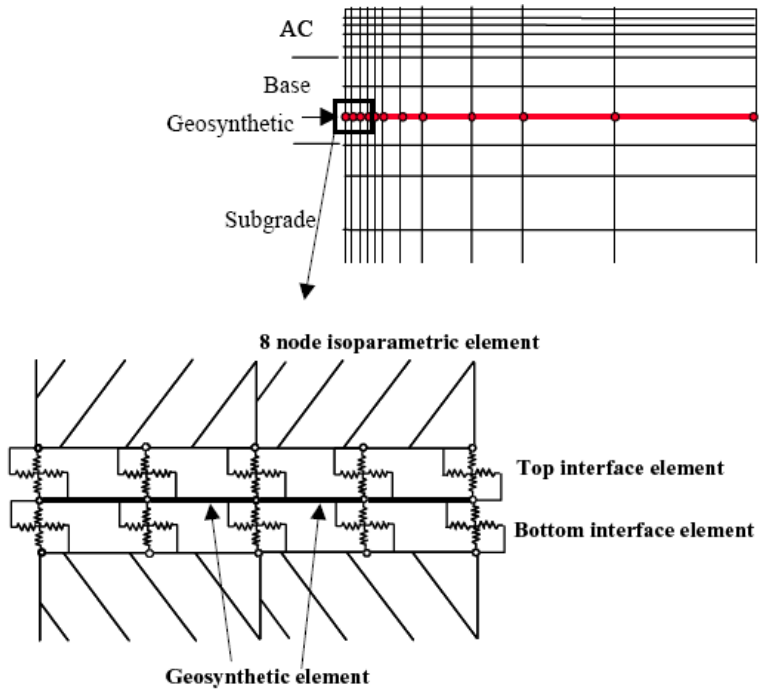

Figure 16. Illustration. Finite element formulation for the axisymmetric mechanistic model of soil / aggregate–geosynthetic interaction.

Source: Kwon et al. (2005)

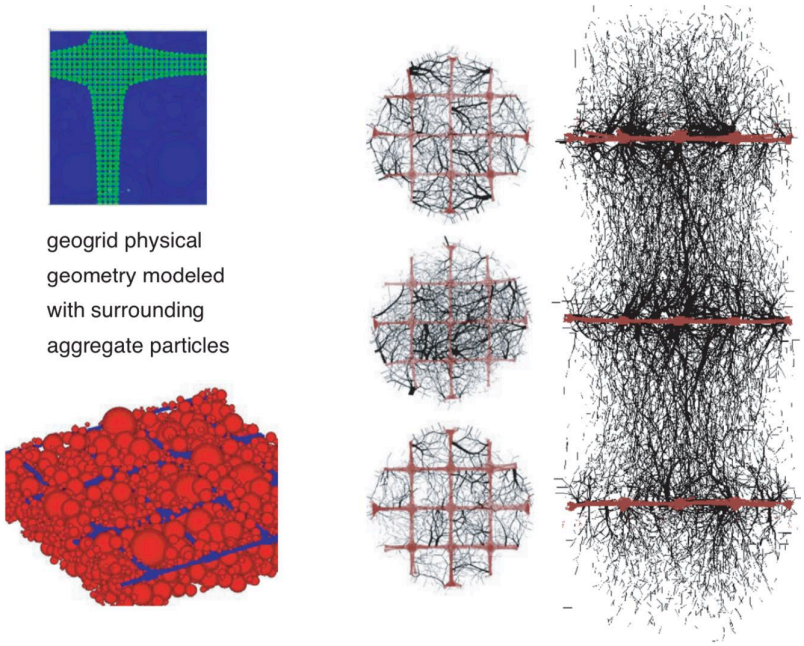

Figure 17. Illustration. Contact force distributions in geogrid-reinforced soil particles after partial horizontal and vertical unloading conditions.

Source: McDowell et al. (2006)

Mechanistic-Empirical Design Approach

Two important components of the *Mechanistic-Empirical Pavement Design Guide* (*MEPDG*) or AASHTO's current pavement M-E method are a mechanistic model to calculate the critical responses of the system, and empirical performance or damage models that relate the critical responses to the accumulated damage and distress levels (AASHTO, 2008).

To develop mechanistic-based design approaches that incorporate the effect of geogrid enhancement of the pavement base or subbase course, several studies have been performed or are in progress. Perkins et al. (2004) developed a mechanistic model that consisted of a compaction module and three subsequent trafficking response modules to describe the effect of geogrid reinforcement during the initial construction operations and in-service traffic loading. The combined use of an empirical damage model for the permanent deformation accumulation of the unbound aggregate layer within a zone influenced by the geogrid reinforcement and finite element response models to account for the effect of increasing lateral confinement with increasing traffic load repetitions showed the benefit of geogrid reinforcement (Perkins & Svano, 2004).

Another mechanistic response model was developed by a research team at the University of Illinois that accounts for the confinement effects in geogrid-reinforced flexible pavements (Kwon et al., 2005, 2007; Al-Qadi et al., 2008). The effects of interlock between the aggregate and geogrid were simulated by considering locked-in horizontal residual stresses in the granular base as initial stresses in the pavement response analysis. This method considered nonlinear stress dependency of the aggregate base and subgrade soil, residual stresses from compaction, and isotropic and anisotropic

behavior of the aggregate base. A stiffening effect above and below the geogrid reinforcement was observed with an increased confinement, and the predicted modulus values increased significantly around the geogrid. Figure 18 shows the software and the mechanism based on the mechanistic model developed at UIUC using FEM.

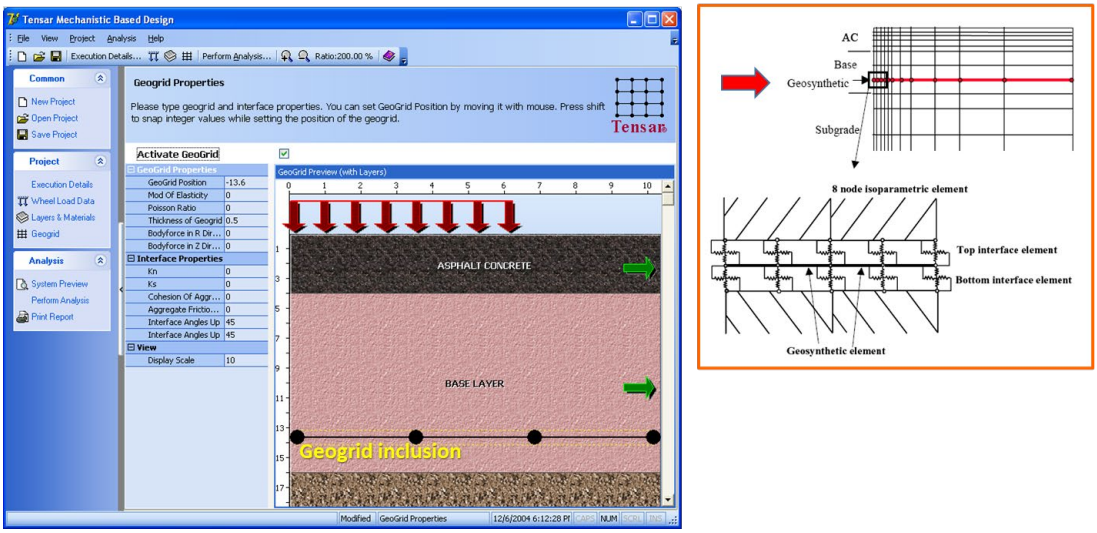

Figure 18. Illustration. Axisymmetric FEM software based on the mechanistic model for geogrid-stabilized pavement.

Source: Kwon et al. (2009)

Attempts were made to validate the UIUC mechanistic finite element model results using pavement responses to accelerated loading from full-scale pavement testing (Al-Qadi et al., 2006, 2007, 2008). Testing conducted at the University of Illinois focused on evaluating the effectiveness of geogrids on the response and performance of low-volume flexible pavements constructed on low-strength subgrade (i.e., CBR = 4%). Nine instrumented pavement sections were designed and constructed to measure pavement responses and monitor pavement performance. All pavement sections consisted of an HMA layer underlain by an unbound aggregate base sitting on a compacted / prepared subgrade. These pavement sections were heavily instrumented with pressure cells, linear variable differential transformers, and strain gauges to measure the pavement response to moving wheel load during testing, as well as with thermocouples, time domain reflectometer, and piezometers to capture environmental changes during testing. The variables considered in the study included HMA and granular base layer thickness as well as the type and location of geogrid within the granular base course. Most of the base-stabilized sections had the geogrid placed at the base-subgrade interface, except for the thicker sections (457 mm or 18 in. aggregate base layer thickness), which also had geogrid layers placed in the upper portions of the base layer.

Testing was conducted using the mobile Accelerated Transportation Loading System for response and trafficking data collection in the UIUC Advanced Transportation Research and Engineering Laboratory. In general, analyses of measured responses indicated that the no-geogrid control sections had higher tensile strains measured at the bottom of the HMA, higher vertical pressure and resilient deformation at the top of the subgrade, and significantly greater lateral deformations in the aggregate base layer,

especially in the direction of traffic, compared to the sections with geogrid-stabilized base. This observation was further validated by the measured surface rutting. The aggregate-geogrid interlock reduced both lateral strain in the aggregate layer and vertical deformation of the pavement surface. At the end of trafficking, the control sections without a geogrid exhibited more pronounced pavement distresses, including greater surface rutting due to subgrade shear failure as well as aggregate lateral movement.

Dynamic cone penetrometer (DCP) tests were conducted along non-trafficked areas on each section immediately after testing to estimate thicknesses and the in situ bearing capacities of the base and subgrade materials. The number of DCP blows needed to penetrate through the base into the subgrade were quantified in non-trafficked pavement test section locations (Kwon & Tutumluer, 2009). The higher number of blows required in the sections with a geogrid-stabilized base showed the stronger behavior of the stabilized base compared to the base with no geogrid. In addition, the DCP results indicated a nonuniform "modulus" throughout the base layer, as well as intermixing of the base aggregate and weak subgrade soils, which was observed after section excavation (Kwon & Tutumluer, 2009).

The UIUC mechanistic model validation efforts involved comparing the outcome of the FEM model to the field data obtained from the full-scale tests. The aggregate-geogrid interlock mechanism from the DEM findings was linked to the continuum analysis technique to improve the finite element-based analysis methodology. It was evident that, when base course anisotropy and compaction-induced residual stresses were considered in the analyses, the main trends in response behavior were in better agreement with that measured in the field. In this finite element modeling approach, an increase in horizontal confinement due to residual stresses can result in significant increases in the moduli of the base and subgrade layers in the vicinity of the geogrid reinforcement. The benefits of including geogrids in the pavement system could be successfully modeled by considering residual stress concentrations assigned in the geogrid-aggregate vicinity. Such residual stresses assigned in the vicinity of the geogrid considerably increased the resilient moduli predicted in the base and subgrade of the modeled pavement section. This resulted in lower vertical pressure on the subgrade, less vertical deflection at the top of the subgrade, and lower aggregate longitudinal deformation in the geogrid base-stabilized sections. Furthermore, the predictions were in good agreement with the measured responses from the full-scale tests (Kwon et al., 2009).

To develop a methodology for quantifying the influence of geosynthetics on pavement performance for use in pavement design and analysis, Luo et al. (2017) developed a computer subroutine for incorporation into the pavement M-E design software to predict pavement performance with geosynthetics. The model required the input of the material properties of the unreinforced, unbound base course, the selected geosynthetics, location of the geosynthetics, geosynthetic sheet stiffness measured at low strain levels (approximately 1%), and the shear interaction coefficient, which was determined by laboratory testing. The model converted the two separate sets of material properties into a composite reinforced base course material property.

Recently, Vavrik (2018) suggested a layer subdivision method to incorporate geogrids in M-E pavement design. The layer subdivision method can account for the different zones a geogrid creates

in the base course as a mechanically stabilized layer (MSL), where the most stiffening effect is seen by the highest lateral confinement near the geogrid. Figure 19 shows an example of the layer subdivision method application for the base layer enhanced with the geogrid installed at the middle of the layer. By applying higher moduli in sublayers in the zones of geogrid influence, the MSL concept can predict the effect of the geogrid enhancement.

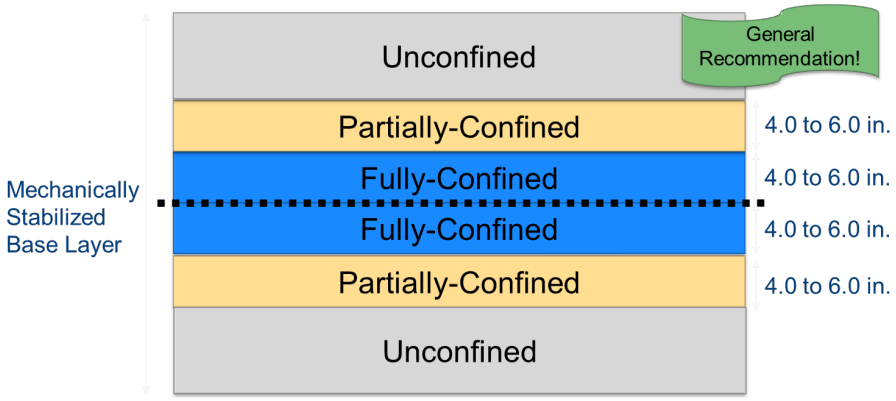

Figure 19. Illustration. Layer subdivision method for the base layer with a geogrid in the middle.

Source: Vavrik (2018)

MSLs with geogrids enhance resilient modulus, provide more uniform support for the surface course, and better control and limit long-term permanent deformation accumulation. Base course mechanical stabilization with geogrids ensures its successful and beneficial application in low- to moderate-volume roads having thin HMA surfaces and subgrade CBRs between 3% and 8%. In addition to potentially reducing shear deformation in aggregates, the control of aggregate movement, especially in the upper part of the layer adjacent to the HMA, may also reduce HMA fatigue distress. Hence, a geogrid interlayer can typically be used to reduce the overall thickness of a pavement system for a target design life or extend the design life of the pavement.

METHODS FOR TESTING GEOGRIDS AND RELEVANT GEOGRID PROPERTIES

Geogrid Property Tests in ASTM

The type of geogrid to be used for reinforcement and stabilization of pavement foundation is chosen based on physical properties and mechanical behavior. Laboratory testing for the integrity of the geogrids as well as the interaction of the geogrids and the stabilized soils are proposed and used for choosing the appropriate geogrid. Koerner (2012) lists several of the mechanical properties that govern the choice of a geogrid. Important physical properties include specific gravity, out-of-plane bending stiffness, and in-plane torsional stiffness. The density of the geogrid is a function of the polymer type from which it is manufactured. Out-of-plane bending stiffness can be determined by ASTM D1388 (2018b), which slides the geogrid on a surface inclined by 41.5 degrees and measures the length required for the geogrid to touch the surface and relates that to the mass or density of the geogrid. The mechanical properties of interest for geogrids and test method specified by ASTM are discussed in Appendix B.

Geogrid Properties Reported by Manufacturers and How They Relate to Functions

As of the date of this report, the Geosynthetic Institute (GSI) (2021) lists seven GSI members as manufacturers of geogrids: Tensar, TenCate, Huesker, NAUE, Propex Geosolutions, Berry Global Inc., and Maccaferri. Currently, most manufacturers provide index properties, structural integrity, and durability of geogrid in their specification sheets. Index properties include aperture dimensions (in.), minimum rib thickness (in.), and tensile strength (lb/ft) at 2% strain and 5% strain and ultimate tensile strength. Structural integrity includes junction strength [lb] / efficiency (node strength / rib strength, %), flexural stiffness (mg-cm), and aperture stability (m-N/deg). Durability includes resistance to installation damage (% clayey sand, % well-graded sand, % graded gravel), resistance to long time degradation (%), and resistance to UV degradation.

Holtz el al. (2008) summarized the survivability requirements for geogrids in stabilization and base reinforcement applications listed in Table 8. Note that no national guide of practice is yet established and the recommended requirements are developed specifically for this manual. According to practice, most commercial geogrids for road applications are biaxial, while triaxial geogrids are also available. However, specification sheets completely miss properties related to stiffness enhancement due to interlocking. Further research and investigation are required to recommend proper geogrids for IDOT practice, and it is noted that some manufacturers (e.g., Tensar) have recommended aggregate gradations to use a certain product.

Table 8. Property Requirements for Geogrid in Stabilization and Base Reinforcement Application

Property	Test Method	Units	Required Value [1,2]
Reinforcement Properties			
Ultimate Tensile Strength	ASTM D6637 *	lb/ft (kN/m)	820 (12)
Geogrid Percent Open Area	CW-02215	%	50
Minimum Aperture Size [4]	Direct measure	In. (mm)	__(__)
Maximum Opening Size [5]	Direct measure	In. (mm)	__(__)
Survivability Index Values			Class 2 [3]
Ultimate Tensile Strength	ASTM D6637 [3]	lb/ft (kN/m)	820 (12)
Junction Strength	GRI GG2	lb(N)	25 (110)
Ultraviolet Stability	ASTM D4355 *	% at 500 hrs	50

Source: adapted from Holtz et al. (2008)

Notes:

1. Values, except ultraviolet stability, are MARVS (average value minus two standard deviations).
2. Minimum strength direction
3. Default geotextile selection. The Engineer may specify a Class 3 geogrid [See Section 5.3-6] based on one or more of the following:

   The Engineer has found Class 3 geogrids to have sufficient survivability based on field experience.

   The Engineer has found Class 3 geogrids to have sufficient survivability based on laboratory testing the visual inspection of a geotextile sample removed from a field test section constructed under anticipated field conditions.
4. Minimum opening size must be $\geq D_{50}$ of aggregate above geogrid to provide interlock, but not less than 25 mm (1/2 in.).
5. Maximum opening size must be $\leq 2D_{85}$ to prevent aggregate from penetrating into the subgrade, but no greater than 75 mm (3 in.).

* References: ASTM D6637 (2015c), ASTM D4355 (2021c)

The current problem with evaluating aggregate-geogrid interlock and the effectiveness of currently available geogrid products is that there is no standard laboratory test to quantify the stiffness enhancement provided by the interlock in the geogrid-aggregate composite system. For example, for unbound aggregates, the properties that seem to be influential may include gradation, angularity, hardness, density, and surface texture / friction, as outlined by Giroud (2009). For a geogrid, the properties that can have great influence on performance include aperture size and geometry, junction strength, as well as rib shape and stiffness (Giroud, 2009).

Experimental Testing Methods

Geogrid stabilization has been reported to improve rutting resistance and bearing capacity of unpaved and paved roads (Tingle & Webster, 2003; Giroud & Han, 2004a; Kwon & Tutumluer, 2009). According to the studies noted in the literature on the governing mechanisms of geogrid stabilization, lateral restraint of aggregate particle movement caused by geogrid-aggregate interlocking has been considered as the primary mechanical stabilization mechanism (US Army Corps of Engineers, 2003). Multiple testing methods for geogrids have been proposed by several researchers.

Pullout Test

The pullout test method is a standard test method specified by ASTM D6706 (2013) intended as a performance test to provide the user with a set of design values for the test conditions examined. A geosynthetic is embedded between two layers of soil using the pullout box, horizontal force is applied to the geosynthetic, and the force required to pull the geosynthetic out of the soil is recorded. Figure 20 shows a schematic of the pullout test box.

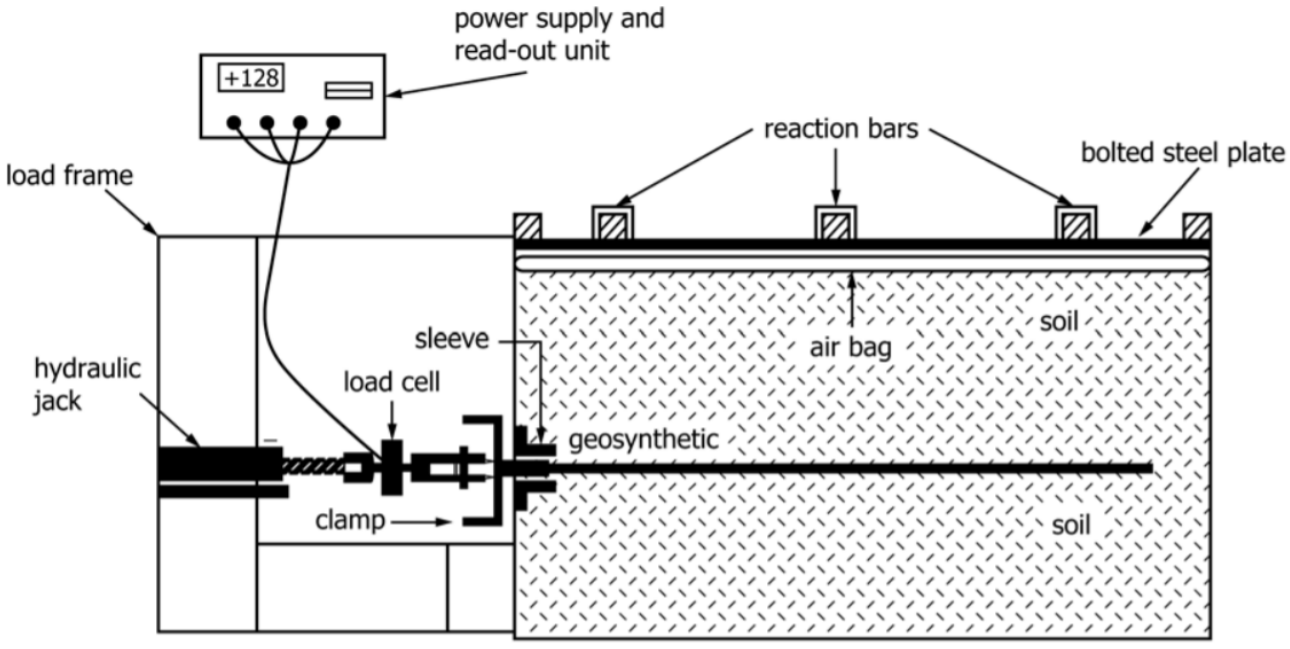

Figure 20. Illustration. Experimental set-up for geosynthetic pullout testing.

Source: ASTM D6706 (2013)

The front displacement and the pullout load are recorded, and the results are given as the efficiency ratio; the ratio of the interface friction angle to soil friction angle ranges from 0.6 to 1.0 (Farrag et al., 1993). For the shear box test, several levels of normal stresses are applied in the direction of the geogrid to develop a normal stress-shear stress behavior and determine the properties governed by the Mohr-Coulomb envelope.

For anchorage strength, the bearing capacity in front of the transverse ribs is an added mechanism that resists pullout in addition to the shear strength from the longitudinal and transverse ribs in the shear box test (Koerner, 2012). In addition, Farrag et al. (1993) discussed the testing parameters that affect the pullout test and the direct shear box test of geogrids resting on soil samples, as well as the desirable rates / ranges for these values. The parameters that affect the results include the pullout rate (desirable rates are less than 6 mm/min), the confinement level, and the side friction on the wall of the box (controlled by clearance distance).

According to Farrag and Griffin (1993), the following are major factors that could affect pullout resistance, namely: 1) testing device, 2) boundary effect, 3) pullout rate, 4) type of reinforcement, 5) soil compaction process, 6) soil properties, and 7) confining pressure. Fannin and Raju (1993) has grouped these factors into three attributes: 1) testing device related, 2) soils related, and 3) reinforcement related. These factors are tabulated in Table 9.

Table 9. Factors Influencing Pullout Resistance

Testing Device Related	Soil Related	Reinforcement Related
1. Lift thickness 2. Front wall effect 3. Side wall effect 4. Pullout rate 5. Confining pressure and its distribution	1. Soil type 2. Soil characters (e.g., shear strength, grain size distribution, density, water content, degree of compaction)	1. Specimen type 2. Specimen width 3. Size of opening

Geosynthetic Composite Stiffness Test

The soil-geosynthetic interaction under small displacements was characterized by an index parameter referred to as the stiffness of the soil-geosynthetic composite (K_{SGC}) (Zornberg et al., 2017; Roodi & Zornberg, 2017; Roodi, 2016). A testing procedure, referred to as the geosynthetic composite stiffness test, was developed to characterize K_{SGC}. This test mobilizes interaction mechanisms between soil and geosynthetics, similar to those mobilized in the conventional pullout test. However, the conventional analysis of the pullout test has been limited to defining the relation between frontal pullout force and frontal pullout displacement to capture ultimate pullout force corresponding to the failure condition. In this approach, linear variable differential transformers are used only to monitor general movement of the geosynthetic. Where this approach is suited to characterizing the failure conditions, it does not provide insight into the interactions developed between soil and geosynthetic at low displacement magnitudes. The focus of the data collection and analysis has been on the onset of movement along the geosynthetic. Specifically, the relationship between load per unit width of the geosynthetic (T) and displacements along the geosynthetic (u) has been determined for

displacements ranging from 0.1 mm (3.94 mils) to 1 mm (39.4 mils). The slope of the linear relationship defined between T and u along the confined length of the geosynthetic has been defined as K_{SGC}.

From the test results, interface shear stiffness K_{SGC} can be calculated using the equation in Figure 21:

$$K_{SGC} = 4\tau_y J_c$$

Figure 21. Equation. Interface shear stiffness.

Source: Roodi et al. (2018)

where τ_y is yield shear stress and J_c is confined stiffness of the soil-geosynthetic system. From the interface shear stiffness, a load per unit width of the geosynthetic can be derived (see Figure 22).

$$T(x)^2 = K_{SGC} u(x)$$

Figure 22. Equation. Unit tension at location x.

Source: Roodi et al. (2018)

where $T(x)$ is the unit tension and $u(x)$ is the geogrid displacement at the location x.

Figure 23 shows the test setup for the geosynthetic composite stiffness test, and Figure 24 illustrates the testing procedure using the test device and a biaxial geogrid tested.

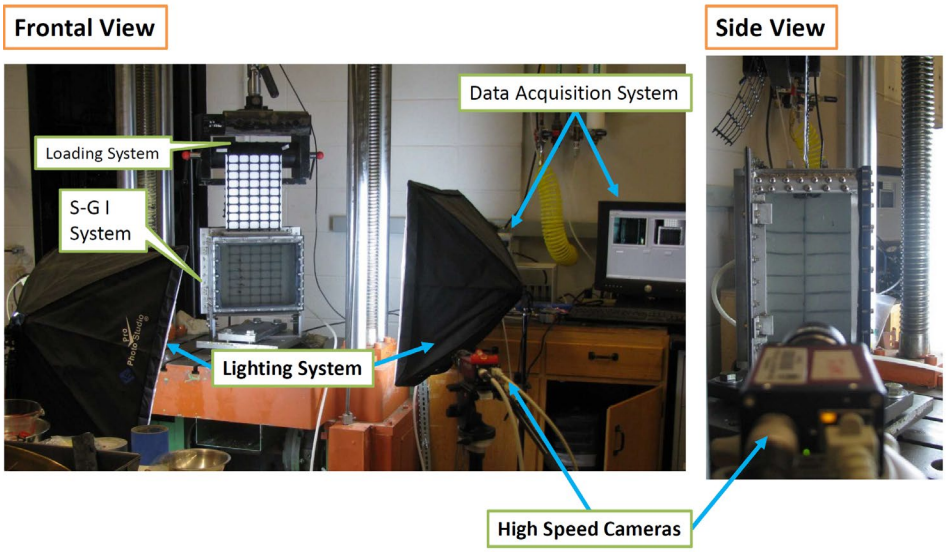

Figure 23. Photos. Test setup for the geosynthetic composite stiffness test.

Source: Roodi et al. (2018)

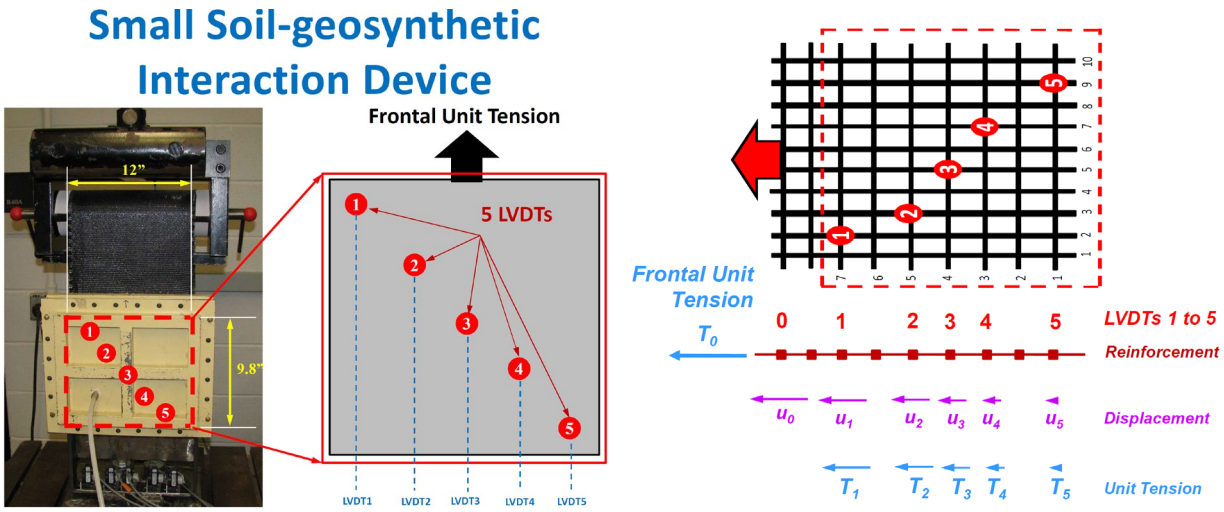

Figure 24. Illustration. Geosynthetic composite stiffness test procedure using the test device and biaxial geogrid.

Source: Roodi et al. (2018)

Shear Wave Measurement Test Using Bender Elements

Geogrids installed in the unbound aggregate base or subbase of the pavement provide the lateral restraint in the layer by interlocking with the aggregate particles. The bender element test is a research approach adopted recently at the University of Illinois to directly measure shear wave velocity in a geogrid influence zone and quantify the stiffening effect in this stiffened zone, which was unavailable through previous research approaches. Shear wave transducers used as a source-receiver pair are called bender elements (BEs), which have been commonly used to evaluate the stiffness of the granular material in laboratory studies (Lee & Santamarina, 2005). A BE transducer is composed of three layers, i.e., a thin metal plate sandwiched between two piezoceramic plates. The piezoceramic plates deform when an electric field passes through them, and the physical deformation generates an elastic wave propagation through the medium, such as an unbound aggregate material. Conversely, the physical deformation of the piezoceramic plate generates the electrical charge. Thus, a BE can be utilized as an elastic wave source or receiver. A flat shape and the fishtail oscillation movement of the BE enable a superb coupling between the transducer and granular materials such as aggregates.

Recent studies using BE pairs to measure the shear wave velocity of geogrid-stabilized cylindrical aggregate specimens during triaxial tests have confirmed that the BE pairs are able to evaluate the characteristics of a geogrid-stiffened zone, i.e., changes in shear wave velocity along with depth above the geogrid (Byun & Tutumluer, 2017; Kang et al., 2020). From the shear wave velocity measured using BEs, a shear modulus can be expressed in terms of shear wave velocity (see Figure 25).

$$G_{max} = \rho V_S^2$$

Figure 25. Equation. Small-strain shear modulus.

where ρ is density of the specimen, G_{max} is small-strain shear modulus, and V_s is shear wave velocity. Further, based on continuum mechanics, the elastic modulus (in a small-strain range) can be estimated (see Figure 26).

$$\mathrm{E_{BE}} = \mathrm{E_{max}} = 2G_{max}(1 + \upsilon)$$

Figure 26. Equation. Small-strain elastic modulus.

where E_{BE} is the elastic modulus from a BE sensor in a small-strain range, and υ is the Poisson's ratio of the aggregate material.

Figure 27 shows the test setup for the repeated load triaxial test with geogrid and bender elements. Bender elements installed at different heights above the geogrid quantified successfully the stiffening effect of the geogrid-stabilized specimen compared to an unstabilized specimen.

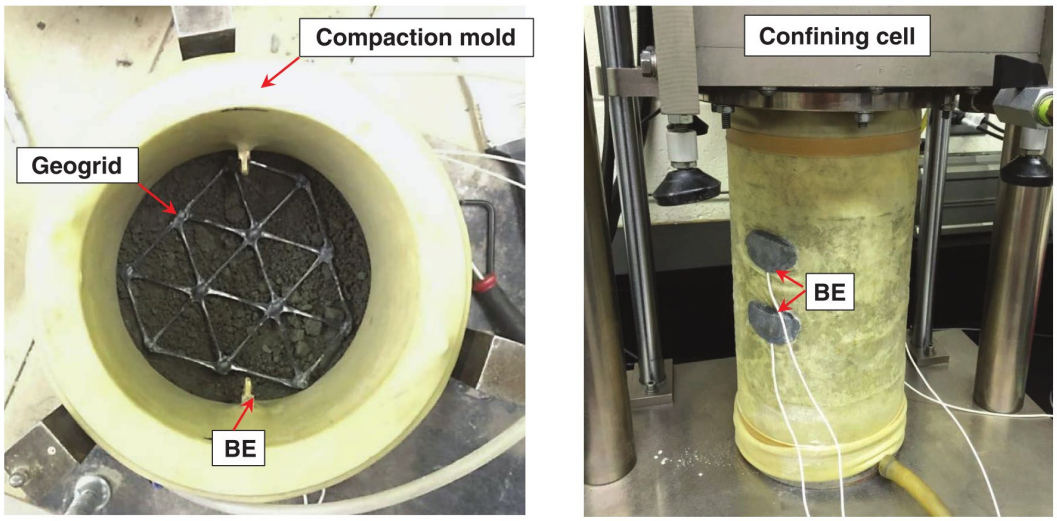

Figure 27. Photos. Images of specimen preparation and test setup with bender elements.

Source: Byun & Tutumluer (2017)

Furthermore, a BE field sensor to monitor and evaluate the shear wave velocity of the unbound aggregate layer of the in situ pavement or full-scale test sections was developed and verified by Kang et al. (2021). The BE field sensor can monitor and quantify the stiffness enhancement in vicinity of the geogrid in pavement. Figure 28 shows a schematic of the BE field sensor along with the shear wave signal measurement system. The test results performed in a large-scale testbed using the BE field sensor indicated the improved stiffness near the geogrid and the existence of MSL profile.

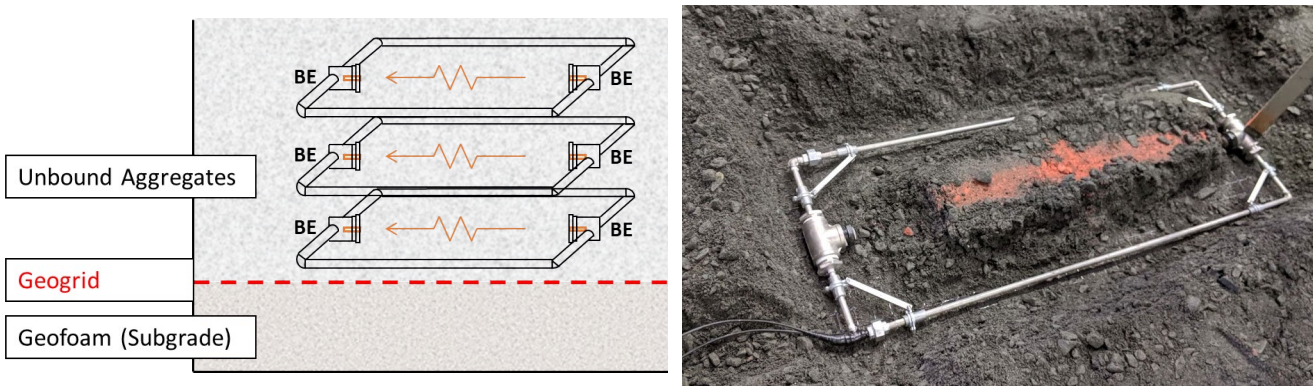

Figure 28. Photos. Schematic of the test setup using bender element field sensor and a picture of the installed bender element field sensor.

Source: Kang et al. (2021)

Modern Geotextiles in Pavement Applications

Geotextiles are the most commonly used type of geosynthetic in transportation applications, and as such, they have been widely investigated by researchers. According to Yeo (2008), geotextiles are permeable fabrics used between soil and structure systems. They are divided into three kinds: woven, nonwoven, or knitted. Geotextiles are composed mostly of polymeric fibers, which are polyamide, polyester, polyethylene, and polypropylene, or sometimes natural materials, such as coconut, jute, cotton wool, and silk.

Al-Qadi and Appea (2003) state that geotextiles are used between aggregate layer (base / subbase) and subgrade, and they can decrease the required excavation depth on weak soil because they increase the performance of pavement sections constructed on weak soil. According to Yeo (2008), geotextiles have four main functions for use in highway design and construction, including separation, reinforcement, filtration, and drainage. Geotextiles can provide reinforcement or stabilization to the aggregate layer by laterally restraining the base or subbase and improving the bearing capacity of the system, decreasing shear stresses on the subgrade. A geotextile with good frictional capabilities can provide resistance to lateral aggregate movement. Geotextiles can increase the interaction with soils to improve the shear capacity of the interface between aggregate layers and soils. Thus, geotextiles for reinforcement / stabilization can improve the mechanical properties of earth structures, which allows for the use of local weak soils.

According to Alungbe (2004), geotextiles perform two main mechanical functions in conventional pavement systems. First, geotextiles provide a physical separation between two layers of different natural material while allowing the water to freely flow through the interface. Second, when geotextiles are in tension they generate tensile resistance to the soils near the interface, allowing the stresses in the base to redistribute more efficiently through the layer and increase the load-bearing capacity. To avoid contamination of unbound aggregate layers with fine-grained subgrade soil particles, geotextiles can provide reduction of layer intermixing by minimizing loss of aggregate particles into underlying soft subgrade, and migration of fine-grained soil particles into overlying unbound aggregate layers. Moreover, as discussed earlier in this chapter, gravity-driven drainage (for

saturated soil conditions) and enhanced drainage due to capillarity (for unsaturated soil conditions) provided by geotextiles can help minimize ingress and accumulation of moisture within structural layers. The elimination of environmental longitudinal cracks along roadways due to the presence of expansive or frost-susceptible subgrade soils can also be achieved by maintaining integrity and uniformity of unbound aggregate layer to minimize stress concentration that triggers longitudinal cracks.

Geotextile Separation Function

Yeo (2008) states that the function of separation is to prevent mutual mixing between a fine soil and a coarse material. Koerner (2012) displays the mechanism of separation in Figure 29. Moreover, pavement performance is improved because separation maintains the integrity and functioning of aggregates and subgrade.

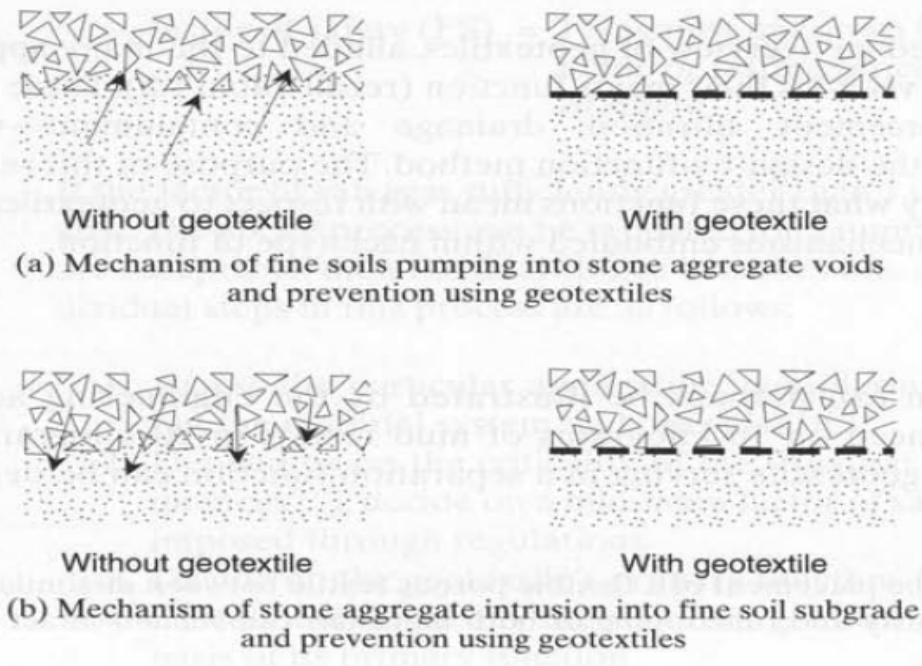

Figure 29. Illustration. Mechanism of geotextile separation.

Source: Koerner (2012)

Geotextile Design for Separation

Geotextiles can work as an efficient separator on subgrade soils with CBR larger than 3 and soils containing fines that are seasonally wet, such as USCS soil classifications CL, ML, SC, SM, GC, and GM (Holtz et al., 2008). According to AASHTO M 288, the geotextile survivability is required to be Class 2 (moderate survivability), the minimum permittivity should be larger than 0.2 sec^{-1}, and the maximum AOS (apparent opening size) should be 0.6 mm, which is equivalent to No. 30 sieve size. According to Hoppe et al. (2019), Virginia DOT requires Class 2 material for separation applications, as listed in Table 10. Also, a subgrade separator geotextile is supposed to be used between soil and any open-

graded aggregate layer and for all jointed concrete pavements constructed on pumping-susceptible subgrades.

Table 10. Geotextile Properties Class 2 (Moderate Survivability)

Property	ASTM Test *	Unit	Elongation < 50%	Elongation ≥ 50%
Grab Tensile Strength	D4632	N	1100	700
Trapezoid Tear Strength	D4533	N	400	250
CBR Puncture Strength	D6241	N	2250	1400
Permittivity	D4491	sec^{-1}	0.02	0.02
Apparent Opening Size (AOS)	D4751	mm	0.60	0.60
Ultraviolet Stability+	D4355	% Ret. @ 500 hrs	50	50

Source: Hoppe et al. (2019)

* References: ASTM D4632 (2015a), ASTM D4533 (2015b), ASTM D6241 (2014a), ASTM D4491 (2021b), ASTM D4751 (2020b), ASTM D4355 (2021c)

+ Evaluation to be on 50 mm strip tensile specimens after 500 hours of exposure.

Research Studies on Separation

Several studies have proven the efficiency and need of using a separation layer to maintain a clean subbase / base layer throughout the design life and prevent the intrusion of fines, which contribute to drainability issues, pumping, and erosion. Common separation layers include dense-graded granular layers and geotextile fabrics. Among the separation geotextiles, a nonwoven geotextile often performs the best because of its high permeability, better durability, better filtration and separation, better lateral transmissivity, and ability to provide gravity-driven lateral drainage and capillary break.

Signore and Dempsey (2002) studied the effects of separation layer type on the pumping resistance of concrete pavement. A laboratory accelerated testing procedure with cyclic loading was applied. Both geotextile separator layers and dense-graded CA 6 aggregate layers were used and compared to a control case with no separation layer employed. Experiments were conducted with both unstabilized and lime-stabilized subgrades to also study the effect of subgrade stabilization on the migration of fines into the overlying layers. According to this study, the use of a geotextile separator reduced pumping by 80% from the nonseparated case. An IDOT CA 06 separation layer offered significant separation benefits while at or below optimum moisture content. However, upon nearing saturation, the CA 06 layer allowed for significant intermixing of the open-graded subbase layer into the dense-graded separation layer. Figure 30 presents a summary of the results. Using a geotextile separator layer provides a more durable and cheaper separation option than a dense-graded aggregate layer for all field conditions, including a nearly saturated pavement structure.

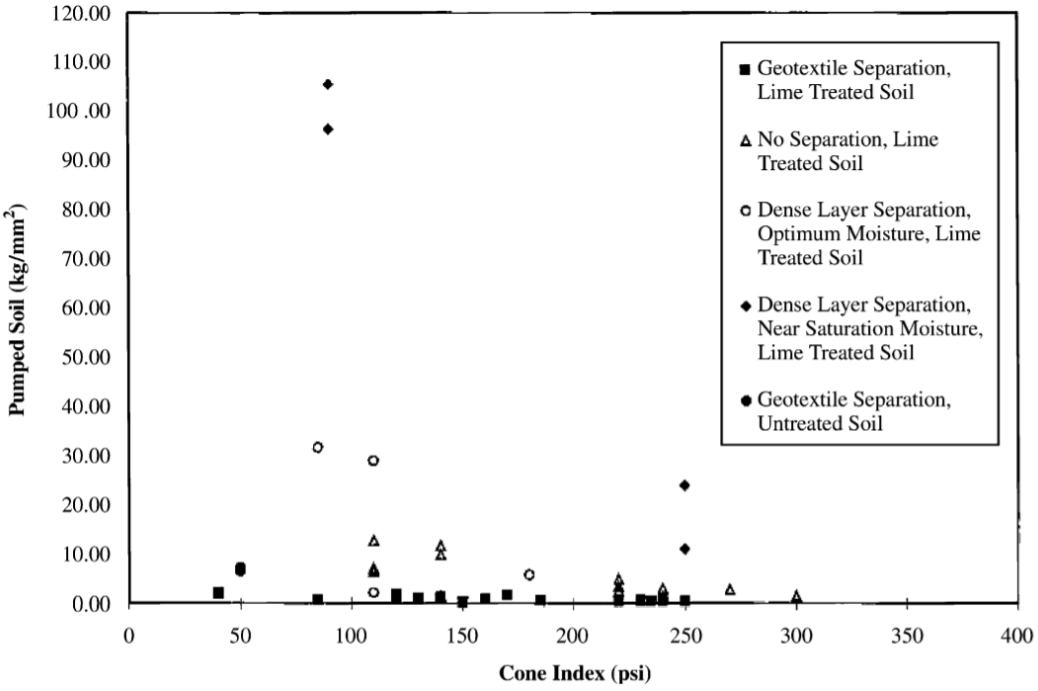

Figure 30. Plot. Pumped material versus cone index for setups of Mexico clay / separation (dense layer or geotextile) / open-graded aggregate subbase.

Source: Signore & Dempsey (2002)

Hoppe et al. (2019) showed that a separator geotextile imparts long-run cost-effectiveness at contamination rates of 0.1/year and greater. Kermani et al. (2018) assessed the capability of geotextile as a separation / filtration layer in reducing subgrade fines migration. A one-third scale model mobile-load simulator was used. There was approximately a 30% reduction in pavement rutting when applying geptextiles at the top of the subgrade layer. Kermani et al. (2020) continued the stimulation study. A control section versus sections with a geotextile placed at the interface of subgrade and subbase were evaluated. Sieve analysis was used to quantify the magnitude and rate of the migration of subgrade particles into the subbase at 200,000 and 1,000,000 loading cycles. The study concluded that the geotextile reduced subgrade migration and faulting by 71% and 52%, respectively. More fines accumulated in the subbase beneath the approach slab than the leave slab, which resulted in faulting of the slabs. As expected, more fines migrated to the bottom half of the subbase closest to the subgrade. Figure 31 presents the percentage of fines migrating into the subbase from the subgrade for the tests with and without a geotextile separator. This study proved the effectiveness of a geotextile separator in reducing fines migration, which maintains the drainability of the subbase and reduces pumping and erosion potentials.

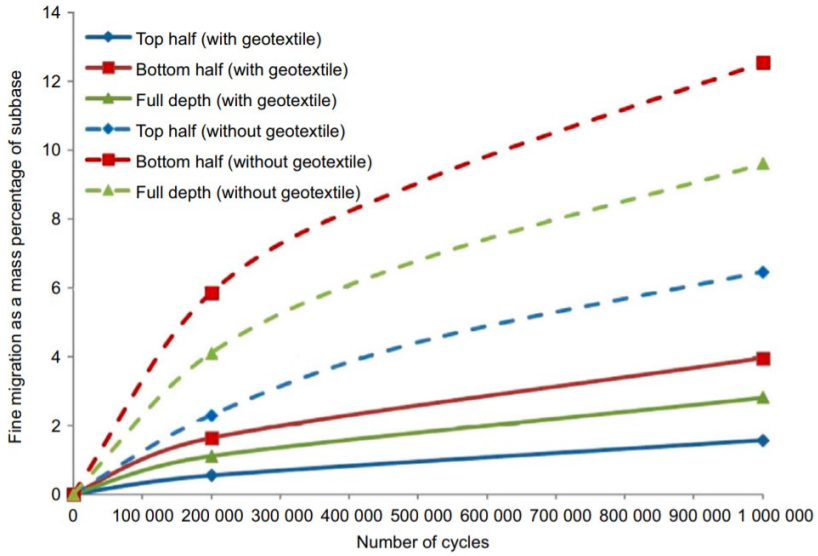

Figure 31. Graph. Percentage of subgrade pumping into the subbase based on the mass of contaminated subbase.

Source: Kermani et al. (2020)

Geotextiles Design for Filtration and Filter Criteria

Geotextiles provide filtration function, as shown in Figure 32. To provide sufficient filtration, geotextiles should meet the following criteria for clogging, permeability, and retention or pumping resistance (fine-grained soil with greater than 50% passing No. 200 sieve). According to the clogging criteria, a woven geotextile is supposed to have an open area percentage larger than 4% and a nonwoven geotextile should have a porosity higher than 30%. According to the permeability criteria, $k_{geotextile}$ = N × k_{soil} (N = 10 to 100). According to the retention or pumping resistance criteria, AOS should be smaller than 0.297 mm (11.7 mils), and AOS of a woven geotextile should be less than D_{85} of the soil and AOS of a nonwoven geotextile should be less than 1.5 × D_{85}.

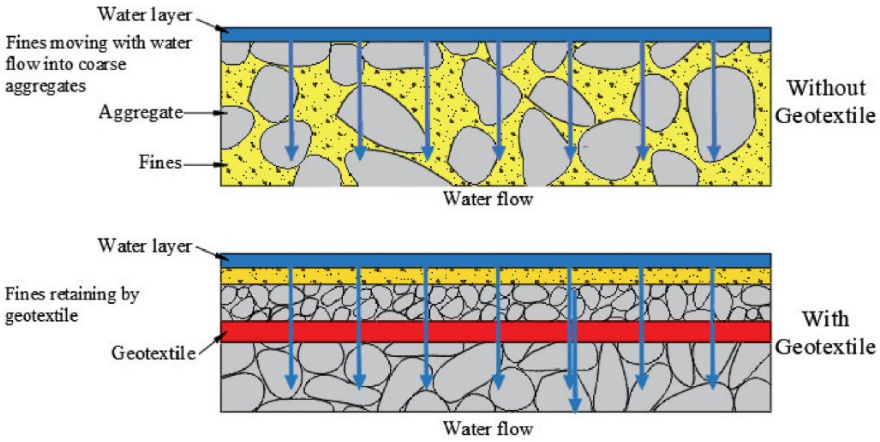

Figure 32. Illustration. Mechanism of geotextiles filtration.

Source: Wu et al. (2020)

According to Koerner (2012), the clogging criteria mentioned above remains unchanged. However, the permeability criteria require that $k_{soil} \leq k_{geotextile}$. Moreover, the retention or pumping resistance criteria are somewhat more detailed. For fine-graded soils with 50% passing the No. 200 sieve, AOS needs to be smaller than No. 50 sieve size, AOS of woven geotextile should be smaller than D_{85}, and AOS of nonwoven geotextile should be smaller than $1.8 \times D_{85}$. For granular materials with 50% or less passing the No. 200 sieve, AOS should be smaller than $B \times D_{85}$, where B = 1 when coefficient of uniformity (C_u) ≤ 2 or $C_u \geq 8$, B = 0.5 C_u when $2 \leq C_u \leq 4$, B = $\frac{8}{Cu}$ when $4 < C_u < 8$.

According to IDOT's *Geotechnical Manual* (IDOT, 2020), a drainage system filter should meet the following criteria:

a) To avoid head loss in the filter: (D_{15} filter ÷ D_{15} protected layer) > 4, and the permeability of the filter must be adequate for the drainage system.

   where D_{15} filter = diameter through which 15% of the filter material will pass by weight, and D_{15} protected layer = diameter through which 15% of the protected layer material will pass by weight.

b) To avoid movement of particles from the protected layer:

   (D_{15} filter ÷ D_{85} protected layer) < 5, (D_{50} filter ÷ D_{50} protected layer) < 25, and (D_{15} filter ÷ D_{15} protected layer) < 20.

   For a very uniform protected layer ($C_u < 1.5$): (D_{15} filter ÷ D_{85} protected layer) may be increased to 6. For a broadly graded protected layer ($C_u > 4$): (D_{15} filter ÷ D_{15} protected layer) may be increased to 40. Note that C_u = (D_{60} ÷ D_{10}) = coefficient of uniformity.

c) To avoid movement of the filter into the drain pipe perforation or joints:

   (D_{85} filter ÷ slot width) > (1.2 to 1.4), (D_{85} filter ÷ hole diameter) > (1.0 to 1.2).

d) To avoid segregation, the filter should contain no particle size larger than 3 in.

e) To avoid internal movement of fines, the filter should have no more than 5% passing the No. 200 (0.075 mm) sieve.

According to Hoppe et al. (2019), the filtration of fine particles can be guaranteed by reduction in AOS, but the flow through geotextiles might be significantly impeded, which can lead to saturated subgrade. Therefore, to provide adequate drainage and redundancy over time, the optimal permittivity determined by Virginia DOT is 0.1 sec^{-1}, matching the AASHTO M 288 minimum permittivity requirement for an erosion control geotextile used with soils containing 50% or more fines. To prevent soil loss with geotextiles when the soil contains more than 30% fines, the coefficient of permeability should be less than 1×10^{-7} cm/s, the plasticity index should be greater than 15, and the undrained shear strength should be more than 200 psf. Thus, the optimal AOS for geotextiles selected by Virginia DOT is less than that of a No. 70 sieve opening (0.212 mm).

Geotextile Lateral Drainage Performance

It is common practice to use a geotextile fabric underneath the granular base / subbase as a separation layer to secure the cleanliness and drainage ability of the base / subbase throughout its life span. Conventional lateral drainage (gravity flow) involves in-plane flow that occurs after saturation of the soil-geotextile interface. If one uses nonwoven geotextiles in conventional lateral drainage, then the flow will pass through the large void spaces in its open structure. If one uses woven geotextiles, then the flow will pass through void spaces of crossed-over yarns. Typically, the utilization of nonwoven geotextiles is recommended unless woven geotextiles are wanted for providing enhanced lateral drainage. Enhanced lateral drainage (capillary flow) contains additional in-plane flow that is mobilized under unsaturated conditions.

A new category of geotextile could offer enhanced (suction-driven) lateral drainage and decrease soil moisture stored within the pores under unsaturated conditions. This new category of geosynthetic materials is called wicking geotextiles, which is a type of woven geotextile. This kind of geotextile is composed of special hydrophilic and hygroscopic 4DGTM (DG = deep groove) fibers with multichannel cross-sections, as demonstrated in Figure 33. According to Wang et al. (2017), the diameters of the micropores range from 5.7 microns to 47.8 microns. Wang et al. (2017) also explained that the multichannel cross-section is capable of enabling the wicking geotextiles to have capillary action and water transport in the unsaturated environment because of its high shape factor and the specific number of channels per fiber. In other words, the wicking fibers are woven into the fabric that has a high strength and high modulus. According to Currey (2016), this kind of fabric combines higher permeability—under both unsaturated and saturated conditions, separation ability, and strength with directional water movement properties.

Wicking geotextiles can remove water from soil at optimum moisture content and under unsaturated condition, as well as mitigate freeze-thaw problems. They perform better in reducing moisture content than non-wicking geotextiles. Wicking geotextiles can increase the modulus of the base by hydraulic stabilization and mechanical stabilization, and significatly reduce permanent deformations of test sections under cyclic loading. The ability of wicking moisture is influenced by relative humidity, temperature, and distance to the wicking geotextile.

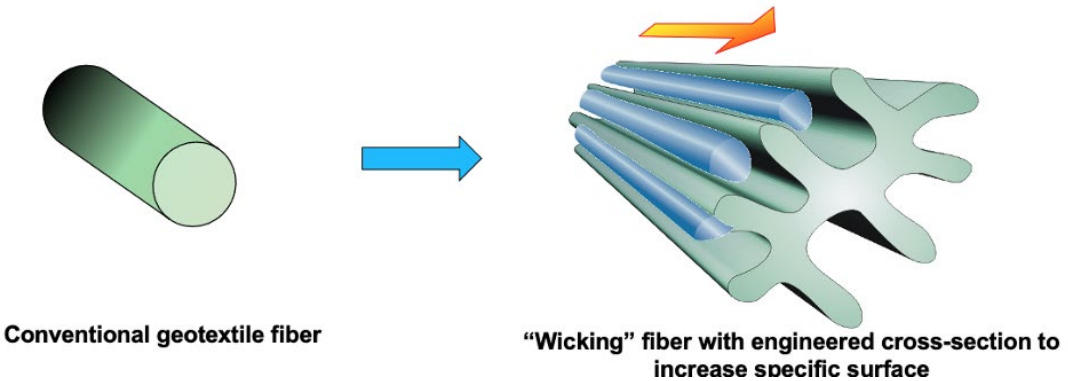

Figure 33. Illustration. Conventional lateral drainage and enhanced lateral drainage.

Source: Zhang et al. (2014)

Currently, wicking geotextiles have been successfully and beneficially used in Alaska, Texas, and Missouri. The H2Ri Wicking Fabric by Tencate was used in Alaska to construct the Dalton Highway MP 197-209 Rehabilitation Project because of its experimental features and properties. The Dalton Highway MP 197-209 Rehabilitation Project was finished between 2012 and 2013 by HC Contractors, Inc. This project was constructed as the second phase of a two-phase project: the mother project—Dalton Highway MP 175-197 Rehabilitation. Originally, the engineers offered "shot rock" and geotextile mitigation designed to fix soft spots in sections of the existing road. However, this solution would add an excessive amount of expense to the estimated total cost. Later, when MP 197-209 got its value engineering study, Northern Region DOT & Public Facilities (PF) partnered with the Alaska University Transportation Center as well as Tencate Mirafi® to propose the H2Ri Wicking Fabric as a cost-saving alternative, replacing the original plan. What makes the H2Ri Wicking Fabric attractive was not only the cost, but also the simplified construction process. After adopting the new geotextiles, the total unit cost came to 34% of the estimated cost of the original proposal, and 17% of the actual cost of the remediation of soft spots in the mother project (Currey, 2016).

During the construction process, workers applied specific installation protocols to maximize the performance of the H2Ri Wicking Fabric. What was different from the installation of the conventional geotextiles was that the new geotextiles must be installed parallel to the centerline. At the same time, the outside edges have to be exposed, and the geotextiles have to be higher than any possible standing water. Another critical step was to make sure that the overlaps between fabric stay clean during the installation for moisture to transfer between adjacent strips. During the process, contractors also avoided the use of heat for cutting rolls to prevent debilitating capillary performance. Last, the fabric was pulled taut and wrinkles minimized to achieve best performance. Although some construction issues happened during the process, affecting the performance of the H2Ri Wicking Fabric, the contractor solved the questions and promised improvements in the future.

Specifically, the H2Ri Wicking Fabric was installed in August and September of 2012. Related personnel reported satisfactory performance during 2013 and summer 2015. Inspections from Tencate Mirafi® also indicated effective and desired results. As depicted by Currey (2016), the pavement was in good condition, and the ride through the entire project was smooth and effortless. The report also mentioned no observable dips, settlement, or distress. Across the 197-209 project, the soil above the new geotextiles was dry, while the soil below it was moist, justifying that the fabric was in good standing for keeping the upper portion of the embankment dry.

A final site inspection took place on August 2, 2016, for the Experimental Features in Construction monitoring, conducted by Jeff Currey and stakeholders from DOT, PF Construction, and FHWA. According to the report, the ride through the 179-197 project was smooth with no observable dips, settlement, or distress. The result was confirmed by maintenance and operations personnel in December 2016. At this point, one could validate the effectiveness of wicking geotextiles in removing moisture and mitigating freeze-thaw problems (Currey, 2016).

In conclusion, wicking geotextiles can remove water from soil under an unsaturated condition and at optimum moisture content. It is also more effective in reducing water content with time than conventional geotextiles.

INTRODUCTION TO GEOCELLS

Geocells, also known as cellular confinement systems, consist of many connected subrounded units usually made with ultrasonically welded high-density polyethylene or novel polymetric alloy (NPA). Geocells have been widely used for erosion control, soil stabilization, slope stabilization, and channel protection. The basic mechanism of geocells is that the walls in each cellular unit can restrict lateral movement and apply confinement on the infill material (see Figure 34) to improve durability, stability, and serviceability of stabilized structures. Benefiting from such mechanism, even some poorly graded materials (e.g., local native soils, quarry wastes, or recycled material) can be used as infill to provide sufficient serviceability without the need of transporting high-quality materials far away from construction sites.

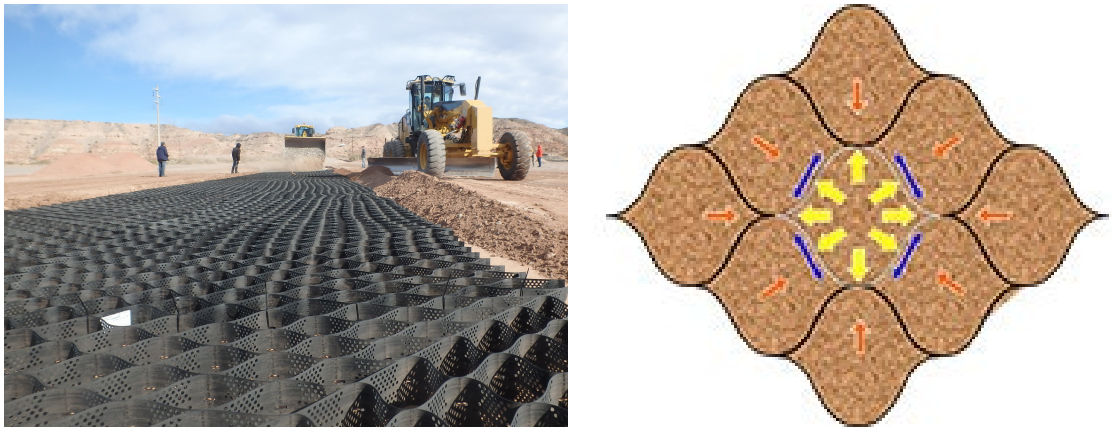

Figure 34. Photo and Illustration. Geocells.

Source: PRESTO (n.d.)

In the field of road engineering, geocells can be used to stabilize base course aggregates and subgrade soils to improve the performance of unpaved or paved roads. NPA geocells could efficiently increase bearing capacity and trafficability of a sand base layer and eventually reduce the rut depth within the aggregate layer on top of the geocell (Yang et al., 2012). Stabilization of reclaimed asphalt pavement (RAP) materials increased the resilient modulus of the RAP base layer by about three times and reduced the permanent deformation of the RAP base layer by over 70% (George et al., 2021).

Design Method for Unpaved Roads Stabilized with Geocells

The Giroud-Han (2004) approach was originally designed for geosynthetic (geotextile and geogrid)-reinforced unpaved roads to determine the required thickness for a base layer. As shown in the equation in Figure 35, Pokharel (2010) modified the original equation by replacing the term for aperture stability with a factor of *k* and involving the modulus improvement factor (MIF) proposed by Han et al. (2007). Note that *k* was calibrated by Pokharel (2010) for a specific NPA geocell with a fill cover of 50 mm (2.0 in.) to 75 mm (3.0), and it can be determined by cyclic plate-loading tests and moving wheel tests on geocell-stabilized bases with different thicknesses.

$$h = \frac{(0.868 + k)\, log\, N}{1 + 0.204(R_E - 1)} \left\{ \sqrt{\frac{\frac{P}{(\pi r^2)}}{\left(\frac{s_a}{f_s}\right)\left[1 - 0.9\, exp\left(-\left(\frac{r}{h}\right)^2\right)\right] N_c c_u}} - 1 \right\} r$$

Figure 35. Equation. Calculating required base course thickness for geocell-reinforced unpaved road.

Source: Pokharel (2010)

where *h* is required base course thickness (m); *k* is a factor that was calibrated by Pokharel (2010), and the calibrated *k* can be calculated with the equation in Figure 36. *N* is number of wheel passes or equivalent single-axle load (ESAL); *P* is wheel load (kN); *r* is radius of tire contact area (m); R_E is the modulus ratio of reinforced base to subgrade and the maximum limit is set to 7.6 (see the equation in Figure 37); s_a is the allowable rutting depth (mm); f_s is equal to 75 mm; *Nc* is the bearing capacity factor that equals 5.14; and c_u is the undrained shear strength of subgrade soil.

$$k = 0.52 \left(\frac{r}{h}\right)^{1.5}$$

Figure 36. Equation. Calculating calibrated k factor for an NPA geocell product.

Source: Pokharel (2010)

where, *k* is the calibrated factor for the equation in Figure 35; *r* is radius of tire contact area (m); and *h* is required base course thickness.

$$R_E = Max\{7.6, MIF * (\frac{3.48 CBR_{bc}^{0.3}}{CBR_{sg}})\}$$

Figure 37. Equation. Calculating modulus ratio of reinforced base to subgrade.

Source: Pokharel (2010)

where R_E is the modulus ratio of reinforced base to subgrade; MIF is determined by the static plate load test on reinforced and unreinforced bases (calculated through the equation in Figure 38) and typically ranges from 1.5 to 2.5; CBR_{bc} is the California Bearing Ratio (CBR) of the unreinforced base course; and CBR_{sg} is CBR of the subgrade.

$$MIF = \frac{E_{bc(reinforced)}}{E_{bc(unreinforced)}}$$

Figure 38. Equation. Calculating modulus improvement factor.

Source: Pokharel (2010)

where $E_{bc(reinforced)}$ is the modulus of the reinforced base, and $E_{bc(unreinforced)}$ is the modulus of unreinforced base.

The undrained shear strength, c_u, of subgrade soil can be estimated by the equation presented in Figure 39.

$$c_u = f_c CBR_{sg}$$

Figure 39. Equation. Estimating undrained shear strength of subgrade soil.

Source: Pokharel (2010)

where f_c is a correlation factor equal to 20.5 kPa for the subgrade used in the cyclic plate loading tests and 19.7 kPa in the moving wheel tests; and CBR_{sg} is CBR of the subgrade.

MITIGATION OF ENVIRONMENTAL DISTRESS WITH GEOSYNTHETICS

Environmental distresses including swelling, expansive soils, and frost heave in pavement are mainly induced by a change in moisture content and temperature, and problematic soils can even aggravate the negative effects. With the functions of separation, reinforcement, drainage, and filtration, geosynthetics are suitable for mitigating environmental distresses.

Mitigating Swelling with Geotextiles

Expansive soil refers to clay with high plasticity index that is volumetrically sensitive to moisture content, i.e., it will gain massive volume when wet and shrink when dried. Such changes in soil volume are detrimental to superstructures (e.g., asphalt or concrete layers) and cause development of cracks on the top surface course. Geotextiles have been applied to alleviate soil swelling.

Biswas et al. (2021) studied the moisture content increase and drainage effect of geotextiles in the laboratory and field. Figure 40-A shows the moisture content variation over time, and Figure 40-B visualizes the water movement and evaporation directions. The sections with the installed geotextile (i.e., MS3 and MS4) rapidly drained out water and decreased the moisture content because water could be drained out along the geotextile. In Figure 40-C, the moisture contents at test sections with a geotextile installed (i.e., TS-1 and TS-2) were much lower than the control section without a geotextile even after several rainfalls. With the function of drainage, geotextiles can maintain moisture content of expansive soil at low level and further reduce the negative effects of excessive water.

Excessive expansion in the vertical direction when expansive soil obtains water usually causes heaving in the superstructure. Badaradinni et al. (2019) studied the geotextile heave relief effect by measuring the footing movement on top of 20 cm (7.87 in.) expansive soil when the soil gradually got saturated. A layer of geotextile was placed at a depth of 0.1B (15 mm) under the footing. To study the effects of multiple layers of geotextile, a second geotextile layer was installed at a depth of 0.3B (45 mm) in addition to the first layer. Note that B is the width of footing and 0.1B was recognized as the optimum depth for placing geotextile in this study. Table 11 compares the footing heave on unreinforced soil, one-layer geotextile reinforced soil, and two-layer geotextile reinforced soil. One layer of geotextile could decrease the heave and two layers of geotextile dramatically reduced the heave by 73.1%.

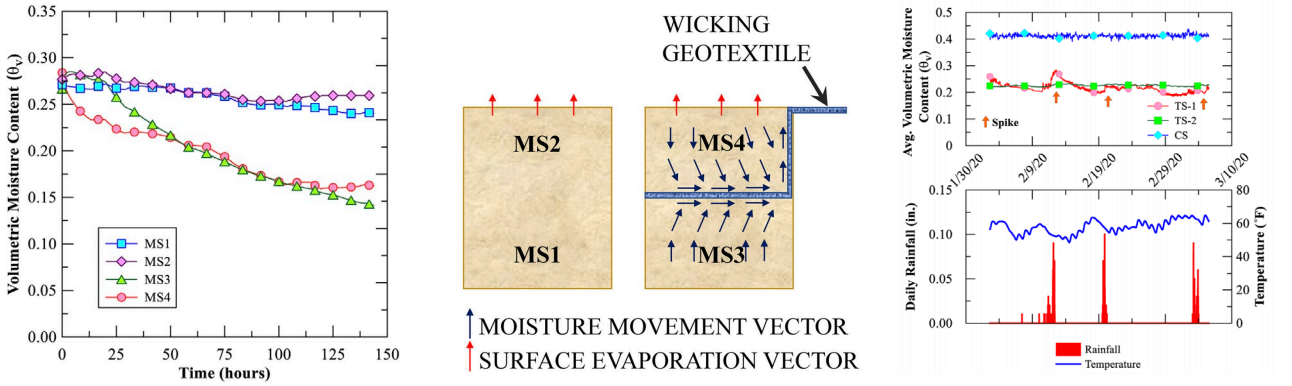

A. Change of moisture content (Lab)

B. Moisture movement & evaporation

C. Change of moisture content (Field)

Figure 40. Moisture content maintaining effect illustration.

Source: Biswas et al. (2021)

Table 11. Heave Results with Geotextile Reinforced

Number of Geotextiles	Depth of Placing	Heave (mm)	Heave Reduction Percentage
0 (unreinforced)	–	31.29	0
1	0.1B	25.26	19.3%
2	0.1B and 0.3B	8.43	73.1%

Source: Badaradinni et al. (2019)

Mitigating Pavement Cracking over Expansive Soil with Geogrid

Alternating dry and wet seasons lead to contraction and expansion in expansive soil and such lateral and vertical deformation can produce tension force in the asphalt layer and lead to longitudinal cracks. Geogrids can restrain lateral movement of interlocked particles in the base course so that it can alleviate the tension force caused by swelling of expansive soil.

In a field test section in Texas, the effect of geogrids on mitigating longitudinal cracks caused by swelling subgrade soil was investigated (Zornberg & Gupta, 2009). Significant longitudinal cracks were observed in the control section without geogrid stabilization even after a few months of use; however, no longitudinal cracks appeared in geogrid-stabilized sections. Luo and Prozzi (2009) applied FEM to study the combination effects of using lime treatment and geogrid reinforcement to control dry land longitudinal cracking and concluded that the best place to install the geogrid was at the interface of the lime-treated layer and an aggregate layer. Luo and Prozzi believed that the geogrid could constrain lateral particle movement near the interface to prevent the initiation of longitudinal cracks at the bottom of the lime-treated layer when the soil was swelling and shrinking.

Mitigating Frost Action with Geofoam

Frost action is a process referring to alternative freezing and thawing of moisture and is a combined consequence of moisture and temperature. Some fine-grained soils such as silt can form a pipe-like

pathway for moisture rising under capillary effects. Then, with freezing and thawing, the voids or gaps within the soil or pavement will develop and may destroy the structure. Geofoam as an insulation layer can reduce the frost penetration and capillary effects, so it is used for mitigating frost action.

Figure 41-A shows a layer of rigid geofoam insulation that was applied under a culvert in Manitoba, Canada. Moussa et al. (2019) collected the temperature data from the thermistors installed under the culvert (see Figure 41-B) and calibrated a numerical model for predicting the freezing and thawing regimes. Figure 42 compares the measured and predicted temperatures over time under the culvert with and without a geofoam insulation layer. The geofoam insulation layer can reduce the temperature variation under the culvert and does not allow freezing so that the frost heave–related pavement distress can be avoided. After calibrating the model with field measurements, Moussa et al. (2019) simulated the cases in which a geofoam insulation layer was installed at different locations and found that the frost depth could be reduced by placing geofoam around the culvert.

A. Geofoam insulation installment B. Layout of thermistors under culvert

Figure 41. Photo and Illustration. Culvert test site in Manitoba, Canada.

Source: Moussa et al. (2019)

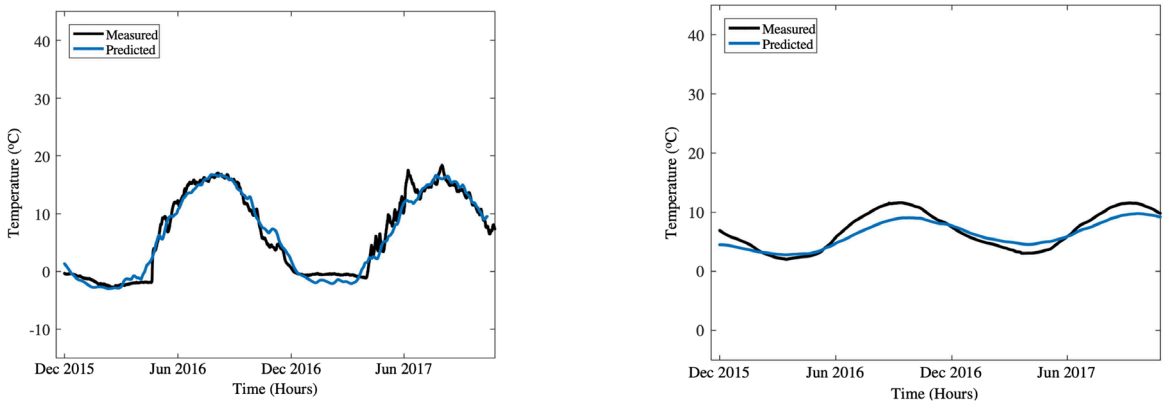

A. Temperature at depth of 3.6 m (no insulation) B. Temperature at depth of 3.4 m (with insulation)

Figure 42. Graphs. Comparisons of temperature variation with or without geofoam insulation.

Source: Moussa et al. (2019)

More details on geotextile properties and testing methods, and more information on geocell properties are presented in Appendix B. Other noteworthy applications of geosynthetics, including case studies, full-scale testing, and relevant research findings from laboratory and field experiments as well as numerical modeling, can be found in Appendix C.

CHAPTER 4: RECOMMENDED MODIFICATIONS TO IDOT PRACTICES AND MANUALS

Applications of geosynthetics in highway pavements involve well-defined mechanisms and functions. Identification of the relevant geosynthetic functions is key to determining the appropriate geosynthetic properties for design. There are significant opportunities for design improvement by using geosynthetics that can be incorporated in IDOT manuals and specifications. These opportunities and other modifications are detailed in the following sections. The list includes geosynthetic functions for:

- Stabilization of Subgrades. For the subgrade restraint function, the use of geogrids, stiff geotextiles, and geocells is proposed and further detailed to update IDOT specifications. Geocells can provide a subgrade restraint method that makes use of standard IDOT aggregate materials, e.g., CA 6 and CA 10 gradations, in addition to local soils and marginal aggregate materials not meeting state requirements inside the "cells." The research team is proposing the use of the Giroud and Han (2004b) design method to account for geosynthetics design for subgrade restraint and soil stabilization. Details of the design method and geosynthetic specifications are presented in Chapter 3 and further elaborated in this chapter and the appendices.

- Reduction of Layer Intermixing (Separation / Filtration). A simple selection criterion for geotextile products that prevent layer intermixing and provide separation between the subgrade and overlaying layers is proposed in this chapter. The proposed criterion can be met by a multitude of commercially available products available in the market by several manufacturers and entails simple, yet conservative and readily available product requirements and specifications that ensure this function is properly achieved.

- Moisture Reduction (Drainage). Similarly, a simple criterion to select geotextiles to perform the drainage function is proposed. The use of modern geotextile materials that are designed to properly drain capillary (suction-driven) water, especially in areas covered with silty soils and shallow groundwater table conditions, is proposed in this chapter.

- Stabilization of Unbound Aggregate Base and Subbase. Some guidelines on geosynthetics and aggregate properties are readily available from the literature. However, the current state of the practice is lacking proper mechanisms to consider properties of both aggregates and geogrids for the best match that would ensure proper interlocking and stiffness enhancement. The use of shear wave propagation using bender element piezoelectric sensors has proven to be an effective method to quantify the local stiffness enhancement in the proximity of a geogrid. This new and promising characterization method can also provide important design parameters for evaluating changes / improvements in aggregate stiffness at different heights above the geogrid and therefore makes it possible to quantify mechanically stabilized layer and adopt proper design methodologies for pavements with geogrids that involves a sublayering technique to

account for geogrid effects. A draft design approach to utilize this in a future study is presented in Appendix D.

- Mitigation of Environmental Distresses (Heaves due to Expansive Soils and Frost Heave Effects). The state of the practice was covered in detail in Chapter 3. IDOT can utilize modern geosynthetic products in projects with such problematic soils encountered through special provisions specifically geared towards using certain geosynthetic products, i.e., geofoams and geogrids, for providing modern geosynthetic solutions.

LIMITATIONS AND PROPOSED MODIFICATIONS TO SUBGRADE STABILITY MANUAL

According to Section 5.4 in the *Subgrade Stability Manual* (*SSM*) (IDOT, 2005), the current developments for reducing aggregate cover thickness when a geogrid or geotextile is used on top of a weak subgrade are based on using several design methodologies based on software programs to determine the aggregate thickness for subgrade restraint with geosynthetics. Examples include Amoco's (now Propex Geosolutions) RACE (Roadways and Civil Engineering) for geotextiles, Tensar's SpectraPave^{TM} for geogrids, and CROW agency developed guidelines in the Netherlands for geosynthetics.

The following limitations were identified related to the current design strategies with geotextiles and geogrids in the *SSM*:

- Generally, geosynthetics could reduce the aggregate cover by as much as 30%, especially when stiffer geogrids are employed. In the *SSM*, a maximum reduction of 152 mm (6 in.) is allowed as a conservative approach.

- The amount of thickness reduction depends on the types and properties of the geosynthetic, aggregate, and the subgrade soil. Currently, no geosynthetic properties are accounted for in the thickness reduction and specified for the selection of the appropriate product. Not all types and/or brands of geosynthetics have the same engineering properties. This makes the performance and, consequently, the specifications of geosynthetics product specific.

- The rut depth assumed in the geosynthetic analyses is 50 mm (2 in.), compared to the currently acceptable rut depth of 12.5 mm (0.5 in.) assumed from empirical sinkage equations for the development of aggregate cover thickness in the *SSM*. So, there is a mismatch between the sinkage amounts or rut predictions during construction trafficking and the bearing capacity improvements adopted by modern geosynthetic solutions.

- IDOT currently does not have generic specifications that could be applied to all geosynthetic products to be used for subgrade restraint.

- Some soils require both a geotextile for separation, to prevent intermixing of the subgrade and the aggregate, and a geogrid for subgrade restraint. This combined geotextile-geogrid option has been used but has proven to be cost prohibitive. The option of using both a

geotextile and a geogrid is not discussed in the *SSM* for appropriate aggregate cover thickness reduction.

An analysis is needed to determine product-specific thickness reductions and to improve guidelines for geosynthetic benefits through the assessment of proper mechanisms provided by geogrids and certain stabilization geotextiles for aggregate cover thickness reductions. This requires a complete study with experimental evaluations and analyses, which is beyond the scope of this project. However, a timely and vital update to the current *SSM* based on the evaluation of the geosynthetic properties reported by manufacturers and the current state of the practice is to add the following statements that limit the selection of proper geosynthetic properties to products that ensure proper subgrade restraint is achieved economically. These statements are recommended to be added to Section 5.4 in the *SSM*:

> *"To ensure a proper geogrid product is selected for aggregate thickness reduction, the selected product needs to have a minimum Junction Efficiency of 93% as determined by ASTM D7737/D7737M (2015d), and a minimum Aperture Stability of 0.32 m-N/degree as determined by ASTM D7864 (2015e)."*
>
> *"To ensure a proper geotextile product is selected for aggregate thickness reduction, the selected geotextile should be a Class 1 non-woven geotextile or a Class 2 woven geotextile, and meet the minimum requirements in accordance with Table 1 of AASHTO M 288 (AASHTO, 2017)."*
>
> *"The use of a geocell product may be permitted under the aggregate cover as a replacement for the geogrid. Thickness reduction must follow the requirements of geogrids in Table 3. The selected geocell product needs to be rated for soil stabilization / subgrade restraint function by the manufacturer."*

PROPOSED MODIFICATIONS TO THE CONSTRUCTION MANUAL AND GEOSYNTHETIC INSTALLATION REQUIREMENTS

In the *Illinois Construction Manual* (IDOT, 2021a), the current definitions for improved subgrade and stabilized subbase are as follows:

> "4. Improved Subgrade: A subgrade that has been modified with lime, by-product lime, cement, or other approved material or, alternatively, has been removed and replaced with aggregate."
>
> "8. Stabilized Subbase: Same as subbase but constructed of an aggregate mixture containing a binder material such as cement, bituminous material or some type of fly ash."

It is proposed that these definitions of improved subgrade / stabilized subbase are modified to include mechanical stabilization as an alternative for pavement foundation improvement. Note that some changes in the definitions might also be required for Chapter 54 of the Bureau of Design and Environment manual and section 312 in the Standard Specifications, where these definitions originate. This will promote more commonplace use of geosynthetics in pavement applications by

IDOT and ensure that economical and beneficial use of geosynthetics is well acknowledged in IDOT manuals as a possible alternative to chemical stabilization and improved subgrade. The proposed modifications for Section 300 are as follows, and the remaining sections are recommended to be corrected accordingly:

> "4. Improved Subgrade. A subgrade that has been ***chemically*** modified with lime, by-product lime, cement, or other approved **admixture/stabilizer**, *or* has been removed and replaced with aggregate**, or, alternatively,** ***has been*** removed and replaced with aggregate ***mechanically stabilized with a geosynthetic product (e.g., geotextile fabric, geogrid, or geocell)***."
>
> "8. ***Chemically*** Stabilized Subbase. Same as subbase but constructed of an aggregate mixture containing a binder material such as cement, bituminous material or some type of fly ash."
>
> "***9. Mechanically Stabilized Subbase. Same as subbase but constructed of an aggregate material stabilized with a geosynthetic material such as a stiff geotextile fabric, a geogrid, or geocell, placed at the interface between the subbase and the subgrade and/or within the aggregate material.***"

Further, the current edition of the *Illinois Construction Manual* (IDOT, 2021a) lacks proper details for handling geosynthetics for pavement applications. Proper construction and inspection of geosynthetic materials is key to ensuring their adequate performance for the intended functions. Proper construction and inspection practices should minimize / avoid tears, rips, and dislocations, thus ensuring performance. For completeness, the following writeup is proposed to warrant appropriate construction protocols are followed when geosynthetics are used in pavement applications. Note that this writeup for construction requirements can partly fit in the *Illinois Construction Manual* (2021a, Article 304.03) and/or as a Bureau of Design and Environment (BDE) Special Provision for a new Section 304; with a material reference to Section 1080.02 in the *Standard Specifications* (IDOT, 2016):

> ***"Geotextile fabrics and geogrids****: geotextile fabrics used for separation, drainage, or stabilization and geogrids used for subgrade restraint/base stabilization shall be placed on top of the graded subgrade (or capping layer of aggregate subgrade improvement where it applies) after the removal of stumps, boulders, etc. The geotextile/geogrid shall be rolled directly over the ground to be stabilized and shall be inspected by the resident engineer to ensure it is free of wrinkles, punctures. Inspection requirements shall follow AASHTO M 288 requirements. Any damaged areas shall be removed and replaced prior to the construction of the aggregate layers.*
>
> *If more than one roll of geogrids/geotextile fabrics is required, rolls shall be overlapped with a minimum 36 in. (914 mm) of overlap. If rolls need to be overlapped side by side, a minimum overlap of 12 (305 mm) is required. The geosynthetic shall be nailed down properly to prevent dislocation due to wind or other factors. No trucks shall drive directly on top of the placed geosynthetic.*

Further, most geosynthetic manufacturers have published installation guidelines and manuals to specifically guide with the installation of their products to ensure performance. Contractors and resident engineers shall refer to and follow these installation guidelines, unless otherwise requested by the resident engineer.

***Geocells**: If specified in the contract documents that a geocell is used, installation guidelines for geocells shall follow the same requirements for geotextiles and geogrids stated above, except that no geocell overlap shall be required. Geocells shall be placed and properly stretched and nailed to ensure pockets have the right geometry, with all pocket openings facing upwards. The resident engineer shall inspect and approve the placement of the geocell prior to filling and compacting a local soil or a designated aggregate material (e.g., CA 6) inside. Proper placement and compaction of soil/aggregates inside geocell pockets is essential to performance. Resident engineer shall inspect the pockets at random spots to ensure they are properly filled and not damaged during construction. Manufacturers' installation guidelines shall be closely followed unless otherwise requested by the engineer."*

DESIGNS WITH GEOTEXTILES FOR DRAINAGE AND SEPARATION

Some modifications for the geotextile physical properties proposed for drainage, filtration, and separation functions are proposed herein. These modifications can be incorporated in the *Standard Specifications* (IDOT, 2016) and/or other IDOT manuals. The intent is to propose simple, broad, and conservative criteria that are met by commercially available geotextile products. For geotextile properties, the AASHTO M 288 (AASHTO, 2017) requirements for a Class 2 separator geotextile should be followed. These specifications are listed in Table 12. For apparent opening size (AOS) and permittivity, the values of these physical properties recently proposed by Hoppe et al. (2019) are met by a multitude of readily available commercial products and provide relatively simple and efficient separation and drainage criteria to be adopted by IDOT, particularly that the proposed values are appropriate for Illinois subgrades and soil and aggregate gradations. As proposed by Hoppe et al. (2019), a maximum AOS of No. 70 sieve size (0.212 mm), and a minimum permittivity of 0.1/sec are proposed for the geotextile fabric used for drainage and separation functions (see Table 13). The use of a nonwoven geotextile is recommended unless a woven geotextile is specially designed to provide the advantage of enhanced lateral drainage and additional suction flow capacity in addition to gravity flow. Nonwoven geotextiles tend to have higher flow rate and drainability by means of gravity.

Table 12. Properties of a Class 2 Geotextile Separator Fabric

Property	Test Method*	Value (N)	
		Elongation < 50%	Elongation ≥ 50% (1)
Grab Strength	ASTM D4632/D4632M	1100 N	700 N
Sewn Seam Strength	ASTM D4632/D4632M	990 N	630 N
Tear Strength	ASTM D4533/D4533M	400 N	250 N
Puncture Strength	ASTM D6241	2200 N	1375 N

Adapted from AASHTO M 288, Table 1 (AASHTO, 2017). *(1) As measured in accordance with ASTM D4632/D4632M*

* References: ASTM D4632 (2015a), ASTM D4533 (2015b), ASTM D6241 (2014a).

Table 13. Physical Properties of Geotextile Separator

Property	Value
Apparent Opening Size, Sieve No. (mm) ASTM D4751 *	No.70 (0.212 mm) maximum
Permittivity, sec-1 ASTM D4491 *	0.1 minimum

* References: ASTM D4751 (2020b), ASTM D4491 (2021b)

The contractor will need to submit to the engineer a manufacturer's certification, which includes the manufacturer's name, address, the geotextile product name, polymer type, and the product's physical properties. The physical properties submitted shall include weight, grab strength, grab elongation, equivalent opening size, permeability, and the allowable strength. The reported permeability of the geotextile shall be higher (preferably an order of magnitude higher) than the permeability of the subgrade ($K_{geotextile} \geq K_{subgrade}$).

DESIGNS WITH GEOGRIDS FOR BASE STABILIZATION IN PAVED ROADS

For geogrids to adequately serve the function of base stabilization and stiffening, geogrid-aggregate interlock should be accounted for in the selection of the proper geogrid product. A proper shear layer lateral restraint creation with good interlock is governed by both aggregate and geogrid properties. Some selection criteria and recommendations are readily available from previous research findings. These include:

- Size of geogrid aperture (A). Some general criteria proposed by previous research studies are as follows:
    - $A = 1.2\ to\ 1.6\ D_{90}$ (Brown et al., 2007)
    - $D_{50} \leq A\ \leq 2D_{85}$ (Holtz et al., 2008)
- Shape of the geogrid apertures. Rectangular apertures in biaxial geogrids have been typical until recently. Newly encountered triangular apertures in certain punched and drawn geogrids can be expected to promote a hexagonal arrangement of aggregate restraint, relating to the densest arrangement in all directions.
- Shape, stiffness, and junctions of ribs. The mechanical behavior of the junctions between ribs is important in the case of stretched geogrids, because they interact with aggregate only through interlocking. Rib shape and thickness are also important when resisting relatively higher wheel loads.

The recommendations listed above are nevertheless general, and as such, a more systematic selection criteria that specifically test various geogrid products for effectively stabilizing local aggregate materials used in the State of Illinois is deemed essential. For that, the use of bender element sensor technology to evaluate the effectiveness of geosynthetics in unbound aggregate base stabilization is proposed for a research study. The proposed analysis involves testing local aggregate materials in the laboratory both in resilient modulus tests following the AASHTO T 307 test procedure

and using large-scale box testing with bender element field sensors embedded in aggregate layers at different heights above the geosynthetic (geogrid). This testing requires (1) the acquisition of a wide variety of stabilization geosynthetic products available; (2) a laboratory quantification of local stiffness enhanced by stabilization geosynthetics using different aggregate materials and gradations; and (3) the performance of box tests utilizing field bender element sensors to quantify local stiffness enhanced by stabilization geosynthetics.

To reduce the testing requirements, the geogrid products are proposed to be grouped into broad categories based on properties, e.g., geogrid group (GG) 1, GG2, GG3 …etc., and the testing is proposed to be performed for certain common IDOT gradation bands, e.g., CA 6 and CA 10. A modulus multiplier (MM), equal to the ratio of the modulus at the bender element location above the geogrid divided by the modulus of the unstabilized case, can be computed for each GG, aggregate gradation, and different heights above the geogrid. These values are proposed to be reported in a table similar to that shown in Table 14 for each common IDOT gradation tested at the upper, lower, and mid-gradation bounds. Once these values are computed from laboratory testing, they can be made available in IDOT manuals for the selection of the proper geogrid and modulus properties in the design of pavements with geogrids. Note that this testing scheme and design approach is proposed herein in anticipation of a follow-up research project for IDOT that will follow the proposed testing procedures and will make these MM factors readily available for IDOT's use in future projects.

Table 14. Sublayer Modulus Multiplier for CA 6 Base/Subbase Layers

	Modulus Multiplier														
Geogrid Type	**GG1**			**GG2**			**GG3**			**GG4**			**GG5**		
Gradation / **Height above GG (in.)**	LB	MG	UB	LB	MG	UB	LB	MG	UB	LB	MG	UB	LB	MG	UB
0.0–1.2															
1.2–4.6															
4.6–6.0															
6.0–≥ 12.0	X 1.0	X 1.0	X 1.0	X 1.0	X 1.0	X 1.0	X 1.0	X 1.0	X 1.0	X 1.0	X 1.0	X 1.0	X 1.0	X 1.0	X 1.0

Note: LB is lower bound, MG is mid gradation, and UB is upper bound of CA 06 gradation.

This approach will allow a more accurate pavement analysis and design methodology for geogrid-stabilized pavements by adopting a sublayering analysis approach where the unbound aggregate base is divided into sublayers, as shown in Figure 43. Each of the sublayers will be assigned a modulus equal to the modulus of the base layer multiplied by a stiffening factor (i.e., MM) prior to conducting the analysis. This is the approach introduced in Chapter 3 by Vavrik (2018) for incorporating stiffened influence zones provided by geogrid into pavement mechanistic analysis following the mechanically stabilized layer concept. The draft design approach with more details is presented in Appendix D.

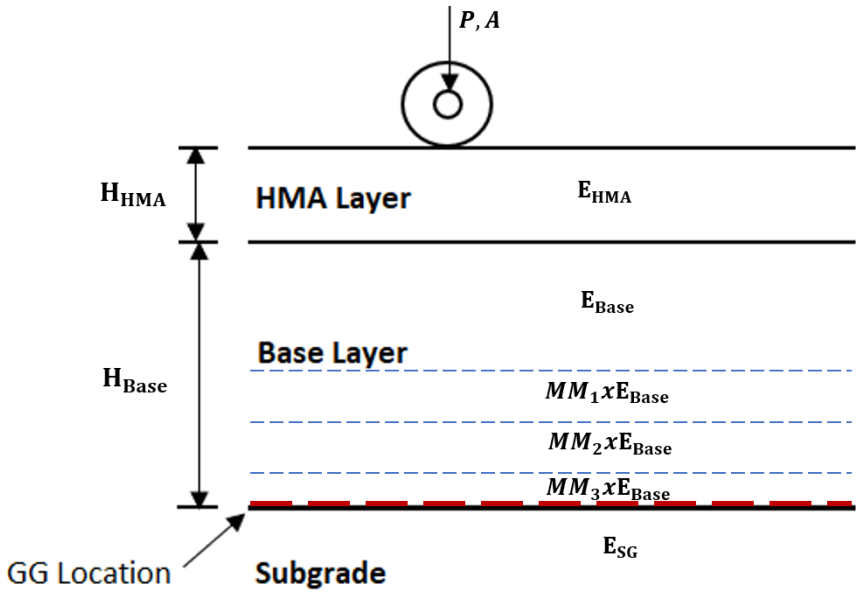

Figure 43. Illustration. Modulus assignment for unbound aggregate base course sublayers for a conventional flexible pavement section stabilized with geogrid (GG).

DESIGNS WITH GEOGRIDS AND A COMBINATION OF GEOTEXTILES AND GEOGRIDS FOR SUBGRADE RESTRAINT AND UNPAVED ROAD APPLICATIONS

For unpaved road applications or subgrade restraint use of geosynthetics, a full review of the available design methodologies was presented in Chapter 3. Revised design methods included the Steward et al. (1977) method, Giroud and Noiray (1981) method, Dutch (CROW) design (2002) method, Army Corps of Engineers (2003) method, and the Giroud and Han (2004a, 2004b) method for unpaved roads. Of these methods, the Giroud and Han (2004b) method for subgrade stabilization using geosynthetics is the state-of-the-art approach to date.

The Giroud and Han method was developed for unpaved roads and is based on Burmister's two-layer solution and data from cyclic plate load tests. Note that this 2004 method is an improvement over the method by Giroud-Noiray (1981) and considers primarily geogrid products for the following improvements: different load / stress distribution angles that can be considered in base layer, variable traffic applications up to 10,000 passes and desired performance, variable modulus / strength ratios of base, and the aperture stability modulus of the geogrid as measured by ASTM D7864 (2015e). For geotextiles, a more appropriate term in lieu of geogrid aperture stability modulus is proposed. Further, this method was calibrated with full-scale test data. For these reasons, a draft design approach based on this method is proposed for IDOT to update their design method for geosynthetic materials used for subgrade restraint in pavements. Drafted design guides for designing with geogrids and geotextiles are presented in Appendix E, while drafted design guides for designing with geocells are presented in Appendix F.

CHAPTER 5: SUMMARY AND CONCLUSIONS

SUMMARY AND CONCLUSIONS

This report presented findings on an Illinois Center for Transportation project to review and update Illinois Department of Transportation (IDOT) specifications and manuals regarding the use of geosynthetic materials in pavements. The project consisted of three tasks: (1) evaluate current IDOT practice related to the use of geosynthetics; (2) review research and state of the practice on geosynthetics applications, available products, design methods and specifications; and (3) propose recommendations to modernize IDOT's practices and manuals for effective solutions with modern geosynthetics utilization in pavements.

As part of the first task, IDOT manuals and standard specifications were reviewed to collect and summarize current IDOT practices for the use of geosynthetics in highway pavements. The reviewed manuals and specifications included the *Illinois Construction Manual* (2021a), *Geotechnical Manual* (2020), *Subgrade Stability Manual* (2005), *Bureau of Design and Environment Manual* (2021b), the *Standard Specifications for Road and Bridge Construction,* and the *Bureau of Local Road and Streets Manual*. In addition, several special provisions and project-specific documents for the use of geosynthetics in pavements were revised. Based on the evaluation of IDOT documents, it was concluded that geotextiles are the most widely used geosynthetic materials in the state, with applications covering subgrade restraint, stabilization, reflective crack control, drainage and separation applications, erosion control, slope stability, and retaining wall applications. Geogrids and other geosynthetic material specifications and applications were not detailed enough except for in some special provisions and specific projects.

In the second task, previous research and state of the practice on geosynthetics usage, products, designs, and specifications were evaluated. A review was conducted for the design methods for stabilization and reinforcement geosynthetics (mostly geogrids, geotextiles, and geocells) used in unpaved and paved road applications. Design methods included the Steward et al. (1977) method, Giroud and Noiray (1981) method, Dutch (CROW) design (2002) method, Army Corps of Engineers (2003) method, and the Giroud and Han (2004a, 2004b) method for unpaved roads. For paved road applications, reviewed design methods included those by US Corps of Engineers (2003), AASHTO (1993), Federal Highway Administration (FHWA) design manual (2008), AASHTO (2013), and other mechanistic-empirical methods using finite and discrete element modeling approaches. Design methods for geotextiles for drainage, separation, and filtration were also fully reviewed, including proper criteria to select geotextile products to ensure drainability, durability, and proper separation. Further, available testing methods for geosynthetic materials, and the geosynthetic properties reported by manufacturers were evaluated to determine the best practice to select proper products for serving a specific function. State-of-the art methods to characterize geosynthetic materials, such as using bender element piezoelectric sensors for local stiffness measurements in the proximity of a geogrid / stiff geotextile. Lastly, case studies and specific field data related to the use of geosynthetics for subgrade restraint, base stabilization, drainage, and mitigation of environmental distresses resulting from expansive soil and frost-heave problems were also reviewed and reported.

Based on the review of IDOT practices and specifications as well as the review of the state of the practice for the use of geosynthetics in roads, the following knowledge gaps were identified:

- Promote economic and beneficial uses of geosynthetic materials with well-documented advantages to pavement performance.
- Better understand governing mechanisms and evaluate soil / aggregate interaction with geosynthetics, primarily geogrids and stiff geotextiles for reinforcement and stiffening, in subgrade restraint and unbound aggregate base stabilization applications.
- Improve guidelines for the *Subgrade Stability Manual* (IDOT, 2005) for selecting geotextiles and geogrids through assessment of target geosynthetic properties in relation to the bearing capacity improvement and lateral restraint governing mechanisms for aggregate cover thickness reductions.
- Develop proper and more relevant specifications based on the lateral restraint governing mechanism and the stabilization / stiffening provided by geogrid-aggregate interaction and quantify geogrid benefits for base stabilization.
- Establish proper standards for geotextiles for separation and pumping resistance by considering criteria for clogging and permeability.
- Consider foundation improvements (uniformity, drainability, and stability) for rigid pavements using geosynthetics. This area was covered in a recent project by the research team (R27-193-5), which recommended the use of a geotextile fabric at the subgrade / subbase interface for concrete pavements constructed on top of daylighted unbound aggregate subbases up to a traffic factor of 10.0 (Qamhia & Tutumluer, 2021).
- Document proper techniques for constructing and conducting quality assurance / control measures when geosynthetics materials are utilized in roadway applications.

Based on the evaluation of IDOT's specifications, the review of available design methods, and available products and characterization techniques, some improvements are recommended to modernize IDOT's practices and ensure utilizing modern geosynthetics to design and construct more reliable, cost effective, and longer lasting pavements. The main proposed modifications include:

1. Establish proper mechanisms for using geogrids, geocells, and geotextiles in subgrade restraint and base reinforcement / stabilization applications. This includes the use of recently developed bender element sensor technology to quantify local stiffness enhancements and incorporate stiffening effects in design methods. It also entails adopting the Giroud and Han (2004b) design method to account for reinforcement and stabilization geosynthetics for unpaved road designs and/or subgrade restraint function.
2. Propose improvements to the *Subgrade Stability Manual* (IDOT, 2005) to add minimum requirements and physical properties for geogrids and geotextiles for subgrade restraint.

3. Establish proper standards on stabilization, separation, and pumping resistance for geotextiles by considering the most recent findings on clogging and permeability criteria.

4. Promote the use of modern geosynthetic products, such as geotextiles with enhanced (suction-driven) lateral drainage, and geocells for subgrade restraint.

5. Modify / update the verbiage in some manuals and specifications related to definitions of mechanical stabilization and elaborate on correct methods to construct pavements with geosynthetics, including the utilization of proper quality control measures.

6. Design guides for designing with geocells, geogrids, and geocells for subgrade restraint, and with geogrids for base stabilization were drafted to update IDOT's practices.

RECOMMENDATIONS FOR FUTURE WORK

Based on the review of the state of the practice for the use of geosynthetics in roads as well as the recommendations obtained from this report, the following areas for future work are proposed:

- There is a need to conduct pilot and small-scale projects to test modern geosynthetic materials based on reported advantages in road design by other states and researchers. Such products include geocell materials filled with local soils for subgrade restraint and modern woven geotextile products that can provide enhanced lateral drainage and additional suction flow capacity in addition to gravity flow. These products are readily available on the market and can prove advantageous for challenging road projects being considered in Illinois. Special provisions and project-specific documents can be drafted as a follow-up to this project for the use of such modern geosynthetic products.

- For the *Subgrade Stability Manual* (IDOT, 2005), minimum requirements for geogrid and geotextile materials were added; however, for more accurate designs, a more comprehensive study may be required to improve guidelines for geotextile and geogrid benefits through the assessment of proper mechanisms provided by geogrids and geotextiles for aggregate cover thickness reductions. Further, aggregate thickness reductions for cases of using both a geogrid and a geotextile or using other geosynthetics (e.g., geocells) may need to be considered and added to the manual as alternative options.

- There is much promise to evaluate the effectiveness of available geosynthetic products in pavement soft subgrade and base / subbase stabilization applications, and to develop modern specifications for IDOT based on the most relevant local stiffness increase mechanism. To achieve this goal, the recently developed bender element sensor technology based on the small-strain shear wave measurement technique can be used to quantify the local stiffness increase by the best match of geosynthetic-aggregate composite and to investigate factors governing the degree of geosynthetic-aggregate interaction through laboratory triaxial specimens and box tests.

REFERENCES

American Association of State Highway and Transportation Officials. (1993). *Guide for design of pavement structures*. AASHTO.

American Association of State Highway and Transportation Officials. (2008). *Mechanistic-Empirical pavement design guide, interim edition: A manual of practice*. AASHTO.

American Association of State Highway and Transportation Officials. (2013). *AASHTO R 50-09: Recommended practice for geosynthetic reinforcement of the aggregate base course of flexible pavement structures*. AASHTO.

American Association of State Highway and Transportation Officials. (2017, June). AASHTO M 288: *Standard specification for geosynthetic specification for highway applications*. AASHTO.

Al-Qadi, I. L., & Appea, A. K. (2003). Eight-year field performance of secondary road incorporating geosynthetics at subgrade-base interface. *Transportation Research Record*, *1849*, 212–220. https://doi.org/10.3141/1849-23

Al-Qadi, I. L., Dessouky, S. H., Kwon, J., & Tutumluer, E. (2008). Geogrid in flexible pavements: Validated mechanism. *Transportation Research Record*, *2045*(1), 102–109.

Al-Qadi, I. L., Dessouky, S., Kwon, J., & Tutumluer, E. (2009). Geogrid in flexible pavements: Validated mechanism. *Transportation Research Record*, *2045*, 102–109.

Al-Qadi, I. L., Tutumluer, E., & Dessouky, S. (2006). Construction and instrumentation of full-scale geogrid-reinforced flexible pavement test sections. In I. L. Al-Qadi (ed.), *Proceedings of the ASCE Transportation and Development Institute (T&DI)* (pp. 131–142). American Society of Civil Engineers.

Al-Qadi, I. L., Tutumluer, E., Dessouky, S., & Kwon, J. (2007). Mechanistic response measurements of geogrid reinforced flexible pavements to vehicular loading. In *CDROM Proceedings of the Geosynthetics 2007 Conference*, Washington, DC.

Alungbe, G. D. (2004). Geotextiles in flexible pavement construction. *Tech Direction 64*(2), 22–23.

ASTM D3887-96. (1996). *Standard specification for tolerances for knitted fabrics*. ASTM International.

ASTM D 693-03a. (2003). *Standard specification for crushed aggregate for macadam pavements (Withdrawn 2008)*. ASTM International.

ASTM D6706-01 (2013). *Standard test method for measuring geosynthetic pullout resistance in soil*. ASTM International.

ASTM D6241-14 (2014a). *Standard test method for static puncture strength of geotextiles and geotextile-related products using a 50-mm probe*. ASTM International.

ASTM D4884 / D4884M-14a (2014b). *Standard test method for strength of sewn or bonded seams of geotextiles*. ASTM International.

ASTM D4632 / D4632M-15a (2015a). *Standard test method for grab breaking load and elongation of geotextiles*. ASTM International.

ASTM D4533 / D4533M-15 (2015b). *Standard test method for trapezoid tearing strength of geotextiles*. ASTM International.

ASTM D6637 / D6637M-15. (2015c). *Standard test method for determining tensile properties of geogrids by the single or multi-rib tensile method*. ASTM International.

ASTM D7737 / D7737M-15. (2015d). *Standard test method for individual geogrid junction strength*. ASTM International.

ASTM D7864 / D7864M-15. (2015e). *Standard test method for determining the aperture stability modulus of geogrids*. ASTM International.

ASTM D378-10. (2016a). *Standard test methods for rubber (elastomeric) conveyor belting, flat type*. ASTM International.

ASTM D1196 / D1196M-12. (2016b). *Standard test method for nonrepetitive static plate load tests of soils and flexible pavement components, for use in evaluation and design of airport and highway pavements*. ASTM International.

ASTM D4595-17 (2017a). *Standard test method for tensile properties of geotextiles by the wide-width strip method*. ASTM International.

ASTM D5101-12 (2017b). *Standard test method for measuring the filtration compatibility of soil-geotextile systems*. ASTM International.

ASTM D5101-12 (2017c). *Standard classification for sizes of aggregate for road and bridge construction*. ASTM International.

ASTM D3786 / D3786M-18. (2018a). *Standard test method for bursting strength of textile fabrics—diaphragm bursting strength tester method*. ASTM International.

ASTM D1388-18. (2018b). *Standard test method for stiffness of fabrics*. ASTM International.

ASTM D1683 / D1683M-17. (2018c). *Standard test method for failure in sewn seams of woven fabrics*. ASTM International.

ASTM D5261-10. (2018d). *Standard test method for measuring mass per unit area of geotextiles*. ASTM International.

ASTM D1505-18. (2018e). *Standard test Method for density of plastics by the density-gradient technique*. ASTM International.

ASTM D6707 / D6707M-06. (2019a). *Standard specification for circular-knit geotextile for use in subsurface drainage applications*. ASTM International.

ASTM D5199-12. (2019b). *Standard test method for measuring the nominal thickness of geosynthetics*. ASTM International.

ASTM D3776 / D3776M-20. (2020a). *Standard test methods for mass per unit area (weight) of fabric*. ASTM International.

ASTM D4751-20b. (2020b). *Standard test methods for determining apparent opening size of a geotextile*. ASTM International.

ASTM D4218-20. (2020c). *Standard test method for determination of carbon black content in polyethylene*. ASTM International.

ASTM D4716 / D4716M-20. (2020d). *Standard test method for determining the (in-plane) flow rate per unit width and hydraulic transmissivity of a geosynthetic using a constant head*. ASTM International.

ASTM D412. (2021a). *Standard test methods for vulcanized rubber and* thermoplastic *elastomers—tension*. ASTM International.

ASTM D4491 / D4491M-21. (2021b). *Standard test methods for water permeability of geotextiles by permittivity*. ASTM International.

ASTM D4355 / D4355M-21. (2021c). *Standard test method for deterioration of geotextiles by exposure to light, moisture, and heat in a Xenon arc-type apparatus*. ASTM International.

Badaradinni, B. M., Hulagabali, A. M., Solanki, C. H., & Dodagoudar, G. R. (2019). Experimental study of heave control technique for expansive soil using micropiles and geotextile layers. In *Ground Improvement Techniques and Geosynthetics* (pp. 35-43). Springer, Singapore.

Barenberg, E. J., Hales, J., & Dowland, J. (1975). *Evaluation of soil-aggregate systems with MIRAFI fabrics* (Report No. UILU-ENG-75-2020). University of Illinois at Urbana-Champaign.

Barker, W. R. (1987). *Open-graded bases for airfield pavements. Miscellaneous Paper GL-86*. U.S. Army Corps of Engineers Waterways Experiment Station.

Benmebarek, S., Berrabah, F., Benmebarek, N., & Belounar, L. (2015). Effect of geosynthetic on the performance of road embankment over sabkha soils in Algeria: Case study. *International Journal of Geosynthetics and Ground Engineering*, *1*(4), 1–8.

Berg, R. R., Christopher, B. R. & Perkins, S. W. (2000). *Geosynthetic reinforcement of the aggregate base/subbase courses of pavement structures GMA white paper II*. Geosynthetic Materials Association.

Biswas, N., Puppala, A. J., Khan, M. A., Congress, S. S. C., Banerjee, A., & Chakraborty, S. (2021). Evaluating the performance of wicking geotextile in providing drainage for flexible pavements built over expansive soils. *Transportation Research Record*, 03611981211001381.

Brown, S. F., Kwan, J., & Thom, N. H. (2007). Identifying the key parameters that influence geogrid reinforcement of railway ballast. *Geotextiles and Geomembranes*, *25*, 326–335.

Byun, Y. H., & Tutumluer, E. (2017). Bender elements successfully quantified stiffness enhancement provided by geogrid–aggregate interlock. *Transportation Research Record: Journal of the Transportation Research Board*, *2656*, 31–39.

Chen, Q., & Farsakh, M. (2012). Structural contribution of geogrid reinforcement in pavement. *GeoCongress*, 1468–1475.

CROW. (2002). Handboek wegontwerp: Publicatie 164a – Basiscriteria [Road design manual: Publication 164a – Basic criteria]

Currey, J. (2016). *H_2R_i wicking fabric experimental feature final report Dalton Highway MP 197-209 rehabilitation*. Alaska DOT Project No. IM-DP-065-4(8)/61214.

Eiksund, G., Hoff, I., Svano, G., Watn, A., Cuelho, E. V., Perkins, S. W., Christopher, B. R., & Schwartz, C. W. (2002). Material models for reinforced unbound aggregate. In *Proceedings of the 6th International Conference on the Bearing Capacity of Roads, Railways, and Airfields* (pp. 133–143).

Fannin, R. J., & Raju, D. M. (1993). Large-scale pull-out test results on geosynthetics. In *Proceedings of Geosynthetics Conference* (pp. 633–643).

Farrag, K., Acar, Y. B., & Ilan, J. (1993). Pull-out resistance of geogrid reinforcements. *Geotextiles and Geomembranes*, 133–159.

Farrag, K., & Griffin, P. (1993). Pull-out testing of geogrids in cohesive soils. In J. Cheng (ed.), *Geosynthetic Soil Reinforcement Testing Procedures, ASTM STP 1190* (pp.76–89).

Gabr, M., (2001). Cyclic Plate Loading Tests on Geogrid Reinforced Roads, Research Rep. to Tensar Earth Technologies, Inc., NC State Univ.

George, A. M., Banerjee, A., Puppala, A. J., & Saladhi, M. (2021). Performance evaluation of geocell-reinforced reclaimed asphalt pavement (RAP) bases in flexible pavements. *International Journal of Pavement Engineering*, *22*(2), 181–191.

Geosynthetic Institute. (2021). *GSI members*. Last modified January 2021. https://geosynthetic-institute.org/mem.htm

Giroud, J. P. (2009), An assessment of the use of geogrids in unpaved roads and unpaved areas. In *Proceedings of the Jubilee Symposium on Polymer Geogrid Reinforcement* (pp. 23–36). Institution of Civil Engineers.

Giroud, J. P., & Han, J. (2004a). Design method for geogrid-reinforced unpaved roads. I. Development of design method. *Journal of Geotechnical and Geoenvironmental Engineering*, *130*(8), 775–786.

Giroud, J. P., & Han, J. (2004b). Design method for geogrid-reinforced unpaved roads. II. Calibration and applications. *Journal of Geotechnical and Geoenvironmental Engineering*, *130*(8), 787–797.

Giroud, J. P., & Noiray, L. (1981). Geotextile-reinforced unpaved road design. *Journal of the Geotechnical Engineering Division*, *107*(9), 1233–1254.

Gniel, J., & Bouazza, A. (2009). Improvement of soft soils using geogrid encased stone columns. *Geotextiles and Geomembranes*, 167–175.

Han, J., Yang, X., Parsons, R. L., & Leshchinsky, D. (2007). *Design of geocell-reinforced bases*. Internal Report to PRS, the University of Kansas.

Hegde, A. (2017). Geocell reinforced foundation beds-past findings, present trends and future prospects: A state-of-the-art review. *Construction and Building Materials*, *154*, 658–674.

Holtz, R. D., Christopher, B. R., & Berg, R. R. (1998). *Geosynthetic design and construction guidelines* (FHWA-NHI-95-038). Course No. 13213. Federal Highway Administration.

Holtz, R. D., Christopher, B. R., & Berg, R. R. (2008). *Geosynthetic design and construction guidelines* (FHWA-NHI-07-092). Federal Highway Administration.

Hoppe, E. J., Hossain, M. S., Moruza, A. K., & Weaver, C. B. (2019). *Use of geosynthetics for separation and stabilization in low-volume roadways* (Report No. FHWA/VTRC 20-R8).

Illinois Department of Transportation. (2005). *Subgrade stability manual*. IDOT Bureau of Bridges and Structures. https://idot.illinois.gov/Assets/uploads/files/Doing-Business/Manuals-Guides-&-Handbooks/Highways/Bridges/Geotechnical/Subgrade%20Stability%20Manual.pdf

Illinois Department of Transportation. (2016). *Standard specifications for road and bridge construction*. IDOT. https://idot.illinois.gov/Assets/uploads/files/Doing-Business/Manuals-Guides-&-Handbooks/Highways/Construction/Standard-Specifications/Standard%20Specifications%20for%20Road%20and%20Bridge%20Construction%202016.pdf

Illinois Department of Transportation. (2018). *Bureau of local roads and streets manual*. IDOT. https://idot.illinois.gov/Assets/uploads/files/Doing-Business/Manuals-Guides-&-Handbooks/Highways/Local-Roads-and-Streets/Local%20Roads%20and%20Streets%20Manual.pdf

Illinois Department of Transportation. (2020). *Geotechnical manual*. IDOT. https://idot.illinois.gov/Assets/uploads/files/Doing-Business/Manuals-Guides-&-Handbooks/Highways/Materials/Geotechnical%20Manual.pdf

Illinois Department of Transportation. (2021a). *Illinois construction manual*. IDOT. https://idot.illinois.gov/Assets/uploads/files/Doing-Business/Manuals-Guides-&-Handbooks/Highways/Construction/Construction-Manual/Construction%20Manual.pdf

Illinois Department of Transportation. (2021b, February). *Bureau of design and environment manual*. IDOT. https://idot.illinois.gov/Assets/uploads/files/Doing-Business/Manuals-Guides-&-Handbooks/Highways/Design-and-Environment/Design%20and%20Environment%20Manual,%20Bureau%20of.pdf

ISO 10319. (2015). *Geosynthetics — wide-width tensile test*. International Organization for Standardization.

ISO 13426. (2019). *Geotextiles and geotextile-related products — Strength of internal structural junctions — Part 1: Geocells*. International Organization for Standardization.

Jewell, R. A., Milligan, G.W.E., Sarsby, R.W., & Dubois, D. (1984). Interaction between soil and geogrids. In *Proceedings Symposium on Polymer Grid Reinforcement in Civil Engineering* (pp. 19-29).

Kang, M., Kim, J. H., Qamhia, I. I.A., Tutumluer, E., & Wayne, M.H. (2020). Geogrid stabilization of unbound aggregates evaluated through bender element shear wave measurement in repeated load triaxial testing. *Transportation Research Record*, *2674*(3), 113–125.

Kang, M., Qamhia, I. I.A., Tutumluer, E., Hong, W. T., & Tingle, J. S. (2021). Bender element field sensor for the measurement of pavement base and subbase stiffness characteristics. *Transportation Research Record*. https://doi.org/10.1177%2F0361198121998350

Kermani, B., Xiao, M., Stoffels, S. M., & Qiu, T. (2018). Reduction of subgrade fines migration into subbase of flexible pavement using geotextile. *Geotextiles and Geomembranes*, *46* (4), 377–383. https://doi.org/10.1016/j.geotexmem.2018.03.006

Kermani, B., Stoffels, S. M., & Xiao, M. (2020). Evaluation of effectiveness of geotextile in reducing subgrade migration in rigid pavement. *Geosynthetics International*, *27*(1), 97–109. https://doi.org/10.1680/jgein.19.00052

Kief, O. (2015). Structural pavement design with geocells made of novel polymeric alloy. In *Proceedings of the 2015 Geosynthetics Conference* (pp. 1–10).

Koerner, R. M. (2012). *Designing with geosynthetics*. Prentice Hall.

Konietzky, H., & Keip, M. A. (2005). *PFC3D discrete element modeling of geogrid pullout Tests* (Interim Progress Report). Prepared for Tensar Earth Tech., Inc., ITASCA Consultants GmbH, Gelsenkirchen, Germany.

Kwon, J., & Tutumluer, E. (2009). Geogrid base reinforcement with aggregate interlock and modeling of associated stiffness enhancement in mechanistic pavement analysis. *Transportation Research Record*, *2116*(1), 85–95. https://doi.org/10.3141/2116-12

Kwon, J., Tutumluer, E., & Al-Qadi, I. L. (2009). Validated mechanistic model for geogrid base reinforced flexible pavements. *ASCE Journal of Transportation Engineering*, 135(12), 915–926.

Kwon, J., Tutumluer, E., & Kim, M. (2005). Development of a mechanistic model for geogrid reinforced flexible pavements. *Geosynthetics International*, *12*(6), 310–320.

Kwon, J., Tutumluer, E., & Konietzky, H. (2007). Aggregate base residual stresses affecting geogrid reinforced flexible pavement response. *International Journal of Pavement Engineering*.

Lee, J. S., & Santamarina, J. C. (2005). Bender elements: Performance and signal interpretation. *Journal of Geotechnical and Geoenvironmental Engineering*, *131*(9), 1063–1070.

Luo, R., Gu, F., Luo, X., Lytton, R. L., Hajj, E. Y., Siddharthan, R. V., Elfass, S., Piratheepan, M., & Pournoman, S. (2017). *Quantifying the influence of geosynthetics on pavement performance* (NCHRP Report No. 235). NCHRP. https://doi.org/10.17226/24841

Luo, R., & Prozzi, J. A. (2009). Combining geogrid reinforcement and lime treatment to control dry land longitudinal cracking. *Transportation Research Record*, *2104*(1), 88–96.

McDowell, G. R., Harireche, O., Konietzky, H., Brown, S. F., & Thom, N. H. (2006). Discrete element modelling of geogrid-reinforced aggregates. *Geotechnical Engineering*, *159*, 35–48.

Mishra, D., & Tutumluer, E. (2012). Effectiveness of geotextiles in unsurfaced pavements over weak subgrade evaluated from accelerated field testing. In *Advances in Transportation Geotechnics II—Proceedings of the 2nd International Conference on Transportation Geotechnics* (pp. 492–497). https://doi.org/10.1201/b12754-72

Mishra, D., Qian, Y., Kazmee, H., & Tutumluer, E. (2014). Investigation of geogrid-reinforced railroad ballast behavior using large-scale triaxial testing and discrete element modeling. *Transportation Research Record*, *2462*(1), 98–108.

Moaveni, M., Wang, S., Hart, J. M., Tutumluer, E., & Ahuja, N. (2013). Evaluation of aggregate size and shape by means of segmentation techniques and aggregate image processing algorithms. *Transportation Research Record: Journal of the Transportation Research Board*, *2335*, 50–59.

Moussa, A., Shalaby, A., Kavanagh, L., & Maghoul, P. (2019). Use of rigid geofoam insulation to mitigate frost heave at shallow culvert installations. *Journal of Cold Regions Engineering*, *33*(3), 05019003.

Norwood, G. J. (2019). *Cyclic plate testing of reinforced airport pavements—Phase I: Geogrid* (Report

No. DOT/FAA/TC-19/30. Federal Aviation Administration William J. Hughes Technical Center Aviation Research Division.

Paradox (2012). *Unpaved access road over muskeg/poor soil, MEG Energy, Christina Lake site, north of Conklin, AB*. Retrieved June 15, 2021, from, https://www.paradoxaccess.com/project-details/meg-energy-christina-lake-4, https://cdn2.hubspot.net/hubfs/5953629/2019-digital-assets-downloadable-resources/CS_2012_LS_MEGEnergy_accessroad_ChristinaLake_101017.pdf

Perkins, S. W., and Ismeik, M. (1997). *A synthesis and evaluation of geosynthetic-reinforced base layers in flexible pavements-part II*. Geosynthetics International, 4(6), 605-621.

Perkins, S. W. (2001). *Mechanistic-empirical modeling and design model development of geosynthetic reinforced flexible pavements: Final report*. (Report No. FHWA/MT-01/002/99160-1A). Montana Department of Transportation.

Perkins, S. W., Christopher, B. R., Cuelho, E. L., Eiksund, G. R., Hoff, I., Schwartz, C. W., Svanø, G., & Want, A. (2004). *Development of design methods for geosynthetic reinforced flexible pavements* (Report No. DTFH61-01-X-00068). Federal Highway Administration.

Perkins, S. W., & Salvano, G. (2004). Assessment of interface shear growth from measured geosynthetic strains in a reinforced pavement subject to repeated loads. In *Proceedings of the 8th International Conference on Geosynthetics*.

Pokharel, S. K. (2010). *Experimental study on geocell-reinforced bases under static and dynamic loading*. Doctoral dissertation, University of Kansas.

PRESTO. (n.d.). Geoweb Load Support. Retrieved May 24, 2021, from, https://www.prestogeo.com/products/soil-stabilization/geoweb-load-support/

PRESTO. (2019). *Geoweb Soil Stabilization System: Material specification*. PRESTO Geosystems. https://www.prestogeo.com/wp-content/uploads/2016/10/GW-geoweb-material-specification.pdf

Qamhia, I. I., & Tutumluer, E. (2021). *Review of improved subgrade and stabilized subbases to evaluate performance of concrete pavements* (Report No. FHWA-ICT-21-011). https://doi.org/10.36501/0197-9191/21-016

Qian, Y., Mishra, D., Tutumluer, E., & Kwon, J. (2013). Comparative evaluation of different aperture geogrids for ballast reinforcement through triaxial testing and discrete element modeling. In *Proceedings of Geosynthetics 2013 Conference*.

Qian, Y., Tutumluer, E., Mishra, D., & Kazmee, H. (2018). Triaxial testing and discrete-element modelling of geogrid-stabilized rail ballast. *Proceedings of the Institution of Civil Engineers: Ground Improvement*, *171*(4), 223–231.

Rao, C., Tutumluer, E., & Kim, I.T. (2002). Quantification of coarse aggregate angularity based on image analysis. *Transportation Research Record: Journal of the Transportation Research Board*, 1787, 117–124.

Roodi, G. H. (2016). *Analytical, experimental, and field evaluations of soil-geosynthetic interaction under small displacements*. Ph.D. dissertation, The Univ. of Texas, Austin.

Roodi, G. H., & Zornberg, J. G. (2017). Stiffness of soil-geosynthetic composite under small displacements: II. *Experimental Evaluation. J. Geotech. Geoenviron. Eng*., *143*(10).

Roodi, G. H., Zornberg, J. G., Aboelwafa, M. M., Phillips, J. R., Zheng, L., & Martinez, J. (2018). *Soil-geosynthetic interaction test to develop specifications for geosynthetic-stabilized roadways* (Report No. FHWA/TX-18/5-4829-03-1). University of Texas at Austin, Center for Transportation Research.

Schary, Y. (2020). Case studies on geocell-based reinforced roads, railways and ports. In *Geocells* (pp. 387–411). Springer, Singapore.

Steward, J. E., Mohney, J., & Williamson, R. (1977). *Guidelines for use of fabrics in construction and maintenance of low-volume roads*. USDA, Forest Service.

Signore, J. M., & Dempsey, B. J. (2002). Accelerated testing procedures for evaluating separation layer performance in open-graded base courses. *Transportation Research Record*, *1808*(1), 134–143. https://doi.org/10.3141/1808-16

Tingle, J. S., & Webster, S. L. (2003). Corps of Engineers design of geosynthetic-reinforced unpaved roads. *Transportation Research Record: Journal of the Transportation Research Board*, *1849*(1), 193–201.

Tutumluer, E., Dombrow, W., & Huang, H. (2008). Laboratory characterization of coal dust fouled ballast behavior. *Proceedings of the AREMA 2008 Annual Conference*.

Tutumluer, E., Huang, H., Hashash, Y. M. A., & Ghaboussi, J. (2006). Aggregate shape effects on ballast tamping and railroad track lateral stability. In *Proceedings of the 2006 AREMA Annual Conference*.

Tutumluer, E., Huang, H., Hashash, Y. M. A., & Ghaboussi, J. (2007). Discrete element modeling of railroad ballast settlement. In *Proceedings of the 2007 AREMA Annual Conference*.

Tutumluer, E., Huang, H., Hashash, Y. M. A., & Ghaboussi, J. (2009). AREMA gradations affecting ballast performance using discrete element modeling (DEM) approach. In *Proceedings of the AREMA 2009 Annual Conference*.

Tutumluer, E., Rao, C., & Stefanski, J. (2000). *Video image analysis of aggregates* (Report No. FHWA-IL-UI-278). University of Illinois Urbana-Champaign.

US Army Corps of Engineers. (2003, February 14). *Use of geogrids in pavement construction*. ETL 1110-1-189. U.S. Army Corps of Engineers.

U.S. Departments of the Army and Air Force (1995). *Engineering Use of Geotextiles*. Army Technical Manual TM 5-818-8 (Air Force Joint Manual AFJMAN 32-1030). U.S. Departments of the Army and Air Force

Wang, F., Han, J., Zhang, X., & Guo, J. (2017). Laboratory tests to evaluate effectiveness of wicking geotextile in soil moisture reduction. *Geotextiles and Geomembranes*, *45*(1), 8–13.

Webster, S. L. (1993). *Geogrid reinforced base courses for flexible pavements for light aircraft: Test section construction, behavior under traffic, laboratory tests, and design criteria* (Technical Report GL-93-6). US Army Corps of Engineers Waterways Experiment Station.

Wu, H., Yao, C., Li, C., Miao, M., Zhong, Y., Lu, Y., & Liu, T. (2020). Review of application and

innovation of geotextiles in geotechnical engineering. *Materials*, 13(7). https://doi.org/10.3390/ma13071774

van Gurp, C.A.P.M. and van Leest, A.J. (2002). Thin asphalt pavements on soft soil, In proceedings of the 9th International Conference on Asphalt Pavements, ISAP, Copenhagen, pp. 1-18.

Vavrik, W. (2018). Recommended practice for incorporating geogrids in ME pavement design. Presentation at the Tensar International Congress, Roatan, Honduras, by Bill Vavrik of Applied Research Associates on July 26, 2018.

Yang, X., Han, J., Pokharel, S. K., Manandhar, C., Parsons, R. L., Leshchinsky, D., & Halahmi, I. (2012). Accelerated pavement testing of unpaved roads with geocell-reinforced sand bases. *Geotextiles and Geomembranes*, 32, 95–103.

Yeo, K. C. (2008). Properties of geotextiles. Retrieved June 15, 2021, from, http://www.service.hkpc.org/hkiemat/previous/2008/mastec03_notes/KYEO.PDF

Zhang, X., Presler, W., Li, L., Jones, D., & Odgers, B. (2014). Use of wicking fabric to help prevent frost boils in Alaskan pavements. *J. Mater. Civ. Eng.*, *26*(4), 728–740. https://doi.org/10.1061/(ASCE)MT.1943-5533.0000828

Zornberg, J. G. (2017a). Functions and applications of geosynthetics in roadways. *Procedia Engineering*, *189*, 298–306.

Zornberg, J. G. (2017b). Functions and applications of geosynthetics in roadways, part II. *Geosynthetics Magazine*, 34–40.

Zornberg, J., & Christopher, B. (2007). *The Handbook of Groundwater Engineering, 2nd Edition*, CRC Press, Retrieved from https://www.caee.utexas.edu/prof/zornberg/pdfs/BC/Zornberg _Christopher_2007.pdf

Zornberg, J. G., & Gupta, R. (2009). Reinforcement of pavements over expansive clay subgrades. In *Proceedings of the 17th International Conference on Soil Mechanics and Geotechnical Engineering* (pp. 765–768).

Zornberg, J. G., & Tutumluer, E. (2020). Geosynthetics in pavements, Discussion Session Presentation, DS 3-GPV, 4th Pan-American Conference on Geosynthetics, GeoAmericas 2020, October 27, 2020.

Zornberg, J. G., Roodi, G. H., & Gupta, R. (2017). Stiffness of soil-geosynthetic composite under small displacements: I. Model Development. *J. Geotech. Geoenviron. Eng.*, *143*(10).

APPENDIX A: DESIGN METHODS FOR UNPAVED ROADS

STEWARD ET AL. (1977) METHOD

The design method proposed by Steward et al. (1977) is based on the subgrade restraint function using geotextiles. The concept of reducing soil movement and soil strain is emphasized, and the geotextile used for confinement can restrain soils against shear failure at low stresses. The soil is expected to hold higher bearing capacity given the soil and geotextile interaction. Such restraint mechanism will predominate only for weak soils stressed to levels at which the soil would fail or rut without the inclusion of a geotextile. Subgrades with CBR values less than or equal to 2 or 3 hold economic benefits in reducing structural thickness based on the restraint mechanism, while for subgrades with CBR values higher than 2 or 3, the separation or filtration function will also be considered predominant functions.

From laboratory model studies using aggregates and geotextiles over soft soils, Barenberg et al. (1975) concluded that the allowable stress (q in Figure 44) on a soft soil under repeated loading could be predicted using the undrained shear strength of the soils (C in Figure 44) and the bearing capacity factor (N_c in Figure 44).

$$q = CN_c$$

Figure 44. Equation. Allowable stress on a soft soil under repeated loading.

The concept of the method is to design sufficient thickness of the base material. The stress on top of the subgrade is calculated using Boussinesq's one-layer solution based on a uniform homogenous elastic half-space, to ensure it does not exceed the allowable stress of the subgrade. Considering vehicle passes, equivalent axle load, tire pressure, subgrade strength, and rut depth, the bearing capacity factor (N_c) proposed by Barenberg et al. (1975) is summarized in Table 15 under different rutting and traffic conditions.

Table 15. Bearing Capacity Factor under Different Conditions

Condition	Rut mm (in.)	Traffic (Passes of 18 kip (80 kN) axle equivalents)	Bearing Capacity Factor, N_c
Without Geotextiles	$< 50\ mm\ (2\ in.)$	$> 1{,}000$	2.8
	$> 100\ mm\ (4\ in.)$	< 100	3.3
With Geotextiles	$< 50\ mm\ (2\ in.)$	$> 1{,}000$	5.0
	$> 100\ mm\ (4\ in.)$	< 100	6.0

Several curves are presented in each chart in Figure 45 for determining the aggregate layer thickness (mentioned as depth for different single, dual, and tandem loading conditions). The curves were developed to reduce stresses from the wheel loads to the allowable level for different combinations of CN_c by incorporating the bearing capacity factors for changing soil shear strengths. These establish the design curves for this method.

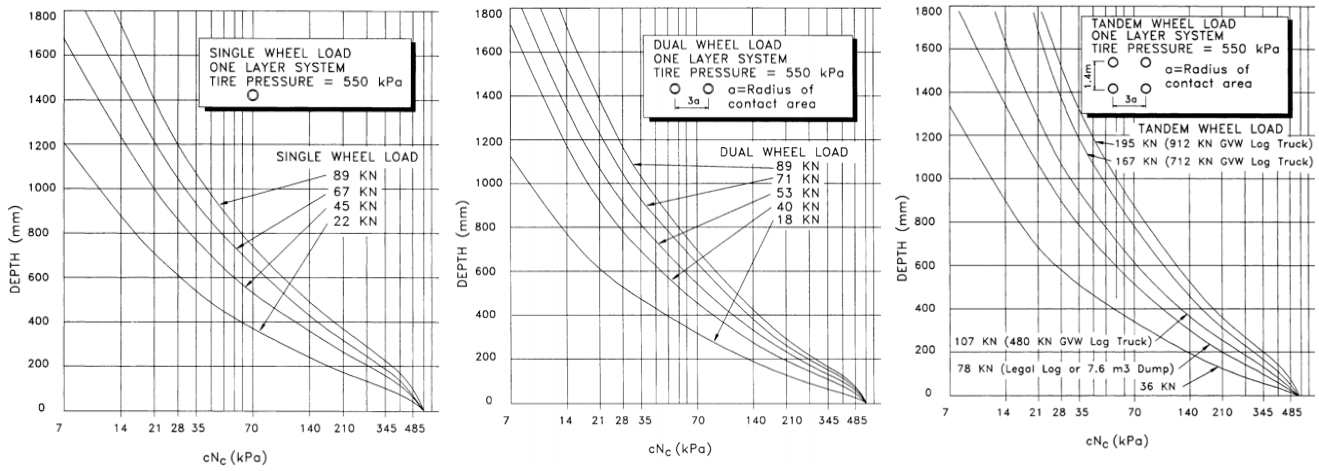

A. B. C.

Figure 45. Graph. US Forest Service thickness design curve (Steward et al., 1977; Holtz et al., 1998) for a) single, b) dual, and c) tandem wheel loads.

Design Procedure

The design procedure using the Steward et al. (1977) method is summarized as follows:

a) Determine the undrained shear strength (*C*) of the subgrade soil using available tests. For example:

- Field California Bearing Ratio (CBR) test (Figure 46).

$$C(kPa) = 30 \times CBR$$

Figure 46. Equation. Determination of undrained shear strength using field CBR test.

- Cone penetration test (Figure 47).

$$C = \frac{Cone\ index}{10}\ or\ \frac{Cone\ index}{11}$$

Figure 47. Equation. Determination of undrained shear strength using cone penetration test.

- Vane shear test where the undrained shear strength (*C*) is directly measured.

b) Determine traffic condition (e.g., wheel loading, amount of traffic) and allowable rutting. Obtain the bearing capacity factor(s) from Table 15.

c) Select design thickness using Figure 45.

d) Check geotextile drainage and filtration characteristics.

e) Determine geotextile survivability requirements. Specify geotextile property requirements and construction requirements.

The limitations of the Steward et al. (1977) method are listed below.

- The method fails to consider the base material properties using Boussinesq's one-layer solution for load distribution.
- The rut depth influence and number of passes are estimated and limited to two cases.
- Theoretical background of bearing capacity factors is not included.
- The tensioned membrane effect of geotextiles is not included.
- The design is limited to geotextiles, and no geotextiles property is considered (only design with or without geotextiles).

GIROUD AND NOIRAY (1981) METHOD

The Giroud and Noiray (1981) method was established as an improvement to the Steward et al. method to more accurately reduce the base thickness when geotextiles were used in the design. The method presented by Giroud and Noiray is also for cohesive subgrade soils and mostly applicable to roads subjected to light to medium traffic. The design procedure is summarized as follows:

a) Determine the required base thickness for an unreinforced case under traffic in terms of number of passes using the simplified US Army Corps method (h_0').

b) Determine the required base thickness for the unreinforced and reinforced case under a static load (h_0 and h_r).

c) Determine the reduction of base thickness ($\Delta h = h_0 - h_r$).

d) Determine the required base thickness for the reinforced case ($h' = h_0' - \Delta h$).

The design is based on the limit equilibrium bearing capacity theory with consideration of the tensioned membrane effect. The applied stress is determined by considering elastic limit plus the base aggregate overburden stress on subgrade. The stress level applied on top of the subgrade without a geotextile is given by the equation in Figure 48, which is the quasi-static analysis concerning theories of elasticity in the case of a loaded aggregate layer. The load applied on the subgrade soil by a dual wheel and by the weight of aggregate layer is equivalent to a uniform pressure presented in Figure 48.

$$p = \frac{P}{2 * (B + 2 * h_0 * tan \propto)(L + 2 * h_0 * tan \propto)} + \gamma * h_0 = \pi c_u + \gamma * h_0$$

Figure 48. Equation. Stress level on top of subgrade.

where p is the stress level on top of subgrade, c_u is the undrained cohesion of the frictionless soil (in Pascals), P is the axle load, and B, L are the loaded area dimensions. γ is the unit weight of aggregate layer, h_0 is the base layer thickness, and $tan\ \alpha$ is usually taken as 0.6. The variables are defined in Figure 49.

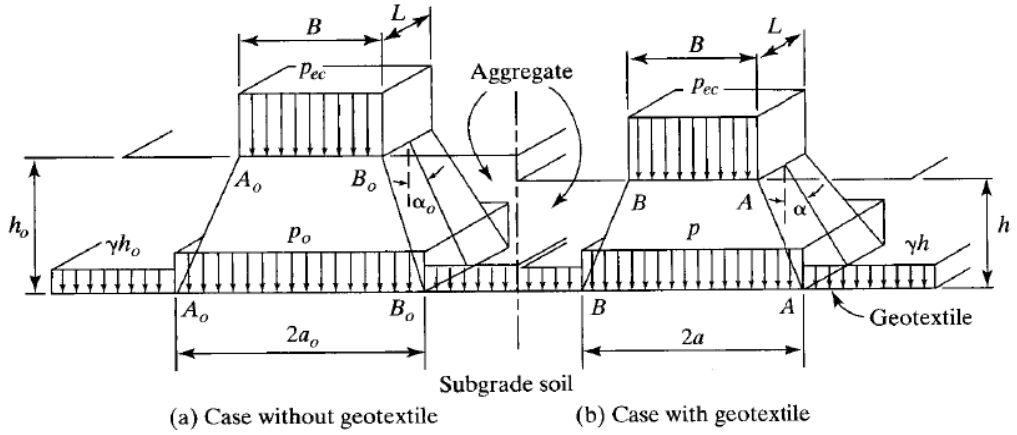

Figure 49. Illustration. Load distribution in an unpaved road with and without geotextile.

Source: Giroud and Noiray (1981)

Once the geotextile is included in the design, the pressure applied on top of the subgrade is reduced. Meanwhile, the elastic behavior of the subgrade can be turned into plastic behavior. Therefore, the equation in Figure 50 gives the vertical stress level applied on the subgrade:

$$p - p_g = (\pi + 2)c_u + \gamma h_r$$

$$\frac{P}{2 * (B + 2 * h_r * tan \propto)(L + 2 * h_r * tan \propto)} - p_g = (\pi + 2)c_u$$

Figure 50. Equation. Stress level after geotextile is placed.

where $\mathrm{p_g}$ is the reduction of pressure resulting from the use of a geotextile in Pascals.

The geotextile is expected to exhibit a wavy shape under the two-wheel loadings and the in-between heave with stretch. The membrane effect takes place, and the two benefits provided by a geotextile are as follows: 1) confinement of the subgrade soil between and beyond the wheels and 2) reduction of the pressure applied by the wheels on the subgrade soil. Based on this theory, the reduction of pressure resulting from the use of a geotextile is quantified as:

$$p_g = \frac{K\epsilon}{a\sqrt{1 + \left(\frac{a}{2s}\right)^2}}$$

Figure 51. Equation. Reduction of pressure resulting from the use of geotextile.

where ϵ is the elongation of the geotextile, K is the geotextile modulus, a is the half length of the chord subtended by the wheel load, and s is the rut depth.

Note that the contribution of geotextile resistance is defined through the tensioned membrane effect, and the Giroud and Noiray (1981) method is the only one that provides the quantification of the tensioned membrane effect. Based on the calculations using the Giroud and Noiray (1981) method, the tensioned membrane effect can be approximately accounted for by multiplying the calculated base thickness by a base reduction factor (R_{TM}). However, when the rut depth is smaller than 75 mm (3 in.), R_{TM} is approximately equal to 1, which indicates the contribution of geotextile resistance through the tensioned membrane effect is negligible. When rut depth increases, R_{TM} becomes below 1 (e.g., when rut depth is 95 mm [3.7 in.], R_{TM} is approximately equal to 0.98). Note that for the tensioned membrane (stretched geotextile) to carry any load, ruts larger than 100 mm (4 in.) are essentially needed.

Practical charts are put forward to simplify the calculation process. Two sets of curves are presented with one giving h_0' as a function of the traffic and the other giving Δh as a function of the geotextile modulus. An example of series of such charts is given in Figure 52 to determine h_0' and Δh given specific traffic patterns and geotextile properties.

The limitations of the Giroud and Noiray (1981) method are listed below.

- The method does not consider the base material quality and uses a fixed stress distribution angle.
- The base thickness reduction design is based on static loading rather than cyclic loading.
- No difference among all geosynthetic materials is presented in the method.
- The influence of rut depth is based on the empirical relationship for paved roads.

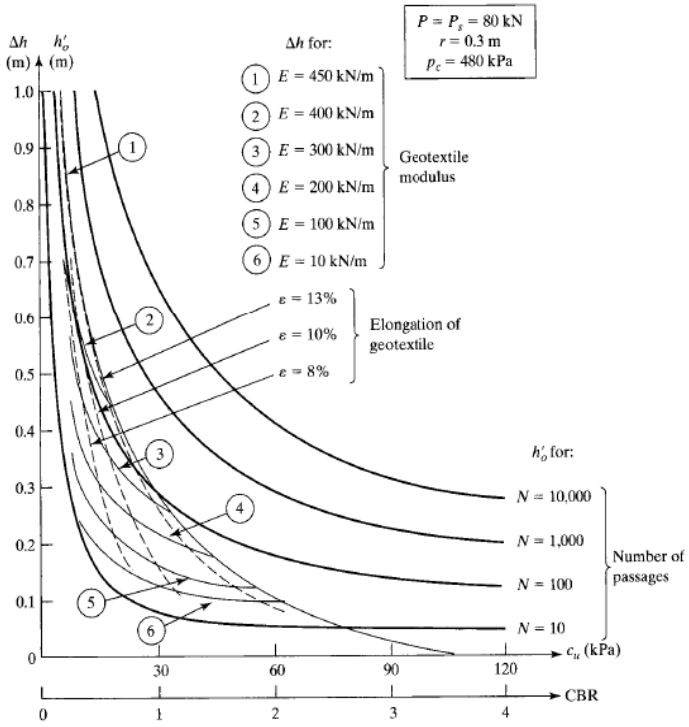

Figure 52. Graph. Design curves with h_0' and Δh for unpaved roads.

Source: Giroud and Noiray (1981)

DUTCH (CROW) DESIGN (2002) METHOD

The Dutch (CROW) Design (2002) method also emphasizes the important function of geosynthetics in terms of base layer thickness reduction. The design procedure is summarized as follows:

a) Design the required base thickness (h_d) for an unreinforced section using the equation in Figure 53.

$$h_d = \frac{125.7 \times \log(N_{const}) + 496.52 \times \log(P) - 294.14 \times RD_{constr} - 2412.42}{f_{undr}^{0.63}}$$

Figure 53. Equation. Thickness reduction calculated using Dutch (CROW) design method.

where f_{undr} is the undrained shear strength of subgrade in Pascals and can be estimated using CBR value ($f_{undr}(Pa) = 20{\sim}30 * CBR$); N_{const} is the number of axle loads during construction, which should be less than 1,000; P is the wheel load; and RD_{constr} is the base thickness reduction factor, which can be obtained from Figure 54, based on geosynthetic properties.

b) Determine applicability of the geosynthetics.

c) Determine reduction of layer thickness.

Note that the absolute value of reduction of layer is limited to 150 mm (6 in.) and the minimum layer thickness of the reinforced base is 150 mm (6 in.).

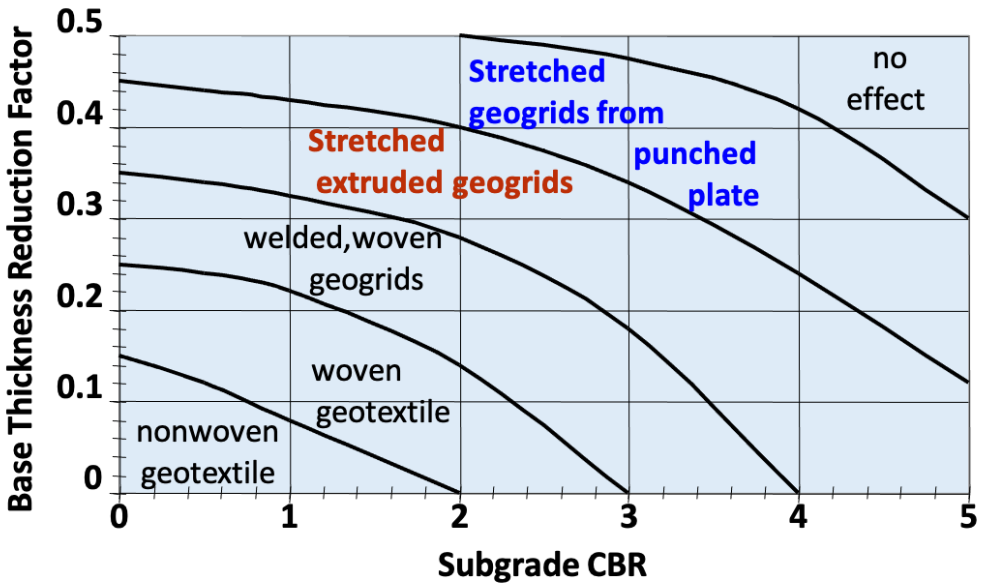

Figure 54. Graph. Base thickness reduction factor using Dutch (CROW) design method.

Source: CROW Design Method (van Gurp & van Leest, 2002)

ARMY CORPS OF ENGINEERS (2003) METHOD

The design method employed by the US Army Technical Manual 5-818-8 (U.S. Departments of the Army and Air Force, 1995) for geotextile-reinforced low-volume unpaved roads is based on the methodology proposed by Steward et al. (1977), which considers the reinforcement function of geotextile in increasing subgrade load-bearing capacity. Tingle and Webster (2003) studied the US Army Corps of Engineers (USACE) approach and modified the criteria for the addition of stiff biaxial geogrid. Historical data were reviewed from a full-scale test section constructed in 1995 under controlled conditions and trafficked with military vehicles, as shown in Figure 55. A high-plasticity clay (CH) subgrade constructed to a design CBR of 1 was constructed. The base course thicknesses and geosynthetics used for each section were based on the criteria presented in Army Technical Manual 5-818-8 and presented in Figure 55. Bearing-capacity factors, N_c, of 2.8 and 5.0 as proposed by Steward et al. (1977) were used for all sections. The design shear strength value of 3.6 psi (computed from as-constructed subgrade strength of 0.7 × CBR shown in Figure 56) was used. Each item was designed to exhibit similar deterioration for a design traffic level of 2,000 military truck passes.

The results of the full-scale test were used for comparison with the design method by the US Army Technical Manual 5-818-8. The aggregate thickness and subgrade strength of each test item were used to back-calculate the experimental value of N_c using Figure 57. Note that the authors presented that the average experimental rut depths [61 mm (2.4 in.) to 76 mm (3.0 in.) for 2,000 truck passes] were reasonable and representative of the conditions applicable to using the design method.

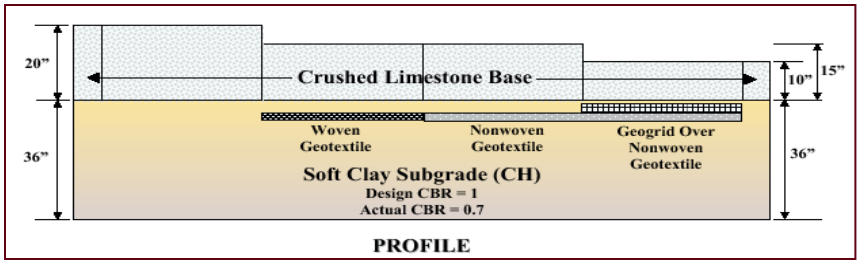

Figure 55. Illustration. Layout of 1995 test section profile (not to scale).

Source: Tingle & Webster (2003)

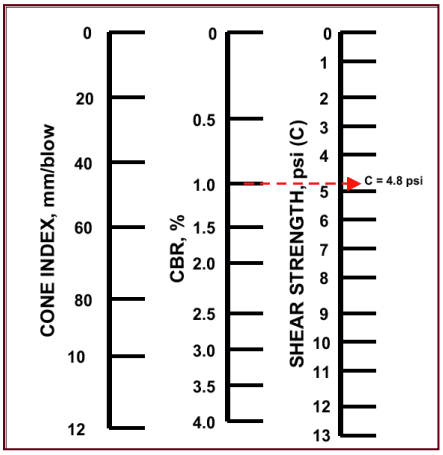

Figure 56. Graph. Shear strength conversion nomograph from USACE design method.

Source: Tingle & Webster (2003)

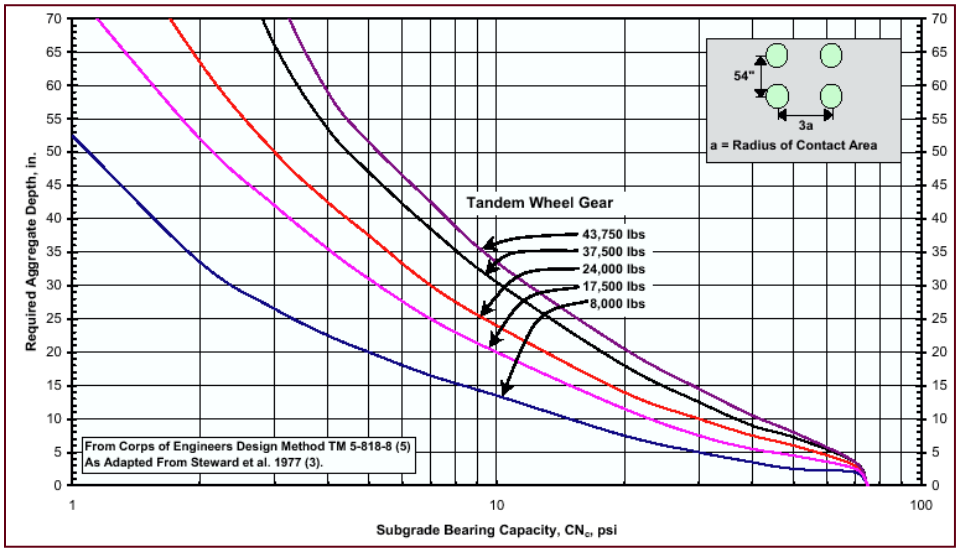

Figure 57. Graph. Dual-tandem (one-layer system, tire pressure = 552 kPa [80 psi]) design curve from USACE design method.

Source: Tingle & Webster (2003)

The experimental calculated N_c values are presented in Table 16. Tingle and Webster (2003) recommended the N_c of 5.0 continue to be used until additional conclusive evidence is developed for its revision. However, for a conservative design of geotextile-reinforced unpaved roads, N_c of 3.6 should be used. N_c of 5.8 should be used for the design of unpaved roads reinforced with both a geotextile and a geogrid under soft cohesive subgrade conditions. Additional field tests were recommended to be conducted to further validate the design method and parameters.

Table 16. Theoretical and Experimental Bearing Capacity Factors

Section	Rut mm (in.)	Traffic*	Bearing Capacity Factor N_c	
			Theoretical	Experimental
Unreinforced	$< 50\ mm\ (2\ in.)$	$> 1{,}000$	2.8	2.6
Geotextile	$< 50\ mm\ (2\ in.)$	$> 1{,}000$	5.0	3.6
Geotextile and Geogrid	–	–	–	5.8

Source: Tingle & Webster (2003)

* Sections were trafficked with a M923 5-ton military truck loaded to a gross vehicle weight of 43.5 kips (194 kN)

GIROUD AND HAN (2004) METHOD

A method for geosynthetic design for unpaved roads was proposed by Giroud and Han (2004a; 2004b). The design method was developed for geogrid-reinforced unpaved roads, although it can also be used for geotextile-reinforced unpaved roads and unreinforced roads with appropriate values of relevant parameters. The method is based on Burmister's two-layer solution and data from cyclic plate load tests by Gabr (2001). Several improvements this methodology has over the method by Giroud-Noiray (1981) are as follows:

- Considers changes in the stress distribution angle in the base layer.
- Considers the number of load repetitions and the desired performance.
- Uses calibrated and verified with full-scale test data.
- Considers the base quality with the modulus / strength input.
- Considers aperture stability modulus of the geogrid and, accordingly, differentiates contribution by the types and properties of geosynthetic materials.

Currently, this is the most used methodology for the design of geosynthetic-reinforced unpaved roads. A single expression is developed that determines the required base course thickness shown in Figure 58.

$$h = \frac{0.868 + (0.661 - 1.006J^2)\left(\frac{r}{h}\right)^{1.5}}{1 + 0.204[R_E - 1]} logN \left[\sqrt{\frac{\frac{P}{\pi r^2}}{\left(\frac{s}{f_s}\right)\left[1 - 0.9exp\left(-\left(\frac{r}{h}\right)^2\right)\right] N_c \cdot f_c \cdot CBR_{sg}}} - 1 \right] r$$

Figure 58. Equation. Thickness design equation by Giroud & Han (2004b).

where *h* is base course thickness (m); R_E is limited modulus ratio of base course to subgrade soil; *r* is equivalent radius for the contact area of the tire (m); *P* is wheel load (kN); *J* is aperture stability modulus of the geogrid; f_s is rut depth factor (often assumed to be 75 mm); f_c is factor relating CBR of subgrade to equivalent undrained cohesion (equal to 30 kPa); *s* is allowable rut depth (mm); *N* is number of equivalent single (80-kN or 18-kip) axle passes; N_c is bearing capacity factor (5.71 for geogrid reinforcement, 5.14 for geotextile reinforced, and 3.14 for unreinforced); and CBR_{sg} is the California Bearing Ratio of the subgrade soil.

The limited modulus ratio of base course to subgrade soil is calculated using the equation in Figure 59 and according to the data collected from the field. This ratio (R_E) should be limited to a maximum value of 5.0.

$$R_E = \min\left(\frac{E_{bc}}{E_{sg}}, 5.0\right) = min\left(\frac{3.48{CBR_{bc}}^{0.3}}{CBR_{sg}}, 5.0\right)$$

Figure 59. Equation. Modulus ratio of base course to subgrade soil.

where E_{bc} and E_{sg} are the resilient moduli of the base course and subgrade soil, respectively, and CBR_{bc} and CBR_{sg} are the CBR values of the base course and subgrade soil, respectively.

The aperture stability modulus of geogrid can be determined from the standard test method for determining the aperture stability modulus of geogrid (ASTM D7864 / D7864M [2015e]).

The design chart where design thickness can be determined along with the CBR of subgrade is presented in Figure 60. For unreinforced unpaved roads, *J* = 0 and N_c = 3.14. For geotextile-reinforced unpaved roads, *J* = 0 and N_c = 5.14 and for geogrid-reinforced unpaved roads, $J > 0$ and N_c = 5.71.

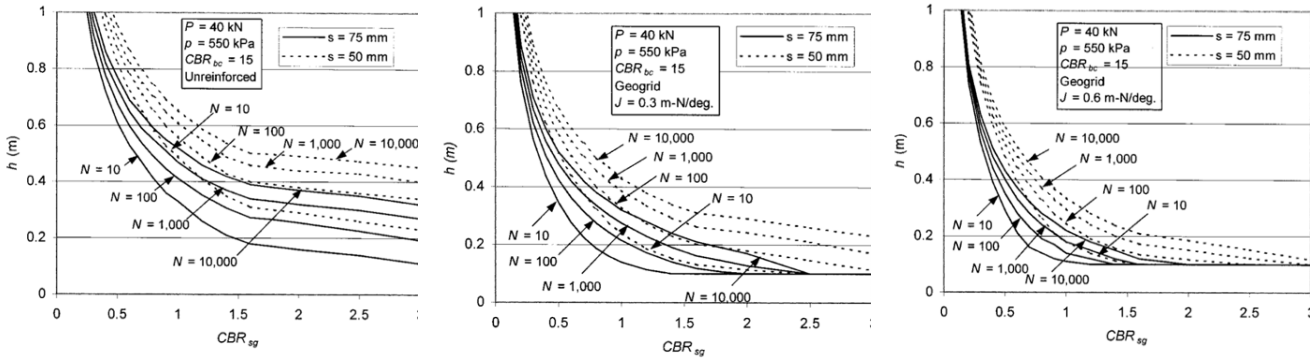

A. B. C.

Figure 60. Graph. Design chart for unreinforced and geogrid-reinforced roads: a) unreinforced, b) geogrid-reinforced with aperture stability modulus of the geogrid as 0.3m-N/°, c) geogrid-reinforced with aperture stability modulus of the geogrid as 0.6m-N/°.

The Giroud and Han (2004a, 2004b) method has some limitations that can only be applied to specific conditions:

- Rut depth ranges from 50 mm to 100 mm (2 in. to 4 in.) and, meanwhile, the tensioned membrane effect is not considered; note that it is negligible for rut depths less than 100 mm (4 in.).
- Field subgrade CBR must be less than 5, and the maximum ratio of base course modulus to subgrade soil modulus is 5.
- Maximum number of passes is limited to 10,000 Equivalent Single Axle Loads (ESALs).
- The influence of geosynthetics (geotextiles and geogrids) is considered through the bearing capacity factor.
- A minimum thickness of 100 mm (4 in.) of base course aggregate is needed.

The above limitations are expected to change as additional empirical data are available, according to Giroud and Han (2004b). However, some limitations are within expectations. For example, typical conditions for unpaved roads over soft subgrade are that the maximum number of passes is limited to 10,000 ESALs and the subgrade CBR must be less than 5.

ILLINOIS DEPARTMENT OF TRANSPORTATION *SUBGRADE STABILITY MANUAL* (2005)

According to Illinois Department of Transportation (IDOT), remedial procedures are required for any subgrade with a CBR, or immediate bearing value (IBV), less than 6. In the current IDOT *Subgrade Stability Manual* (*SSM*) (2005), it is pointed out that when a geosynthetic is placed at the subgrade / aggregate interface, subgrade restraint may occur to increase the support of the construction equipment over a weak subgrade. The tensile resistance and lateral restraint provided by geosynthetics can help reduce rutting in the subgrade when wheel loads are applied. The guidelines for the preliminary aggregate thickness design when using geosynthetics for subgrade restraint are recommended by IDOT as presented in Table 1. The geosynthetics should only be considered when the subgrade is very weak (with an IBV / CI smaller than 3 / 120); the greatest benefits can be achieved when the IBV / CI is 1.5 / 60 or smaller. Note that the allowable rut depth 12.5 mm (0.5 in.) is not included in the geosynthetic analysis, while a rut depth of 50 mm (2 in.) is incorporated. The required thickness of an aggregate layer above subgrade is therefore obtained from Table 1. The minimum aggregate thickness is 152 mm (6 in.) and maximum thickness reduction is 152 mm (6 in.) when geotextiles / geogrids are considered in design.

According to the above guidelines by the IDOT *SSM* (2005), engineering properties of geosynthetics may vary from types and brands, and no generic specifications could be applied currently for subgrade restraint. There are also cases when both a geotextile and a geogrid are required because geotextiles can be effective in preventing the intermixing of the subgrade and the aggregate, while geogrids can provide subgrade restraint. This combination may or may not be economical. It is

recommended that the District Geotechnical Engineer be consulted in designing the geosynthetic for subgrade restraint.

FHWA NHI-07-092 MANUAL (HOLTZ ET AL., 2008)

The FHWA NHI-07-092 Manual (Holtz et al., 2008) adopted the method proposed by Giroud and Han (2004a, 2004b). The design procedure is summarized as follows:

a) Determine soil subgrade strength in the field using the field CBR, cone penetrometer, vane shear, resilient modulus, or any other appropriate test.

b) Determine the maximum single-, dual-, and dual-tandem wheel loads anticipated for the roadway during the design period.

c) Estimate the maximum amount of traffic anticipated for each design vehicle class.

d) Select allowable rut depth depending on the road use, and calculate the radius of the equivalent rut depth using the equation presented in Figure 61.

$$r = \sqrt{\frac{P}{\pi p}}$$

Figure 61. Equation. Radius of the equivalent rut depth calculation.

where *P* is the wheel load, *r* is the radius of tire contact, and *p* is the tire pressure.

If necessary, determine the undrained shear strength of the subgrade soil from available data or correlations.

e) Check capacity of subgrade soil to support wheel load without reinforcement using the equation presented in Figure 62.

$$P_{h=0,unreinf} = \left(\frac{s}{f_s}\right)\pi r^2 N_c c_u$$

Figure 62. Equation. Capacity of subgrade soil without reinforcement.

where P_h is the support capacity of subgrade, *s* is the allowable rut depth, and f_s is 75 mm (3 in.). N_c is the bearing capacity factor for unreinforced case, which is equal to 3.14, and c_u is the subgrade undrained shear strength. If $P < P_{h=0,unreinf}$, then the subgrade soil can support the wheel load and a minimum thickness of 100 mm (4 in.) base course is recommended to prevent disturbance of the subgrade. If $P > P_{h=0,unreinf}$, the use of reinforcement is required, and the solution continues to the next step.

f) Determine the required base course thickness for reinforced or unreinforced roads using the equation presented in Figure 58. The calculation of the base course thickness requires iteration. The minimum thickness of the base course is 100 mm (4 in.).

APPENDIX B: PROPERTIES AND TESTING METHODS OF GEOSYNTHETIC MATERIALS

GEOGRID PROPERTY TESTS IN ASTM

The type of geogrid to be used for reinforcement and stabilization of pavement foundation is chosen based on physical properties and mechanical behavior. Laboratory testing for the integrity of the geogrids as well as the interference of the geogrids and the stabilized soils are proposed and used for choosing the appropriate geogrid. Koerner (2012) lists several of the mechanical properties that govern the choice of a geogrid. Important physical properties include specific gravity, out-of-plane bending stiffness, and in-plane torsional stiffness. The density of the geogrid is a function of the polymer type from which it is manufactured. Out-of-plane bending stiffness can be determined by ASTM D1388 (2018b), which slides the geogrid on a surface inclined by 41.5 degrees and measures the length required for the geogrid to touch the surface and relates that to the mass or density of the geogrid. The mechanical properties of interest for geogrids and test method specified by ASTM are discussed in this appendix.

- Tensile Properties of Geogrids (ASTM D6637 [2015c]): This test method covers the determination of the tensile strength properties of geogrids by subjecting strips of varying width to tensile loading. Single rib strength and secant modulus are calculated through the test. In addition, wide width tensile strength testing can be carried out for a number of repeated rib units when clamped and tested both in the longitudinal and transverse directions for biaxial geogrids.

- Aperture Stability Modulus (ASTM D7864 [2015e]): This test method covers the procedure for measuring the aperture stability modulus of a geogrid. The test measures in-plane stability of a geogrid by clamping a center node and measuring the stiffness over an area of the geogrid. Aperture stability modulus is referenced in the FHWA Geosynthetics Design and Construction Guidelines NHI-07-092 (Holtz et al., 2008) as an input parameter for the design of geogrid-reinforced unpaved roads using punched and drawn biaxial geogrids.

- Individual Geogrid Junction Strength (ASTM D7737 [2015d]): This test is conducted for determining the strength of an individual geogrid junction, also called a node. The test is configured such that a single rib is pulled from its junction with a rib(s) transverse to the test direction to obtain the maximum force, or strength of the junction. The procedure allows for the use of two different clamps with the appropriate clamp selected to minimize the influence of the clamping mechanism on the specific type of geogrid tested.

GEOTEXTILE PROPERTIES REPORTED BY MANUFACTURERS

There are approximately 13 geotextile manufacturers listed as members of the Geosynthetic Institute, including SOLMAX, TenCate, Huesker, Propex Geosolutions, NAUE, Berry Global Inc., Afitex-Texel, Maccaferri, AGRU, InterGEO Services, Kaytech Group, Owens Corning, and SKAPS. According to the majority of the manufacturers, geotextiles have three categories of properties: mechanical,

hydraulic, and durability. Mechanical properties include five specific attributes that describe the ability of geotextiles, including grab tensile strength, grab elongation, trapezoidal tear strength, CBR puncture resistance, as well as wide width tensile strength and strain (for woven geotextiles). There are three attributes for hydraulic properties, including permittivity, water flow rate, and AOS. Furthermore, durability explains UV resistance after 500 hours.

While geotextiles have two divisions, woven and nonwoven, all manufacturers report the same or similar geotextile properties. FHWA published a manual (Holtz et al., 2008) for geotextile property requirements with explicit explanations. Because there are many accessible products, IDOT can specify properties mentioned previously in generic specifications and choose appropriate products from the market accordingly. Some major products from manufacturers for nonwoven geotextiles are Maccaferri MaxTex N, Propex Geotex, and TENCATE Mirafi. One piece of information that needs to be mentioned is that many commercially available geotextiles might not have their porosity values listed in the specification sheets. For nonwoven geotextiles, porosity must be equal to or greater than 30% in order to meet the clogging criteria. Most commercially available geotextiles will pass such criteria, but one must pay attention to this detail. Some obtainable products include Maccaferri Matex and TENCATE Mirafi H_2Ri. All design parameters like hydraulic properties required to use a geotextile for drainage / separation / filter applications are readily available by manufacturers.

Some recommended values for geotextile properties can be found in Table 17 and Table 18.

Table 17. Geotextile Strength Properties

		Class 1 Geotextiles		Class 2 Geotextiles	
Property	ASTM Test *	Elongation < 50%	Elongation > 50%	Elongation < 50%	Elongation > 50%
Grab Strength	D4632/D4632M	1400 N	1400 N	1100 N	700 N
Sewn Seam Strength	D4632/D4632M	1260 N	1260 N	990 N	630 N
Tear Strength	D4533/D4533M	500 N	500 N	400 N	250 N
Puncture Strength	D6241	2750 N	2750 N	2200 N	1375 N

Source: AASHTO (2017)

* References: ASTM D4632 (2015a), ASTM D4533 (2015b), ASTM D6241 (2014a).

Table 18. Geotextile Hydraulic and Physical Properties

Property	Value
Apparent Opening Size, Sieve No. (mm) ASTM D4751 *	No. 70(0.212 mm) maximum
Permittivity, sec^{-1} ASTM D4491 *	0.1 minimum
Ultraviolet Stability (Retained Strength), %, ASTM D4355/D4355M *	50% after 500 h of exposure

Source: AASHTO (2017)

* References: ASTM D4751 (2020b), ASTM D4491 (2021b), ASTM D4355 (2021c).

GEOTEXTILE PROPERTIES AND REQUIREMENTS FOR STABILIZATION FUNCTION

To provide separation and reinforcement / stabilization functions in saturated or unstable conditions, stabilization geotextiles should be used. To increase the bearing capacity of soft subgrade soils, stabilization geotextiles can help develop vertical restraint beyond the wheel path, and some membrane-induced tension under the wheel path. They can decrease time-dependent rutting by minimizing vertical and shear stresses in the subgrade under the wheel path, and redistributing shear and normal stresses beyond the wheel path. To minimize time-dependent lateral spreading and associated modulus decrease in base aggregate, stabilization geotextiles can help develop lateral restraint and shear resistance to minimize the tendency of unbound aggregates to displace laterally. They can decrease time-dependent rutting by providing an increased modulus of unbound aggregates at the time of construction and minimizing degradation of the modulus of unbound aggregates over time.

According to Hoppe et al. (2019), Virginia DOT requires Class 1 material for subgrade stabilization applications. Note that slit-film woven fabrics are not allowed to be used. For subgrade stabilization geotextiles, the minimum permittivity determined by Virginia DOT is 0.1 sec^{-1}, and the optimal AOS for a geotextile is less than that of a No. 70 sieve opening (0.212 mm). For embankments up to 1.83 m (6 ft) high, the seam strength determined for stabilization geotextiles is 90% of specific grab strength, and the optimal AOS for a geotextile is less than that of a No. 20 sieve size (0.85 mm). Stabilization geotextiles are typically applied between the replacement granular material and the undercut subgrade; they can also work as wrapping fabrics around the open-graded aggregate, which is used in a drainage blanket below the pavement section.

Table 19 presents the properties and requirements for stabilization function, as stated in FHWA NHI-07-092 report (Holtz et al., 2008).

GEOTEXTILE LABORATORY TESTING

To develop geotextile specifications, material properties should be investigated and fully understood by designers. According to Zornberg and Christopher (2007), Table 20 presents the laboratory tests commonly performed on geotextiles. In addition, one of the leading laboratories for testing geosythetics in the United Kingdom, British Textile Technology Group (BTTG™), also offers more laboratory tests to help designers comprehensively understand the properties of geotextiles. Those laboratory tests are listed as follows: determination of the long-term protection efficiency of geotextiles in contact with geosynthetic barriers, compressive properties, compressive creep properties, tensile creep and creep rupture behavior, durability tests, determination of the resistance to weathering, abrasion damage simulation, and so on.

Table 19. Geotextile Property and Requirement for Stabilization

Property	ASTM Test Method *	Units	Separation Application Class 2[1]		Separation Application Class 1[2]	
			Elongation < 50%[3]	Elongation ≥ 50%[3]	Elongation < 50%[3]	Elongation ≥ 50%[3]
Grab Strength	D4632	N	1100	700	1400	900
Sewn Seam Strength [4]	D4632	N	990	630	1260	810
Tear Strength	D4533	N	400[6]	250	500	350
Puncture Strength	D6241	N	2200	1375	2750	1925
Permittivity	D4491	sec^{-1}	0.02[5]		0.05[5]	
Apparent Opening Size	D4751	mm	0.60 max		0.43 max	
Ultraviolet Stability (Retained Strength)	D4355	%	50% after 500 hours of exposure			

Source: adapted from Holtz et al. (2008)

Notes:

[1] Default geotextile selection. Class 1 should be specified for more severe or harsh conditions where there is a greater potential for geotextile damage. The engineer may specify a Class 3 geotextile based on one or more of the following:
- a) The Engineer has found Class 3 geotextiles to have sufficient survivability based on field experience.
- b) The Engineer has found Class 3 geotextiles to have sufficient survivability based on laboratory testing and visual inspection of a geotextile sample removed from a field test section constructed under anticipated field conditions.
- c) Aggregate cover thickness of the first lift over the geotextile exceeds 300 mm (12 in.) and aggregate diameter is less than 50 mm (2 in.).
- d) Aggregate cover thickness of the first lift over the geotextile exceeds 150 mm (6 in.), aggregate diameter is less than 30 mm (1.2 in.), and construction equipment contact pressure is less than 80 psi (550 kPa).

[2] Default geotextile selection. The Engineer may specify a Class 2 or 3 geotextile based on one or more of the following:
- a) The engineer has found the class of geotextile to have sufficient survivability based on field experience.
- b) The engineer has found the class of geotextile to have sufficient survivability based on laboratory testing and visual inspection of a geotextile sample removed form a field test section constructed under anticipated field conditions.

[3] As measured in accordance with ASTM D4632 (2015a).

[4] When sewn seams are required.

[5] Default value. Permittivity of the geotextile should be greater than that of the soil ($\psi_g > \psi_s$). The Engineer may also require the permeability of the geotextile to be greater than that of the soil ($k_g > k_s$).

[6] The required MARV tear strength for woven monofilament geotextiles is 250 N.

* References: ASTM D4632 (2015a), ASTM D4533 (2015b), ASTM D6241 (2014a), ASTM D4491 (2021b), ASTM D4751 (2020b), ASTM D4355 (2021c)

Table 20. Standard Tests for Geotextiles

Property	Test standard *	Test name
Thickness	ASTM D5199	Standard Test Method for Measuring Nominal Thickness of Geotextiles and Geomembranes
Mass per unit area	ASTM D5261	Standard Test Method for Measuring Mass per Unit area of Geotextiles
Grab rupture	ASTM D4632	Standard Test Method for Breaking Load and Elongation of Geotextiles (Grab Method)
Uniaxial tensile strength geotextile	ASTM D4595	Standard Test Method for Tensile Properties of Geotextiles by the Wide-Width Strip Method
Multiaxial tensile, puncture or burst tests	ASTM D6241	Standard Test Method for the Static Puncture Strength of Geotextiles and Geotextile Related Products Using a 50-Mm Probe
Trapezoid tear strength	ASTM D4533	Standard Test Method for Trapezoid Tearing Strength of Geotextiles
Apparent opening size	ASTM D4751	Standard Test Method for Determining Apparent Opening Size of a Geotextile
Permittivity	ASTM D4491	Standard Test Methods for Water Permeability of Geotextiles by Permittivity
Gradient ratio	ASTM D5101	Standard Test Method for Measuring the Soil-Geotextile System Clogging Potential by the Gradient Ratio
Transmissivity	ASTM D4716	Standard Test Method for Constant Head Hydraulic Transmissivity (In-Plane Flow) of Geotextiles and Geotextile Related Product
Ultraviolet resistance	ASTM D4355	Standard Test Method for Deterioration of Geotextiles from Exposure to Ultraviolet Light and Water (Xenon-Arc Type Apparatus)
Seam strength	ASTM D1683	Failure in Sewn Seams of Woven Fabrics
Seam strength	ASTM D4884	Standard Test Method for Seam Strength of Sewn Geotextiles

Source: Zornberg & Christopher (2007)

* References: ASTM D5199 (2019b), ASTM D5261 (2018d), ASTM D4632 (2015a), ASTM D4595 (2017a), ASTM D6241 (2014a), ASTM D4533 (2015b), ASTM D4751 (2020b), ASTM D4491 (2021b), ASTM D5101 (2017b), ASTM D4716 (2020d), ASTM D4355 (2021c), ASTM D1683 (2018c), ASTM D4884 (2014b).

PROPERTIES OF GEOCELLS

Knowing the properties of geocells is necessary before applying specific geocells from manufacturers in preliminary design and field construction. The essential properties commonly reported by manufacturers include cell dimensions, strip thickness, density, surface area, tensile strength, and seam strength, while other additional and advanced properties such as creep reduction factors, durability to UV degradation, and allowed strength for design of 50 years may also be found (Hegde, 2017). Table 21 summarizes common characteristics, typical values (if applicable), and test methods that are usually reported by manufacturers. More detailed explanations to some properties are given in the following subsections.

Table 21. Common Properties of Geocells

Properties	Typical Values	Units	Test Methods *
Density	0.95	g/cm	ASTM D1505
Strip Thickness	1.53 (±10%)	mm	ASTM D5199
Cell Depth	75–200	mm	–
Tensile Strength	–	N (lbf)	ISO 10319 ASTM D4595
Short-Term Seam/Junction Peel Strength	–	N(lbf)	ISO 13426 GEOWEB's METHOD
Long-Term Seam/Junction Peel Strength	Pass/Fail	–	GEOWEB's METHOD

* References: ASTM D1505 (2018e), ASTM D5119 (2019b), ISO 10319 (2015), ASTM D4595 (2017a), ISO 13426 (2019). For GEOWEB's method, see https://www.prestogeo.com/products/soil-stabilization/geoweb-geocells/ for example specifications.

Cell Depth

Benefiting from confinement and lateral restriction generated by cell walls, geocells can improve bearing capacity of base course or subgrade soil. The cell depth directly relates to the size of the confining zone. Geocells with larger cell depth tend to produce a larger stabilization area and eventually more dramatically improve the performance of infilled materials. Cell depth of geocell products in the market usually varies from 75 mm (2.95 in.) to 200 mm (7.87 in.), providing several options for specific stabilization tasks.

Tensile Strength

In this report, tensile strength refers to strip shear strength, which is different from seam shear strength. Tensile strength determines the strength of geocell material rather than the junction / seam. Many manufacturers are following different specifications but mainly using a wide-width strip method as in ISO-10319 and ASTM D4595 (2017a). Note that ASTM D4595 is originally designed for determining geotextile strength. The main differences among test methods are the cut size of the specimen and shear rate. In ISO-10319, a specimen with dimensions of 100 mm × 100 mm (3.94 in. x 3.94 in.) is tested at a shear rate of 20% strain per minute, while ASTM D4595 applies a specimen with dimension of 200 mm × 200 mm (7.87 in. x 7.87 in.) and a shear rate of 10% strain per minute. Additional attention needs to be drawn to investigating the specimen dimension and the shear rate selected and performed by manufacturers.

Short-Term Seam / Junction Peel Strength

The short-term seam peel strength is applied to determine the strength near the seam parts of two contiguous cells. Figure 63 presents the fundamental design of short-term seam peel strength test: a trimmed sample with two 102 mm (4 in.) seamed cells is fixed by a clamp at top, and peeling is exerted on the bottom at a constant rate. Different manufacturers or specifications may select different peel rates (e.g., 20% strain/min in ISO 13426 versus 300 mm/min in GEOWEB's method).

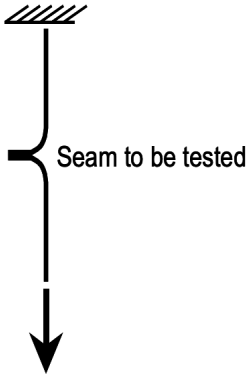

Figure 63. Illustration. Short-term seam / junction peel strength test.

Source: PRESTO (2019)

Long-Term Seam / Junction Peel Strength

The long-term seam / junction peel strength test evaluates the long-term performance of the junction and simulates temperature change in the field. The same sample is cut out from the geocells as from the short-term test in Figure 63, whereas a weight of 72.5 kg (160 lb.) is hung at the bottom instead of applying a constant peel rate. During the peel testing, the sample undergoes a temperature change on a one-hour cycle from room temperature (in accordance with ASTM E41) to 54˚C (130˚F). The sample passes the test if no failure (i.e., seam rupture) exists after 168 hours (7 days) of testing. PRESTO suggests performing 10 replicate tests, and all 10 samples need to pass the test.

Other Properties

Other environmentally related properties such as environmental stress-cracking resistance, durability to UV degradation, and coefficient of thermal expansion may also be provided by manufacturers. Such properties can help determine the suitability of geocell products under certain environmental conditions.

APPENDIX C: CASE STUDIES, FULL-SCALE TESTING, FINDINGS BY RESEARCHERS, AND FIELD EXPERIMENTS

FULL-SCALE PAVEMENT STUDIES BY US ARMY CORPS OF ENGINEERS

Open Graded Bases for Airfield Pavements (Barker, 1987)

Early research works on pavement application were conducted by a geotechnical laboratory at the Waterways Experiment Station (WES) of United States Army Corps of Engineers (USACE). A research performed by Barker mainly focused on the permeability of the open graded aggregate base layer of an airfield pavement as a drainage layer. However, field tests of the structural feasibility of using open-graded base in a flexible pavement were performed with heavy aircraft load included geosynthetics in the base layer.

The pilot test section planned was to be 15 ft wide and 70 ft long having a sandy silt subgrade, a 6-in. cement stabilized clay gravel subbase, a 6-in. open-graded base, and a 3-in. asphalt concrete (AC) surface, as shown in Figure 64. The section was subdivided into three base test sub-sections above the subbase. The first sub-section was a section 15 ft wide and 15 ft long having an open-graded base of crushed limestone following the ASTM Specifications D448 (2017c) and D693 (2003, withdrawn 2008) for a No. 57 stone. The second sub-section was also 15 ft wide and 15 ft long and had a base of the same stone with a geoweb fabric located at mid-height of the base. The geoweb used was tensor SS-2 geoweb having a web dimension of approximately 1.1 by 1.5 in. There was a 10-ft-long transition zone between the sub-section 2 and sub-section 3 to allow for transition of the base. Sub-section 3 was 15 ft wide and 30 ft long, and the base was the same aggregates stabilized with 2 percent asphalt. A cement-stabilized sandy gravel with 8 percent of cement and 7.3 percent of moisture content was chosen for the subbase to provide a stiff working platform for the placing of the base and as protection for the subgrade during the load test.

The traffic placed on the test section was to simulate traffic from an F-4 aircraft. The loading was applied by a single tire loaded to 27,000 lb and inflated to 265 psi tire pressure. At intervals during traffic the application of traffic was stopped, and data on the performance of the test sections were obtained. Photographs were taken and cross-section data were obtained at traffic coverage levels of 0, 10, 30, 100, 300, and 1,000. Falling weight deflectometer (FWD) data were collected at 0, 100, 300, and 1,000 coverages using a nominal 15 kip-loading.

Figure 65 shows a plot of the development with traffic of permanent deformation for each of the sub-sections. The deformation under the load was more noticeable for open-graded aggregates than asphalt stabilized aggregates. As can be seen by 100 coverages, the deformation of open-graded aggregates was approximately twice that of asphalt stabilized aggregates. After 100 coverages, the deformation in unstabilized aggregates increased at a greater rate than the deformation in geoweb-stabilized aggregates. At the end of traffic, the deformation of geoweb-stabilized aggregates was 79 percent of the deformation of unstabilized aggregates, this 21 percent of permanent deformation was achieved by mechanical stabilization. The deformation of asphalt stabilized aggregates was 44 percent that of unstabilized aggregates.

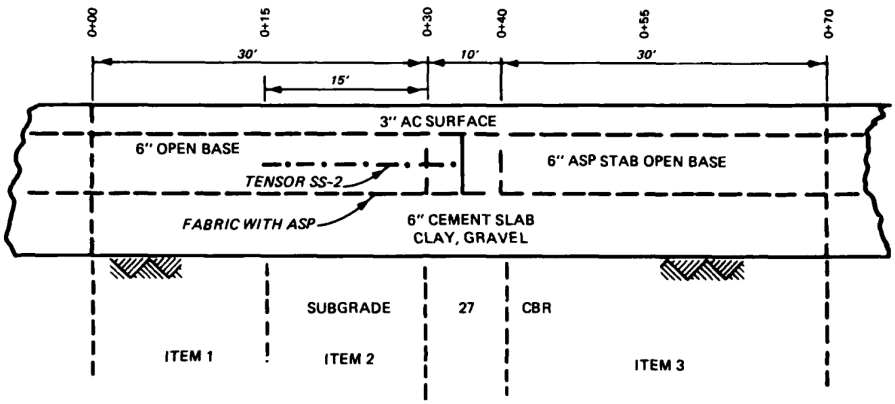

Figure 64. Illustration. Longitudinal cross-section of the test section.

Source: Barker (1975)

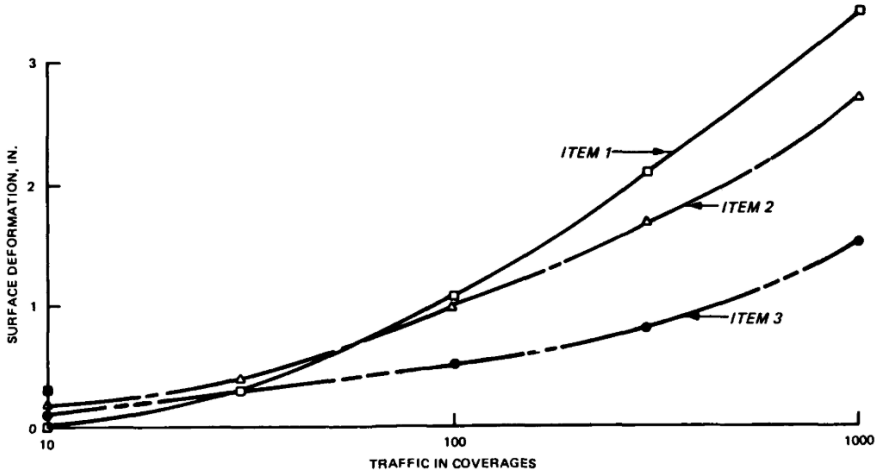

Figure 65. Graph. Permanent deformation as a function of traffic; Item 1 is unstabilized base, Item 2 is geoweb-stabilized base, and Item 3 is asphalt stabilized base.

Source: Barker (1975)

Geogrid-Reinforced Bases for Flexible Pavements for Light Aircraft (Webster, 1993)

To determine the potential application of geogrid stabilization for an airfield base, extensive full-scale tests with three control factors, geogrid, subgrade strength and base layer thickness, were designed and carried out. This report describes the construction of the field test section, the behavior of the test section under traffic testing using a 30,000 lb single tire load, the data collected, laboratory tests various geogrid products used in the field test design criteria for geogrid base reinforcement for flexible pavements for light aircraft.

The test section contained 4 traffic lanes and each traffic lane includes 4 sub-sections. All test items were surfaced with a 2-in asphalt concrete surface meeting FAA Item P-401 requirements for pavements designed for aircraft weights less than 60,000 lbs or tire gross pressure less than 100 psi.

Figure 66 shows a profile section of traffic lane 1, 2, 3 and 4. The subgrade under all test sections consist of a heavy clay (CH) material with plastic limit of 45 and liquid limit of 67. A marginal-graded crushed limestone following the FAA P-208 for Aggregate Base Course specification was used as base material. Three products (SS-1, SS-2, and Geogrid X) had a sheet type structure with a polypropylene polymer composition. The remaining three products (FX-3000, GB-3022, and Miragrid 5T) were coated polyester with a woven structure.

Test traffic was applied using a 30-kip single-wheel-assembly test cart. The test wheel and tire were for a C-130 aircraft with contact pressure of 68 psi. The tire load was 30,000 lb with a contact area of 442-in^2. Failure of a test section was defined as 1 in. of rutting. Traffic was continued on a test section until 3 in. of rutting occurred or until each sub-section in the traffic lane reached 1 in. of rutting.

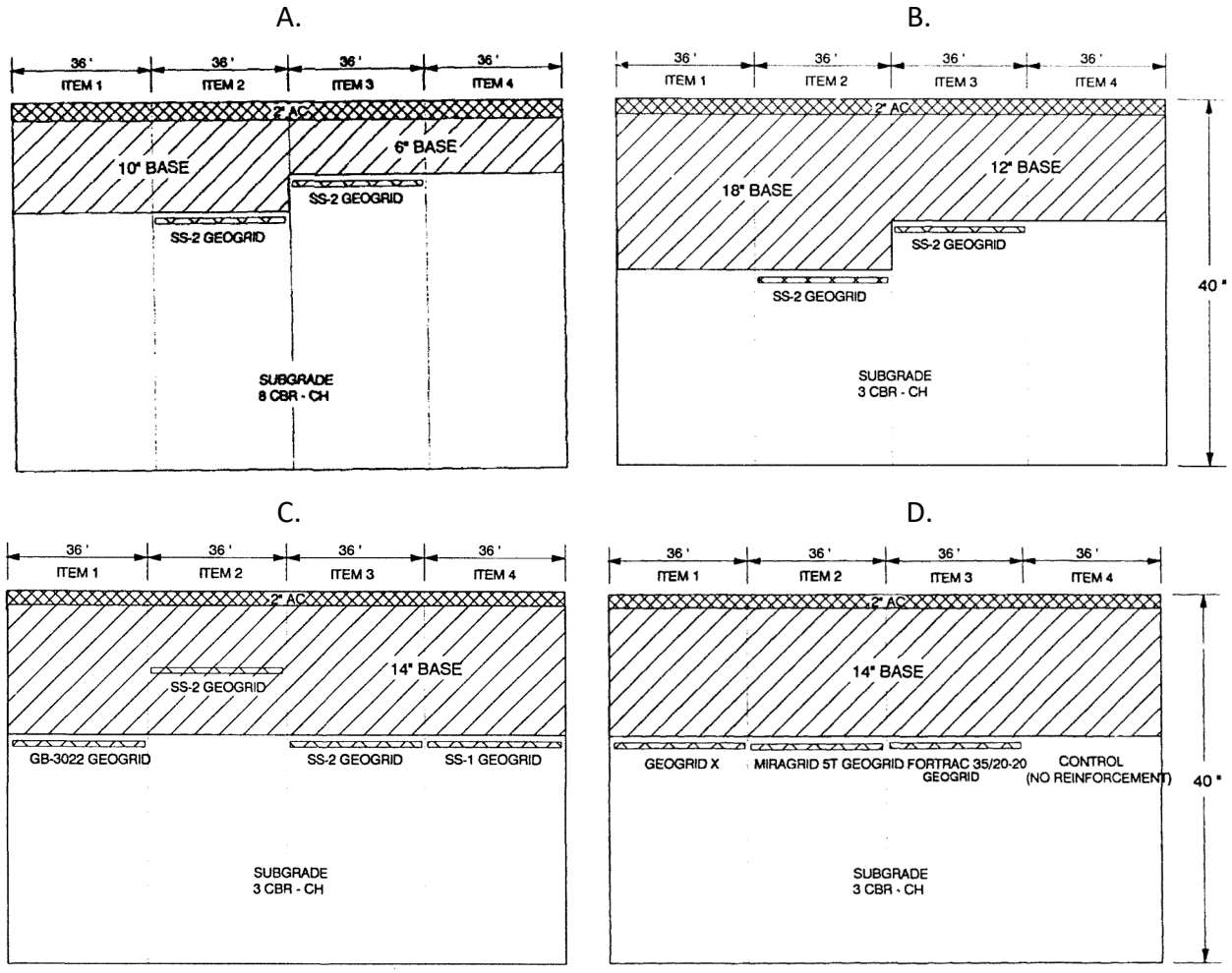

Figure 66. Illustration. Profile section of geogrid test section: (a) lane 1, (b) lane 2, (c) lane 3, (d) lane 4.

Source: Adapted from Webster (1993)

Rut depth and surface cross section elevation measurements were recorded at intervals throughout the traffic test period. The rut depth included both the permanent deformation and upheaval within the traffic lane. Cross section measurements were also made on the top of the base and geogrid or geogrid/subgrade interface in a test pit dug. The after-traffic application, CBR, water content, and density of the base and subgrade materials were collected. Nondestructive tests were also performed on each traffic lane with the falling weight deflectometer (FWD).

The traffic improvement factor is defined as a ratio of reinforced traffic passes to unreinforced traffic passes to produce a 1 in. rut and 1 in. permanent surface deflection. The traffic improvement factor ranged from 0.9 to 22.4 for the 1-in rut. The depth of placement of the geogrid reinforcement in the pavement structure is critical to the traffic improvement factor. The optimum depth of the geogrid reinforcement for the 30,000-lb tire load was approximately 8 in. And geogrid reinforcement at the bottom of the base was more effective than in the middle of base for 14-in.-thick base layers surfaced with 2 in. of AC. Therefore, it is recommended that the geogrid should always be placed at the bottom of the base course. This paper also demonstrated the geogrid mechanisms to improve the aggregate base layers. The improvement mechanisms for geogrid reinforcement over subgrade strengths greater than 1.5 CBR include grid interlock with aggregate base material, subgrade confinement, and to some extent a tensioned membrane effect when placed under relatively thin base courses.

From the results of test lanes 1 and 2, the equivalent base layer thickness relationship between reinforced and unreinforced base was carried out. Figure 67 shows the results of pavement thickness versus traffic passes for a 1-in. rut failure for lane 1 (8 CBR subgrade) and lane 2 (3 CBR subgrade). Lines extended through these data points were used to map out the shaded zone which was used to develop equivalent thicknesses between the unreinforced and reinforced conditions. The shaded zone was not extended below the recommended minimum geogrid placement depth of 6 in. Figure 68 shows a suggested conversion relationship from an unreinforced base thickness to an equivalent reinforced base thickness. This relationship can be utilized to design a base layer thickness of geogrid-reinforced airfield pavement for light weight aircraft.

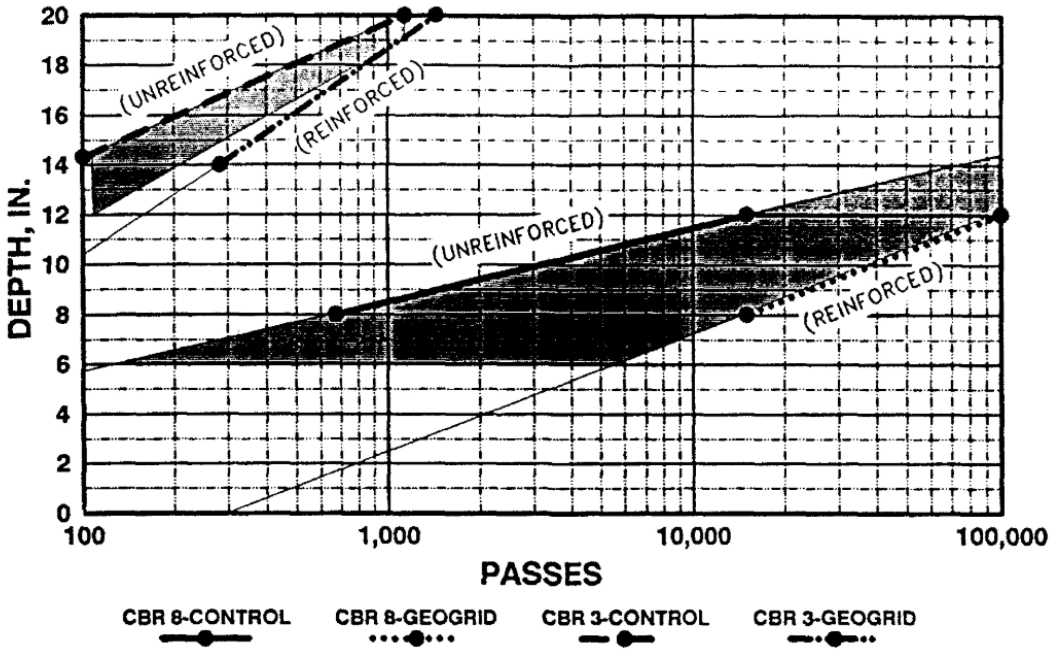

Figure 67. Plot. Pavement thickness versus traffic passes for a 1-in. rut failure for lane 1 (8 CBR subgrade) and lane 2 (3 CBR subgrade).

Source: Webster (1993)

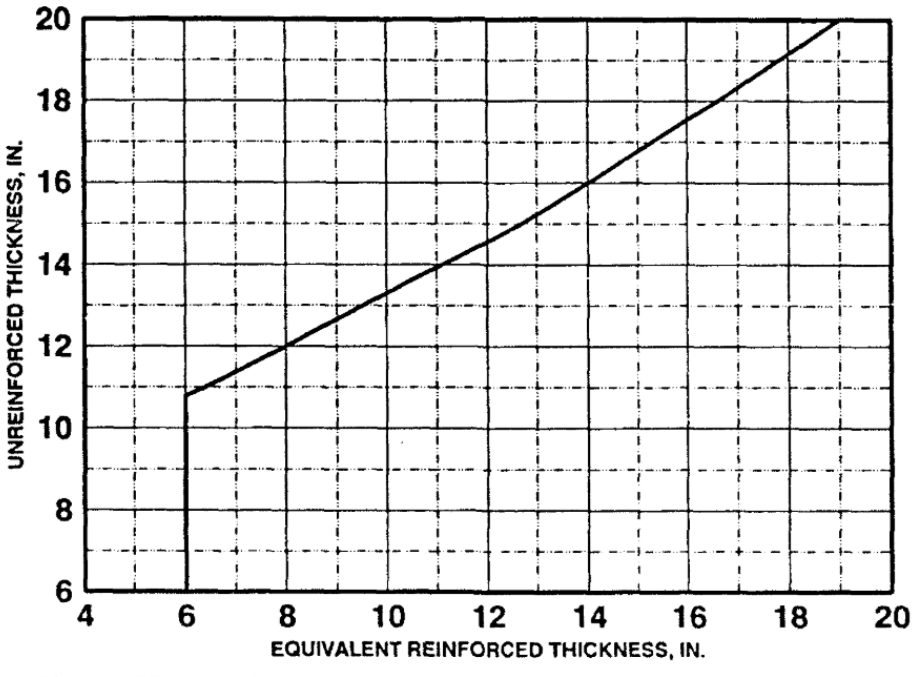

Figure 68. Graph. Relationship for the conversion from an unreinforced base thickness to an equivalent reinforced base thickness.

Source: Webster (1993)

RECENT RESEARCH EFFORT ON GEOGRID APPLICATION IN PAVEMENTS

Following the early full-scale tests by USACE engineers, the efficiency of using geogrids for stabilization of weak soil layers or for reinforcing unbound aggregate layers have been studied extensively (Al-Qadi & Appea, 2003; Chen & Farsakh, 2012; Al-Qadi et al., 2008). While the early research mostly focused on the rut depth measurement research, the focus of the research on geogrid stabilization can be divided into two main approaches. Geogrids can be used to improve the field performance, measured by lower rutting and rutting rate. For this stabilization purpose, geogrids can be applied at the interfaces between the subgrade and the base layer or the interface between the hot mix asphalt layer and the base layer. Another use for geogrids is reinforcement of the unbound aggregate layers for improving the resilient modulus and/or layer thickness optimization. These two applications are discussed in detail below.

A study by Al-Qadi and Appea (2003) demonstrated that the use of geogrids for stabilization can highly improve the performance of pavements built on subgrades with low CBR values (2–6%) and the improvement was quantified. In the same study, the use of geotextiles on the boundary between the base course and the subgrade layer was shown to improve pavement performance, concluded by observing that the same pavement structure with same layer thicknesses was able to withstand from 1.7 to 2.5 times more load repetitions for a 25 mm rutting compared to the control sections. The findings also show that the use of geogrids can reduce the rutting rate by preventing the penetration of the unbound aggregates in the base or subbase layer to the subgrade. At one point of the pavement life when the pavement started to deteriorate, the control sections experienced an increase in the rutting rate with time, while the pavement sections that were stabilized with geogrids still showed a reduction in the rutting rate with the continuously increasing load repetitions. Finally, it was concluded that geosynthetic-stabilized pavement sections can have up to two times the service life of unstabilized pavements.

One more use for geogrids is as reinforcement in the base layer. Chen and Farsakh (2012) investigated using geogrids for reinforcing base layers with geogrid layers placed in the middle of the base layer, at the interface of the base and subgrade as well as at the upper one third of the base layer. A total of seven geogrid-stabilized and two control pavement sections were tested under cyclic plate loading. The obtained results show that the contribution of geogrid reinforcement is lower permanent deformation for the same number of load repetitions. The authors found that the contribution of the geogrid to pavement performance is directly proportional to the tensile modulus of the geogrids and is also affected by the position of the geogrid in the base layer. The geogrids placed at the upper one third of the base layer outperformed the ones placed at the interface with the subgrade, which in turn slightly outperformed the ones that were placed in the middle of the base layer. The results of the study are shown in Figure 69. The authors recommended that the reinforcement contribution of the geogrids to the base layer can be incorporated in the mechanistic empirical pavement design guide (MEPDG) method in two ways: the first is by increasing the base resilient modulus to account for the stiffening effect of the geogrids. The second way is by reducing the required thickness of the base layer by a certain base reduction factor (BCR).

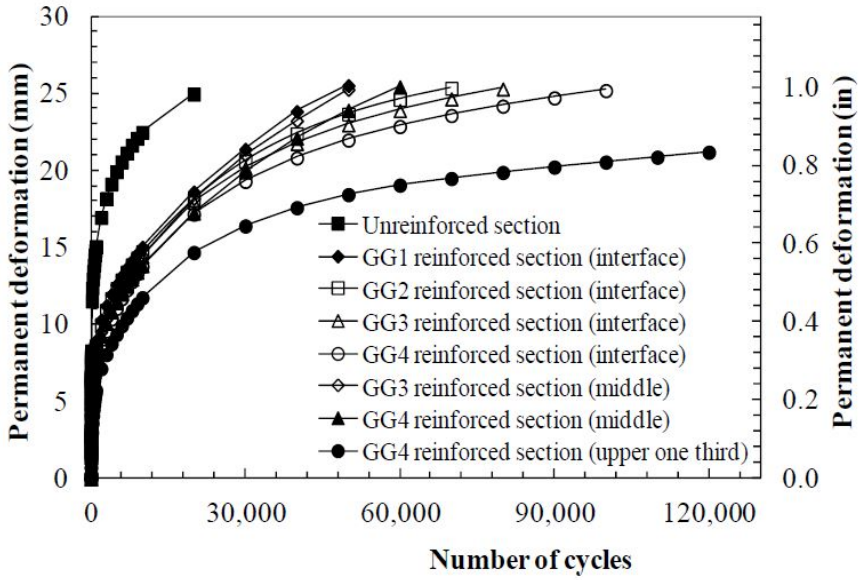

Figure 69. Graph. Permanent deformation results.

Source: Chen & Farsakh (2012)

Another study by Al-Qadi et al. (2008) evaluated the effectiveness of geogrids on the performance of flexible pavements. The study comprised a full-scale accelerated testing for a low-volume flexible pavement sections having an HMA thickness of 76 mm (3 in.) in three sections and 127 mm (5 in.) in one section, built on top of a base layer with thicknesses ranging from 203-457 mm (8-18 in.) and a subgrade having a California Bearing Ratio (CBR) of 4%. The advantages of using geogrids on pavement were found to be the resistance of the lateral movement of the granular base layer by increasing confinement, enhancing the pavement structural capacity, and reducing the potential of distresses such as the horizontal shear deformation in the base layer in the direction of traffic. The study also revealed that the optimal position of the geogrid layer for effective performance and cost effectiveness is dependent on the thickness (stiffness) of the base layer and the thickness of the HMA layer. For aggregate base layers with thicknesses of 203-457 mm (8-18 in.), the optimal position of the geogrid was determined to be at the interface of the unbound aggregate-subgrade boundary. For thicker base layers, the optimum location is at the top one third of the base layer and one more layer may be added at the interface with the subgrade for stability purposes.

Similar to this study, a study by Mishra et al. (2014) concluded that the optimal performance for geogrids was obtained when two layers of geogrids were placed 10 inches from the top and bottom of a 24 in. triaxial specimen of ballast size unbound aggregates (i.e., two layers of geogrids placed near the middle of the unbound aggregate layer). The reason for the optimal performance was attributed to that the reinforcing geogrid layers are intersecting the failure shear plane thus increasing shear strength and preventing lateral bulging.

Another use of geogrids for weak subgrade stabilization and reinforcement is by using geogrid-encased stone columns. The encasement can be done using both Geogrids and geotextiles, depending on the encased soil. The columns are made of highly compacted gravel size materials and

are pushed through weak soils by displacement methods. The use of geogrid-encased stone columns is researched extensively in literature. The proposed used are mainly for the construction industry as a form of pile foundation and the use for transportation systems foundations for flexible pavements. These encased columns work by distributing stresses in the upper soil depths as the columns bulge under loading; thus, less stress is transferred to the lower weaker depths (Gniel & Bouazza, 2009).

Federal Aviation Administration (FAA) recently performed study to examine the effect of using geosynthetics as a reinforcement agent in airfield pavement design with pavement structures subjected to heavy aircraft loadings (Norwood, 2019). The technical objective of this effort is to conduct medium-scale laboratory testing of representative flexible airfield pavements including different types of geosynthetic reinforcement. Pavement performance was measured by accumulated rut depth, which was used to calculate a traffic benefit ratio (TBR) for each product tested. The subgrade was constructed using locally available clay, known as Vicksburg Buckshot Clay. The subbase was constructed using a locally available granular material that met the gradation requirements for FAA P-154 material, and it was classified as a poorly graded sand (SP) according to the Unified Soil Classification System (USCS) and an A-1-b according to the AASHTO procedure. The base course was crushed limestone material. The crushed limestone aggregate base was classified as a poorly graded gravel with silt and sand (GP-GM) according to the USCS and an A-1-a according to the AASHTO procedure. Three geogrids were tested during this suite of tests including TX140, BX1200, and HUESKER Fornit 30/30. After construction, the test items were loaded to failure via cyclic loading of a 12-in.-diameter plate. The load was applied with 0.3 seconds of loading followed by a 0.9-second rest period. A load of approximately 28,800 lb was applied to achieve the targeted 254 psi pavement loading. Testing was conducted until each test item registered greater than 2-in. permanent surface deformation beneath the loading plate.

Table 22 summarizes the load level required for each test item to reach 2-in. of permanent surface deformation. Figure 70 presents summary plots of the permanent layer deformations for control section and reinforced section. The testing result indicated that the pavement test section performance noticably improved with the geogrid-reinforced test items compared to the unreinforced control item. The traffic benefit ratio (TBR) values for the geogrid-reinforced items with a 7-inch base course ranged from 20.3 to 29.7. The TBR values for the 6-inch base when compared to the 7-inch base unreinforced item were 3.3 and 3.4. Subgrade rutting and damage was exhibited in the unreinforced control item, whereas no measureable rutting was present for any of the geogrid-reinforced items.

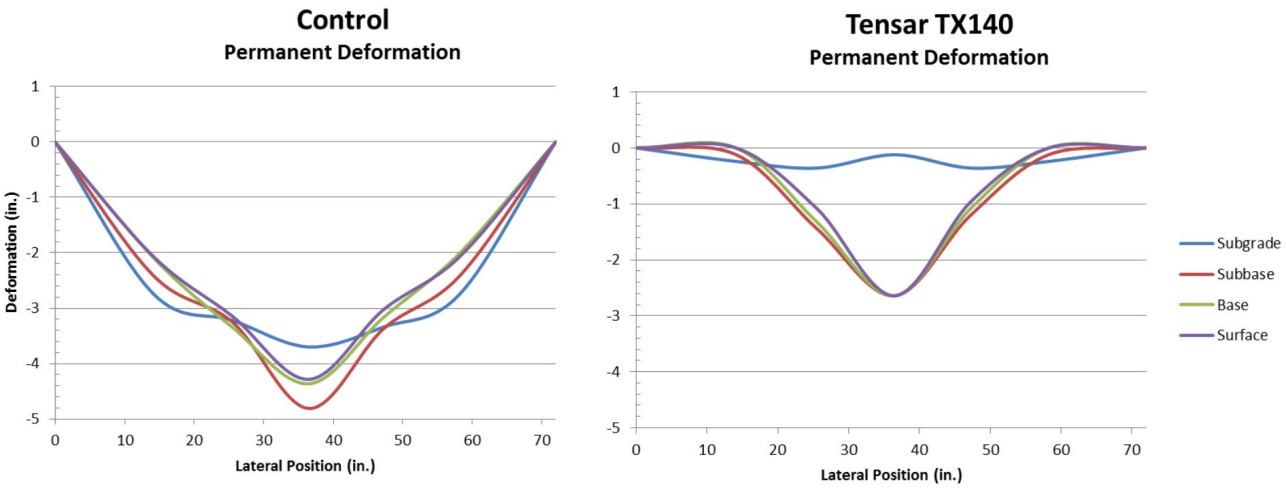

Figure 70. Graphs. Summary plots of the permanent layer deformations.

Source: Norwood (2019)

Table 22. Summary of the Load Level and Traffic Benefit Ratio (TBR) at Failure

Product	Load level at 1-in. permanent deformation	Load level at 2-in. permanent deformation	TBR at 1-in. permanent deformation	TBR at 2-in. permanent deformation
Control	304	1278		
TX140	1000	4304	3.3	3.4
BX1200	6322	25960	20.8	20.3
Fornit 30/30	9024	34901	29.7	27.3

Source: Norwood (2019)

RECENT RESEARCH EFFORT ON GEOTEXTILE APPLICATION IN PAVEMENTS

To study the effectiveness of geotextiles in unsurfaced pavements over a weak subgrade, Mishra and Tutumluer (2012) conducted full-scale pavement testing considering the geotextile separation and reinforcement functions of the aggregate-subgrade interface. The study showed that geotextiles could significantly reduce interlayer material migration. Figure 71 demonstrates that geotextiles are able to reduce the rate of wheel path rut accumulation and allow a larger number of load applications.

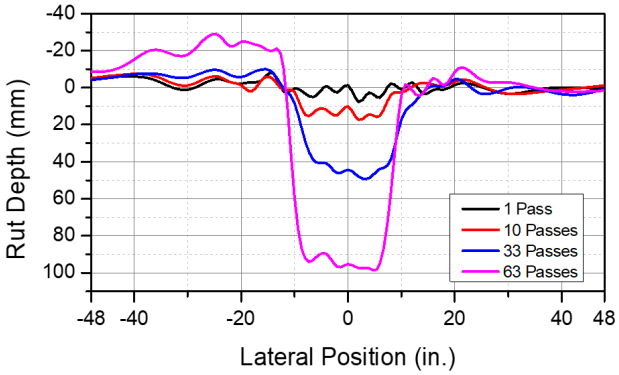

A. Rut depth of north wheel path without geotextile.

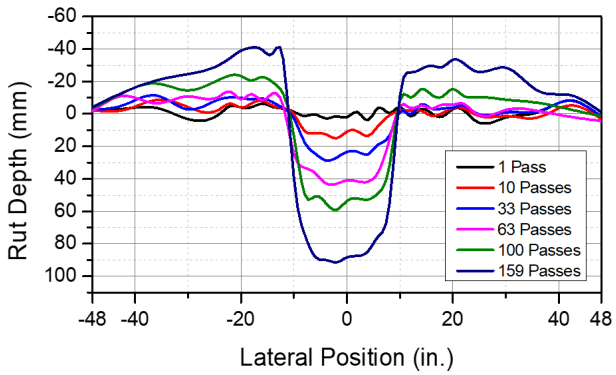

B. Rut depth of south wheel path with geotextile.

Figure 71. Graph. Geotextile effects on separation and gradual rut accumulation in wheel path.

Source: Mishra & Tutumluer (2012)

Benmebarek et al. (2015) conducted full-scale embankment testing over a section of about 11 km (6.8 miles) on sabkha soils of Chott El Hodna in Algeria. The sabkha surface had problems such as poor bearing capacity and rising water table over the surface. The geosynthetic applied on the road embankment significantly improved the soil bearing capacity, as shown in Figure 72.

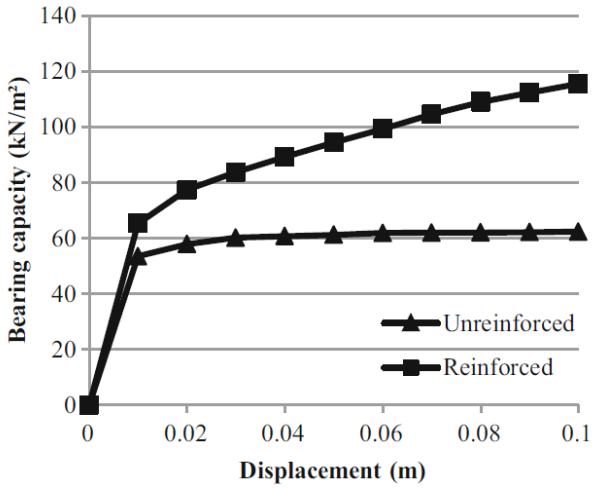

Figure 72. Graph. Effect of geosynthetics on the improvement of bearing capacity.

Source: Benmebarek et al. (2015)

RECENT RESEARCH EFFORT ON GEOCELL APPLICATION IN PAVEMENTS

Application in Mining Access Road (Paradox, 2012)

In 2012, MEG Energy's oil sand mining operations at Christina Lake in Alberta, Canada, were expanding; however, the existing road with high-saturated muskeg presented difficulties for allowing mining traffic approaching the drilling sites. Figure 73-A illustrates the deep muskeg subgrade with water content greater than 800% on the existing road. Constructing a durable and trafficable access road to the drilling site was required. Because removing and replacing the problematic muskeg subgrade with other materials was economically infeasible, a solution with geosynthetic stabilization was proposed and applied.

The total length of the road is 2 miles approximately across 0.9-mile muskeg subgrade and non-swamp 1.1 mile subgrade. The number of traffic passes was 2.5 million ESALs and the maximum load was from a CL-800 truck trailer with 800 kN of total semi-trailer load. The tolerable rut depth was 75 mm (3 in.), which was a typical value in unpaved road design. To achieve such requirements, two layers of geocells were applied in the muskeg area and one layer of geocells were installed in other areas. The geocells used in this project had a height of 150 mm (6 in.) and a width of 8 m (8 ft). One layer of nonwoven geotextile was placed under each layer of geocells to block the moisture from the swampy subgrade. Along with drainage facilities installed, the initial layer of geocells (on top of the muskeg subgrade) was installed on a nonwoven geotextile layer and filled with local sand, as shown in Figure 73-B and Figure 73-C. After sufficient compaction, another geotextile layer was placed, and a second geocell-stabilized layer was constructed by filling gravel finer than 40 mm sieve (1.5 in.) (see Figure 73-E). The fill thickness between two geocell layers varied with base thickness from 50 mm (1.97 in.) to 500 mm (19.7 in.). After completion of construction (Figure 73-F), the thickness of covered gravel material was 175 mm (7 in.).

A. Muskeg subgrade

B. Installation of initial layer of geocells

C. Filling with local sand

D. Compaction

E. Second layer of geocells filled with gravel

F. Completed road

Figure 73. Photos. Access road construction in Christina Lake, Alberta, Canada.

Source: Paradox (2012)

Application in Airport Roads (Schary, 2020)

The New International Airport Mexico City (NIACM) was constructed on unstable, saturated, and sinking clay mud, which was originally from the ancient Lake Tenochtitlan lakebed. The on-site soil consisted of two layers: a top layer of 20 cm (7.9 in.) to 25 cm (9.8 in.) clay with 1% CBR and 30 m to 60 m deep layer of clay mud with 0.6% CBR under that. Nevertheless, high groundwater level was

observed, and seasonal rain made this project more challenging. It was not economical to conduct soil replacement because of the amount of soil needing replacement.

To solve the challenges with this soil, many conventional soil stabilization methods were proposed and tested, such as placing multiple geogrid layers in the four-month solution comparison period, but all failed. Figure 74-A shows the on-site test section with geogrid stabilized and the truck still sank into the soil. Finally, as the only solution, neology geocells were proven effective during the on-site testing without observation of surface deformation, as shown in Figure 74-B. Figure 75 shows the pavement design in which a 120 mm (4.7 in.) geocell-reinforced layer with local rock as infill material was placed on top of a natural soil and below the base and asphalt pavement layers. The use of geocells in the NIACM airport project made the constructed road sustainable and durable through the six-month rain season each year.

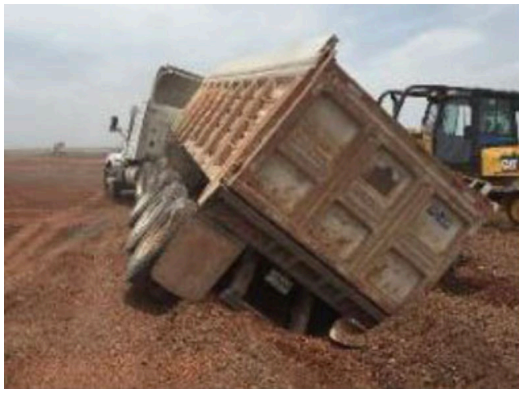

A. Truck on soil geogrid-reinforced soil

B. Truck on geocell-reinforced soil

Figure 74. Photos. Comparison of geogrid and geocells stabilization in NCIAM airport project.

Source: Schary (2020)

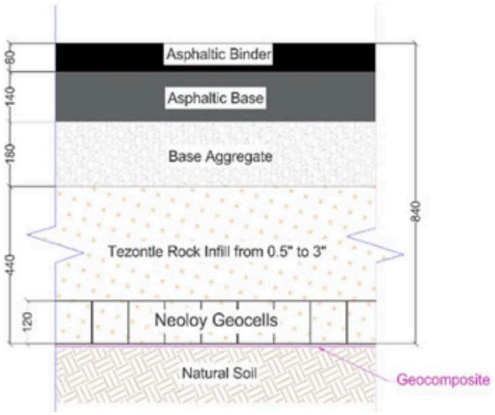

Pavement Structure Design (typical)

- 8 cm Asphalt Wearing Surface
- 14 cm Asphalt Base
- 18 cm Aggregate Base Layer
- 32 cm Tezontle rock infill
- 12 cm Neoloy-330-120-C
- Biaxial Geogrid
- Non-woven Geotextile

Figure 75. Illustration. Geocell-reinforced pavement section design.

Source: Schary (2020)

Application in Highway Road

The 26 km (16.2 miles) western high-speed diameter road (WHSD) in Saint Petersburg, Russia, was designed for relieving congestion traffic and planned for a traffic capacity of 1,000,000 vehicles monthly. Initially, a conventional pavement design was raised, and it was comprised of a 70 mm (2.8 in.) subbase layer, a 410 mm (16.1 in.) granular base layer, and a 230 mm (9 in.) asphalt layer. Importing high-quality granular base materials for providing sufficient bearing capacity and modulus was costly and time-consuming. A more economical alternative solution was using local materials reinforced with geocells.

To verify the feasibility of using local sand reinforced with geocells, field tests were performed by Kief (2015) and proved that the geocells could improve the granular subbase modulus by a factor of 2.45 and reduced the vertical stress by 50% on the subgrade. Such findings also presented that geocells could allow a 13% reduction in asphalt thickness and further decrease the budget. As a result, geocells with local infill were selected for constructing the WHSD highway, and the geocell-reinforced pavement could sustain double service time than the conventional pavement design with less cost (Kief, 2015).

APPENDIX D: DESIGN APPROACH WITH GEOGRIDS FOR BASE STABILIZATION IN PAVED ROADS (DRAFT)

SIGNIFICANCE AND USE: This draft design approach is introduced here for measuring the local stiffness enhancement in an unbound base or subbase layer in the proximity of a geogrid by using bender element (BE) piezoelectric sensors to determine the extent of the stiffened zone and the stiffness enhancement due to the presence of a geogrid.

This approach can be used to evaluate the effectiveness of a geogrid placed under or within an unbound aggregate layer. This approach can be used for geogrids (or stiff geotextiles) intended to serve the function of base mechanical stabilization. This geogrid function is suitable for asphalt paved or surface treated roads when dense-graded unbound aggregate base/subbase layers are placed on top of a natural subgrade with an immediate bearing value ranging between three and eight percent ($3\% \leq IBV \leq 8\%$).

DESIGN APPROACH: Divide a base/subbase layer stabilized with a geogrid into sublayers as shown in Figure 76. Assign each of the sublayers a modulus equal to the modulus of the base layer multiplied by a stiffening factor (modulus multiplier, MM); which is a function of the height above the geogrid, geogrid type, and the grain size distribution of the stabilized base/subbase.

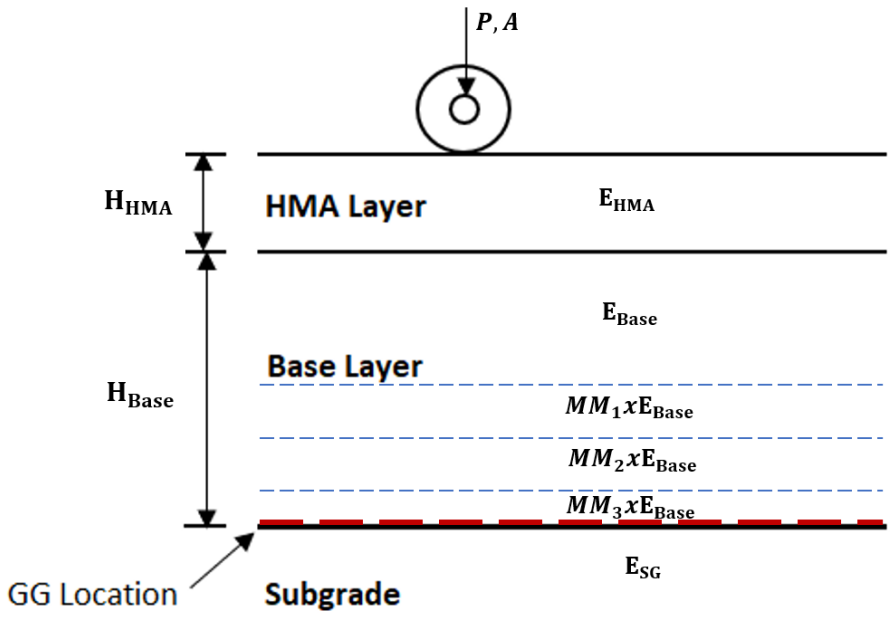

Figure 76. Illustration. Modulus assignment for base course sublayers in a pavement section with geogrid.

Follow procedure A or Procedure B to determine the stiffened zone properties (stiffness profile) in the proximity of a geogrid depending on aggregate gradation and geogrid type:

Procedure A: For unbound aggregate gradations and geogrid types that have already been tested, obtain stiffness properties of sublayers using Table 23 and Table 24. Select the stiffness multipliers closest to the grain size distribution and geogrid properties from these tables. Interpolation is recommended for gradations and/or geogrid properties that lie within testing ranges.

Table 23. Sublayer Modulus Multiplier for CA 6 Base/Subbase Layers

	Modulus Multiplier														
Geogrid Type	GG1			GG2			GG3			GG4			GG5		
Gradation / Height above GG (in.)	LB	MG	UB	LB	MG	UB	LB	MG	UB	LB	MG	UB	LB	MG	UB
0.0 – 1.2															
1.2 – 4.6															
4.6 – 6.0															
6.0 – ≥ 12.0	X 1.0	X 1.0	X 1.0	X 1.0	X 1.0	X 1.0	X 1.0	X 1.0	X 1.0	X 1.0	X 1.0	X 1.0	X 1.0	X 1.0	X 1.0

Note: LB is Lower Bound, MG is Mid Gradation, UB is Upper Bound of CA 06 gradation

Table 24. Sublayer Modulus Multiplier for CA 10 Base/Subbase Layers

	Modulus Multiplier														
Geogrid Type	GG1			GG2			GG3			GG4			GG5		
Gradation / Height above GG (in.)	LB	MG	UB	LB	MG	UB	LB	MG	UB	LB	MG	UB	LB	MG	UB
0.0 – 1.2															
1.2 – 4.6															
4.6 – 6.0															
6.0 – ≥ 12.0	X 1.0	X 1.0	X 1.0	X 1.0	X 1.0	X 1.0	X 1.0	X 1.0	X 1.0	X 1.0	X 1.0	X 1.0	X 1.0	X 1.0	X 1.0

Note: LB is Lower Bound, MG is Mid Gradation, UB is Upper Bound of CA 10 gradation

Note 2: Modulus multipliers in the tables above are proposed be filled based on the results of laboratory testing of the different gradations CA 06 and CA 10 (UB, MG, LB) with various geogrid products as part of a proposed research study. Geogrid products are proposed be divided into categories (GG1-GG5) for aperture shape and size and stiffness properties to allow for a broad use of available products from suppliers in the market.

Procedure B: If an aggregate gradation or a geogrid with aperture size/shape outside the range of tested properties is selected, determine the stiffened zone properties through laboratory testing using the prospective geogrid and aggregate material, upon the approval of the engineer. Use the

test setup shown in Figure 77. The wave measurement system consists of signal generator, pre-amplifier, filter-amplifier, and oscilloscope. First, input signal as source can be triggered from the signal generator. Amplification of signal magnitude is often crucial, and the magnitude can be controlled by the pre-amplifier and filter and amplifier. After filtering noise in the output signal, the shear wave can be properly recorded by the oscilloscope.

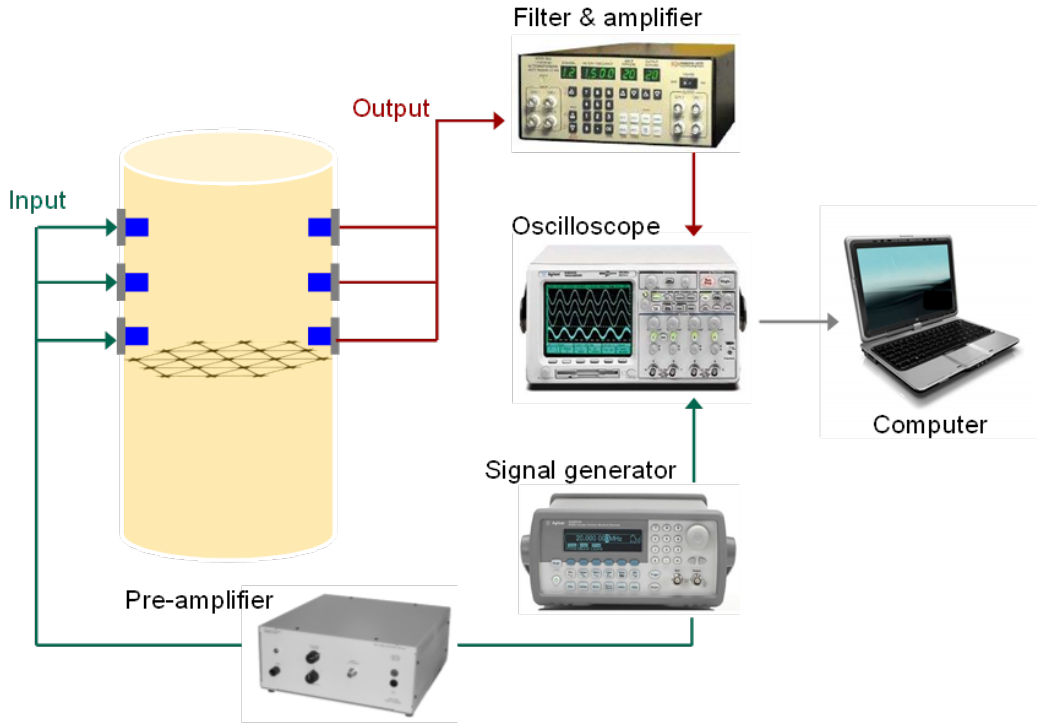

Figure 77. Illustration. Test setup for determining stiffened zone properties near a geogrid using bender elements.

Conduct repeated loading resilient modulus tests following AASHTO T 307 standard testing procedure on geosynthetic-stabilized and non-stabilized aggregate (control) specimens. Samples shall be instrumented with bender elements to determine the specific modulus multipliers to be assigned to the various sublayers.

APPENDIX E: DESIGNING WITH GEOGRIDS AND GEOTEXTILES FOR SUBGRADE RESTRAINT AND UNPAVED ROADS (DRAFT)

SIGNIFICANCE AND USE: This design guide is for using geogrids and geotextiles to increase the bearing capacity of weak subgrade soils having an immediate bearing value (IBV) of 5% or less.

DESIGN PROCEDURE: This draft design procedure for unpaved roads with geogrids and geotextiles uses the Giroud-Han 2004 design method for unpaved roads. Use the following equation to determine the base thickness with geogrids/geotextiles:

$$h = \frac{0.868 + (0.661 - 1.006J^2)\left(\frac{r}{h}\right)^{1.5} logN}{1 + 0.204[R_E - 1]}\left[\sqrt{\frac{\frac{P}{\pi r^2}}{\left(\frac{s}{f_s}\right)\left[1 - 0.9exp\left(-\left(\frac{r}{h}\right)^2\right)\right]N_c \cdot f_c \cdot CBR_{sg}}} - 1\right]r$$

Figure 78. Equation. Thickness design equation for geogrids and geotextiles by Giroud & Han (2004b).

where

h =base course thickness (m)

r = equivalent radius for the contact area of the tire (m). A typical value of 0.152 m (6 in.) may be assumed if this value is unknown.

P = wheel Load (kN). A typical value of 40 kN (9 kips) may be used if this value is unknown.

s = allowable surface rut depth

f_s = a factor for surface rut depth often assumed to be 75 mm (serviceability limit)

f_c = a factor relating CBR of subgrade to equivalent undrained cohesion (equal to 30 kPa)

N = number of equivalent single (80-kN or 18-kip) axle passes

N_c = bearing capacity factor (5.71 for geogrid reinforcement and 5.14 for geotextile reinforcement)

R_E = limited modulus ratio of base course to subgrade soil, and calculated as follows:

$$R_E = \min\left(\frac{E_{bc}}{E_{sg}},\ 5.0\right) = min\left(\frac{3.48{CBR_{bc}}^{0.3}}{CBR_{sg}}, 5.0\right)$$

Figure 79. Equation. Modulus ratio of base course to subgrade soil.

CBR_{sg} and CBR_{bc} are the California Bearing Ratios (CBRs) of the base course and subgrade soil, respectively.

J= aperture stability modulus of the geogrid (with J=0 for unreinforced and geotextile-reinforced unpaved roads). Obtain the value of J from product specification sheets.

SELECTION OF PROPER GEOTEXTILE PRODUCT: Geotextile used for subgrade restraint/stabilization should conform to the requirements of AASHTO M288 for Class 1 geotextiles. Requirements for Table 1 for Class 1 geotextiles in AASHTO M288 shall be all met for strength requirements (also shown in Table 25 below) unless the engineer has found a lower class of geotextile to have sufficient survivability based on field experience or laboratory testing and visual inspection of a geotextile sample removed from a field test section constructed under anticipated field conditions. For other physical properties (stability, apparent opening size, and permittivity), the geotextile needs to meet the minimum requirements presented in Table 26 below to ensure proper drainage, durability, and separation. The separation and drainage requirements assume the subgrade is fine grained with more than 50% silt- and clay-sized fractions.

Table 25. Strength Properties of a Class 1 Geotextile Separator

Property	Test Method *	Value (N)	
		Elongation < 50%	Elongation ≥ 50% (1)
Grab Strength	ASTM D4632/D4632M	1400 N	900 N
Sewn Seam Strength	ASTM D4632/D4632M	1260 N	810 N
Tear Strength	ASTM D4533/D4533M	500 N	350 N
Puncture Strength	ASTM D6241	2750 N	1925 N

Adapted from AASHTO M 288 (2017 Table 1)

* References: ASTM D4632 (2015a), ASTM D4533 (2015b), ASTM D6241 (2014a).

(1) As measured in accordance with ASTM D4632/D4632M

Table 26. Other Stabilization Geotextile Property Requirements

Property *	Value
Apparent Opening Size, Sieve No. (mm) ASTM D4751	No.70 (0.212 mm) maximum
Permittivity, sec^{-1} ASTM D4491	0.1 minimum
Ultraviolet Stability (Retained Strength), %, ASTM D4355/D4355M	50% after 500 h of exposure

References: ASTM D4751 (2020b), ASTM D4491 (2021b), ASTM D4355 (2021c).

ALLOWABLE REDUCTION IN THICKNESS: Allowable thickness reduction in base course aggregate layer thickness shall not exceed 6 inches from the original design thickness where no geosynthetic product is used.

APPENDIX F: DESIGNING WITH GEOCELLS FOR SUBGRADE RESTRAINT AND UNPAVED ROADS (DRAFT)

SIGNIFICANCE AND USE: This design guide is for using geocells to increase the bearing capacity of weak subgrade soils having an immediate bearing value of 5% or less.

DESIGN PROCEDURE: Unpaved roads with geocells should be designed using the modified Giroud-Han design method approach for unpaved roads. The following equation is used to determine the base thickness with geocells:

$$h = \frac{(0.868 + k)\, log\, N}{1 + 0.204\left(E_{bc(r)}/E_{sg} - 1\right)} \left\{ \sqrt{\frac{P/(\pi r^2)}{(s_a/f_s)[1 - 0.9\, exp(-(r/h)^2)]N_c c_u}} - 1 \right\} r$$

Figure 80. Equation. Thickness design equation for geocells by Pokharel (2010).

where:

h = base course thickness (m)

r = equivalent radius for the contact area of the tire (m). A typical value of 0.152 m (6 in.) may be assumed if this value is unknown.

P = wheel Load (kN). A typical value of 40 kN (9 kips) may be used if this value is unknown.

s_a = allowable surface rut depth

f_s = a factor for surface rut depth often assumed to be 75mm (serviceability limit)

N = number of equivalent single (80-kN or 18-kip) axle passes

N_c = bearing capacity factor (5.71 with geocells)

$E_{bc(r)}/E_{sg}$ = modulus ratio of base to subgrade (RE). $RE = \frac{E_{bc(r)}}{E_{sg}} = \frac{MIF\, E_{bc}}{E_{sg}} = MIF\, \frac{E_{bc}}{E_{sg}}$

E_{bc} and E_{sg} = resilient moduli of the base course and subgrade soil, respectively

c_u = undrained shear strength of subgrade soil in kPa

MIF = Modulus Improvement Factor. This term was proposed by Han et al. (2007) to quantify the base modulus increase due to closed confinement by a geocell. MIF can be determined by static plate load tests, following ASTM D1196 (2016b) standard, on reinforced and unreinforced bases. The value of MIF is typically 1.5 to 2.5, corresponding to a 33% to 60%

reduction in base thickness, respectively. If MIF cannot be measured, it should be assumed 1.5 conservatively.

k, a calibration factor, depends on geocell properties: cell dimension, material, and manufacture process, and should be calibrated for different geocell products. For example, $k = 0.52(r/h)^{1.5}$ for a specific product and a 50 to 75 mm fill on top. Use this equation if 'k' could not be determined with lab/field testing. Parameter 'k' can be determined by plate load tests on base course with and without geosynthetic to obtain modulus improvement factor (MIF) or with cyclic plate loading tests and/or trafficking tests on geosynthetic-stabilized bases with different thicknesses.

SELECTION OF PROPER GEOCELL PRODUCT: Check if product is rated for road construction applications – many geocells available in the US are for slope protection or agricultural applications.

ALLOWABLE REDUCTION IN THICKNESS: Allowable thickness reduction in base course aggregate layer thickness shall not exceed 6 inches from the original design thickness where no geosynthetic product is used.


Illinois Department
of Transportation


ILLINOIS